

# Matched Spectral-Null Codes for Partial-Response Channels

Razmik Karabed and Paul H. Siegel, *Member, IEEE*

**Abstract**—A new family of codes is described that improve the reliability of digital communication over noisy, partial-response channels. The codes are intended for use on channels where the input alphabet size is limited. These channels arise in the context of digital data recording and certain data transmission applications. The codes—called *matched-spectral-null codes*—satisfy the property that the frequencies at which the code power spectral density vanishes correspond precisely to the frequencies at which the channel transfer function is zero. It is shown that matched-spectral-null sequences provide a distance gain on the order of 3 dB and higher for a broad class of partial-response channels, including many of those of primary interest in practical applications. The embodiment of the matched-spectral-null coded partial-response system incorporates a sliding-block code and a Viterbi detector based upon a reduced-complexity trellis structure, both derived from canonical diagrams that characterize spectral-null sequences. The detectors are shown to achieve the same asymptotic average performance as maximum-likelihood sequence-detectors, and the sliding-block codes exclude quasicatastrophic trellis sequences in order to reduce the required path memory length and improve “worst-case” detector performance. Several examples are described in detail.

**Index Terms**—Spectral-null codes, partial-response channels.

## I. INTRODUCTION

PARTIAL RESPONSE signaling has been widely used in data transmission since its introduction in the 1960's by Lender [46] and Kretzmer [44]. Partial-response models fit a wide range of linear channels with intersymbol interference, as described by Kabal and Pasupathy [26]. Forney [13] utilized the Viterbi algorithm to accomplish maximum-likelihood sequence detection of binary data transmitted over certain partial-response channels in the presence of additive white Gaussian noise (AWGN). The channels he considered had transfer polynomials of the form  $h(D) = (1 - D^N)$ , which comprise the class of “interleaved dicode” channels, but his results effectively provided a method for maximum-likelihood detection applicable to any digital partial-response channel corrupted by AWGN. The dicode channel, with transfer polynomial  $h(D) = (1 - D)$ , and the class-4 (PR4) channel, with transfer polynomial  $h(D) = (1 - D^2)$ , were shown by Kobayashi and Tang [42] to be attractive models for magnetic record-

ing channels. Kobayashi [43] also gave an algorithm for maximum-likelihood detection for these channels that is essentially equivalent to the trellis-based Viterbi algorithm proposed by Forney. Simulation studies and experimental evaluation of binary partial-response signaling with maximum-likelihood detection in the context of magnetic recording were carried out by Wood and Peterson [68]. See also Dolivo [9].

Thapar and Patel [65] proposed a more general class of models for magnetic recording, defined by transfer polynomials of the form  $h(D) = (1 - D)(1 + D)^N$ , where  $N$  is a nonnegative integer. In subsequent literature related to recording, the channel corresponding to  $N = 2$  has figured prominently, and has often been called *extended class-4* partial-response (EPR4), a practice we will follow.

Trellis-coding techniques for binary partial-response channels with transfer polynomials  $h(D) = (1 \pm D^N)$  have been recently proposed by Wolf and Ungerboeck [66], Calderbank, Heegard, and Lee [5], Immink [24], and Karabed and Siegel [30], [34]. In all of these, the constructions are based upon binary codes, typically convolutional, that have attractive Hamming distance properties for a given rate and decoder complexity. In [66], the code is concatenated with a precoder that essentially inverts (modulo 2) the channel transfer function. The minimum squared-Euclidean distance at the channel output is then lower bounded by the smallest, even integer greater than or equal to the minimum Hamming distance of the code. In [5], an inversion technique is used to design a new code that will produce, at the channel output, sequences that correspond to the original code sequences (modulo 2). This approach leads to a lower bound on minimum Euclidean distance that is similar to the one based on the channel precoder technique. The lower bounds suggest the use of codes that achieve the largest minimum Hamming distance for a given rate and complexity. The codes are usually extracted from tables of convolutional codes, such as those found, for example, in Lin and Costello [47, p. 331]. In most cases examined in [66] and [5], the lower bound proves to be tight.

In applications involving partial-response class-4 (twice-interleaved dicode) with maximum-likelihood detection, certain constraints on runlengths of zero samples at the channel output and in the interleaved substrings are desirable for purposes of timing and gain control, as well as to reduce path-memory requirements in the Viterbi detector. See, for example, Marcus and Siegel [51], [52].

Manuscript received May 9, 1990; revised February 22, 1991. This work was presented in part at the IEEE International Symposium on Information Theory, Kobe, Japan, June 19–24, 1988.

The authors are with the IBM Research Division, Almaden Research Center, K65/802, 650 Harry Road, San Jose, CA 95120-6099.

IEEE Log Number 9144340.

To ensure zero-runlength constraints on the trellis-coded partial-response output sequences, a coset of the underlying convolutional code is used in both [66] and [5]. Since the binary partial-response channels addressed by these methods have uncoded minimum Euclidean distance  $\sqrt{2}$ , the gain in minimum distance provided by the trellis code in this context is, in a sense, 3 dB less than the gain in the minimum Hamming distance that the code provides on a memoryless channel, as noted in [66].

In [24], [30], [34] the convolutional code is used in conjunction with an inner code that produces channel output sequences whose minimum squared-Euclidean distance is bounded below by a multiple of the minimum Hamming distance of the original code. Significant increases in the minimum Euclidean distance at the channel output can be achieved using this approach, but at the expense of significant losses in overall code rate. Zero-runlength constraints are provided directly by the inner codes. As with all of the techniques discussed so far, the trellis structure of the maximum-likelihood detector reflects the combined memory of the code and the partial-response channel.

The purpose of this paper is to describe a new class of trellis codes for partial-response channels. These codes exploit, rather than nullify, the channel memory in order to enhance minimum distance properties, while reducing the complexity of the Viterbi detectors, relative to the previously developed codes reported in [66] and [5].

The key idea underlying the new technique is the use of codes with a spectral null of order  $K$  in the code power spectrum, where  $K > 1$ , at the frequencies where the channel transfer function has a spectral null of order  $L$ , where  $L \geq 1$ . We refer to this new class of trellis codes as *matched-spectral-null (MSN) codes*. The general theory of MSN codes was first reported in [29], [30], [31], [33], [36]. The theoretical basis and construction techniques for MSN codes were shown to involve ideas and results from several different areas, including: characterization of sequences with (possibly higher order) spectral nulls at zero frequency or any rational submultiple of the symbol frequency, as developed by Yoshida [69], Pierobon [59], Marcus and Siegel [53], Monti and Pierobon [55]; distance properties of these sequences, as studied by Imminck and Beenker [25]; symbolic dynamics and its application to sliding-block code construction, as pioneered by Adler, Coppersmith, and Hassner [1], Marcus [50], and Karabed and Marcus [28]; and, finally, classical number-theoretic results related to the equal-power-sums problem [19, p. 328], [22, Chapter 18], cyclotomic polynomials [54, p. 72] and the Gaussian sum formula [45, p. 56].

The paper is organized in such a way that it breaks naturally into three parts. Part 1 attempts to give a high-level view, consisting of this introduction (Section I) and a detailed description and analysis of several MSN-coded partial-response systems (Section II). Part 2 addresses the characterization of spectral null sequences (Section III) and their distance properties (Section IV). Part 3 examines the coding gain provided by MSN-codes on partial-response channels (Section V), as well as issues

related to the construction of efficient MSN codes and their demodulation using reduced-complexity detector trellis structures (Section VI).

A more detailed description of the remainder of the paper is as follows.

In Section II, several examples of matched-spectral-null codes are discussed. In Sections II-A, II-B, and II-C we describe the examples that provided the motivation for this investigation and that nicely illustrate key aspects of the MSN coding technique. Section II-A examines the biphasic code for the dicode channel, first (to our knowledge) mentioned in [5], and independently investigated by Imminck [24], Zehavi [70], and Karabed and Siegel [34]. Section II-B describes the even-mark modulation code for the class-1 (duobinary, PR1) channel, discussed by Karabed and Siegel [32], [35]. These examples demonstrate the increased minimum Euclidean distance produced by MSN codes, as well as the existence of reduced-complexity Viterbi detectors that achieve the same asymptotic performance as a maximum-likelihood detector in the presence of AWGN. Section II-C presents further beneficial applications of these codes to other partial-response channels, in particular the interleaved-biphase (IB) code on the PR4 and EPR4 channels [24], [34], and the EMM code on the class-2 (PR2) channel. These applications, initially unexpected, turn out to be quite natural in the context of MSN coding.

In Section II-D, we present new MSN codes, with rates  $R = 2/3$ ,  $R = 3/4$ , and  $R = 4/5$ , for the binary dicode channel. We compare the codes, on the basis of simulated performance and detector complexity, to their counterparts among the codes developed by Wolf and Ungerboeck [66], illustrating some of the potential practical advantages of the MSN coding method.

The examples in this section reflect the original motivation for this investigation, namely the need for high-rate codes for binary partial-response channels relevant to digital data recording. The general theory of MSN codes, however, applies to multilevel partial-response channels, as well, and several authors have investigated and designed interesting quaternary MSN codes; see, for example, Haeb [18] and Eleftheriou and Cideciyan [10]–[12].

Section III addresses the characterization of sequences with higher order spectral null constraints. In Section III-A, we give several equivalent necessary and sufficient conditions for ensembles of sequences, representable as functions of a finite-state Markov-chain, to have a spectral null of order  $K$  at zero frequency or any rational submultiple of the symbol frequency, meaning that their power spectral density and its derivatives through order  $2K - 1$  vanish at the specified frequency. The necessary and sufficient conditions for a spectral null of order  $K$  extend in a natural way the previous results reported in [53], [55], [59], and [69]. Specifically, the conditions are expressed in terms of vanishing order- $K$  power-sums (moments), bounded order- $K$  running-digital-sums, and order- $K$  coboundary conditions at the spectral null frequency. In Section III-B, the coboundary conditions are used to define canonical diagrams for order- $K$  spectral

lossless of finite order can be viewed as "deterministic with bounded delay."

Fig. 2. Example for bound of Theorem 5.

null sequences, generalizing results in [53] and [55]. These diagrams later play an important role in the design of MSN codes and their reduced-complexity Viterbi detectors (Section VI).

Section IV investigates distance properties of spectral null codes. In Section IV-A, we derive lower bounds on the minimum Euclidean distance of integer sequences with a spectral null of order  $K$  at zero frequency or a rational submultiple of the symbol frequency. These bounds generalize earlier results of Imminck and Beenker [25] for binary block codes with  $K$ th-order zero-disparity. We give two proofs of the lower bound in the case of integer sequences with null of order  $K$  at zero frequency. One is based upon Newton's identities, extending the proof for binary block codes in [25]. The other, making use of Descartes' rule of signs, keeps track of sign changes in the sequences, and provides additional insight into the structure of sequences with spectral null of order  $K$  at zero frequency and the known solutions of the number-theoretic equal-power-sums problem.

The extension of the distance bounds to other spectral null frequencies required new techniques, and the proof presented in Section IV-B uses certain tools and results from number theory, including the Legendre symbols (see, for example, Niven and Zuckerman [57, p. 69]) and the Gaussian sum formula (see, for example Lang [45, p. 56]) that have also surfaced in other signal processing applications, as described by McClellan and Rader [54, p. 204] and Schroeder [60, p. 172].

In Section V, the distance properties of spectral null sequences, as developed in Section IV are used to prove the main results about the asymptotic coding gain attainable with matched-spectral-null codes on partial-response channels. In Section V-A, we address the case of certain multilevel code symbol alphabets. Applying the number-theoretic results related to the equal-power-sums problem, we derive a lower bound on the asymptotic coding gain for channels with a spectral null of order  $L$  at zero frequency or at a rational submultiple of the symbol frequency, when  $1 \leq L \leq 10$ , and the symbol alphabet is large. In Section V-B, for a more restricted set of spectral null frequencies and channel null orders, we obtain a lower bound on the asymptotic coding gain of MSN codes for channels with binary input alphabet.

In Section VI, we discuss the structure of practical encoders, decoders, and demodulators (Viterbi detectors) for MSN trellis codes. The canonical diagrams for spectral null constraints, as described in Section III, provide the framework for addressing two key problems related to practical realization of the MSN coding gains. Section VI-A briefly reviews some basic results in symbolic dynamics required in the following sections. In Section VI-B, we define reduced-complexity Viterbi detectors that can be used to demodulate the MSN codes. The trellis structures underlying the demodulators are based upon the canonical diagrams describing the spectral null constraints, rather than upon an actual encoder finite-state-machine or other presentations of the actual code con-

straints. Using results from Marcus [50], we investigate the problem of quasicatastrophic error-propagation (in the sense of Forney and Calderbank [14]) and prove that it can be prevented by requiring that the code avoid certain sequences, called *quasicatastrophic sequences*, that are characterized in terms of the trellis structure underlying the detector. This additional constraint on the code eliminates the potential loss in effective asymptotic coding gain that can arise, in the presence of a finite path memory in the detector, when the code contains these sequences. In Section VI-C, we apply the sliding-block code design methods of Adler, Coppersmith, and Hassner [1], Marcus [50], and the more recent work of Karabed and Marcus [28] to prove the existence of efficient sliding-block codes with specified spectral null constraints at rates arbitrarily close to 1, and to indicate algorithms for their construction. We also show that, in the design of a MSN code for use with a given detector trellis, the quasicatastrophic sequences can be avoided without incurring any additional rate penalty. Finally, in Section VI-D, we show that the reduced-complexity demodulators achieve effectively maximum-likelihood performance (in the presence of AWGN).

In the conclusions, we summarize the main results and indicate some of the future research directions suggested by this work.

## II. MOTIVATING EXAMPLES AND FURTHER APPLICATIONS

This section describes in detail several examples of matched-spectral-null (MSN) codes applicable to digital and optical recording channels. We begin with two specific codes that nicely illustrate (and, historically, motivated) the MSN coding technique. These examples are followed by higher rate MSN codes for the dicode channel that will be compared to previously proposed trellis codes with the same rates and asymptotic coding gains.

*Remarks on Terminology:* Throughout this paper, we will use the term *binary* to refer to the alphabet  $\{0,1\}$ , and the term *bipolar* to refer to the alphabet  $\{\pm 1\}$ . The bipolar version of a binary sequence will mean the sequence obtained by substituting the symbol  $-1$  for the symbol 0.

The expression *free Euclidean* (respectively, *Hamming*) distance, denoted  $d_{\text{free}}$  (respectively,  $d_{\text{free}}^H$ ), used in reference to the set of sequences generated by a specified directed, labeled graph, will mean the minimum Euclidean (respectively, Hamming) distance among pairs of sequences corresponding to paths in the graph that differ in only a finite number of edges. Various concepts of free or minimum distance that are important in evaluating the performance of MSN codes will be addressed in more detail in Section VI.

### A. Biphasic Code for Dicode Channel

As mentioned in the introduction, the binary  $1-D$  channel (dicode) and binary  $1-D^2$  channel (class-4) are useful partial-response models for the magnetic recording

TABLE I  
ENCODER FOR BINARY  
BIPHASE CODE

0	⇒	01
1	⇒	10

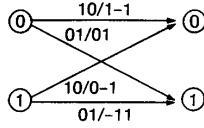


Fig. 1. Trellis for biphas-coded dicode channel.

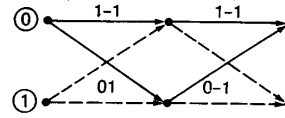


Fig. 2. Worst case error event for biphas-coded dicode channel.

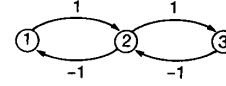


Fig. 3. FSTD for bipolar biphas sequences.

channel. Since the class-4 channel is simply “interleaved dicode,” previous techniques have concentrated on codes for the  $1 - D$  channel. For example, the precoding method of [66] and the inversion technique of [5] yield codes of comparable complexity for a given code rate  $R$  and asymptotic coding gain (ACG). The ACG for channels with binary (or bipolar) input restriction is given by

$$ACG = 10 \log_{10} R \frac{d_{free}^2(\text{coded})}{d_{free}^2(\text{uncoded})},$$

where  $d_{free}$  is the minimum Euclidean distance between channel output sequences corresponding to channel inputs differing in a finite number of positions.

*Remark:* For channels with multilevel inputs, the definition of asymptotic coding gain should incorporate a measure of average input power, as is done in [18] and in [10]–[12]. Also see Section V-C.

To achieve  $R = 1/2$  with  $ACG = 1.8$  dB, both prior approaches generate a code requiring 8 states in the trellis of the Viterbi detector incorporating the structure of the code and the characteristics of the dicode channel. In [5] (see also [24], [70]), however, it is pointed out that the simple block code known as the “biphase code” also satisfies these parameters, although it is not produced by direct application of the techniques of [66], [5]. Moreover, the corresponding Viterbi detector has only two states. The binary biphas code is defined by the encoding rule in Table I.

The trellis that represents the output sequences of the biphas-coded  $1 - D$  channel is shown in Fig. 1. The labels of the edges are  $x_1x_2/y_1y_2$  where  $x_1x_2$  is the biphas codeword corresponding to the channel input, and  $y_1y_2$  is the associated  $1 - D$  channel output. It is not difficult to see that the free Euclidean distance of the coded channel satisfies  $d_{free}^2 = 6$ , as illustrated by the pair of paths shown in Fig. 2. Since the uncoded  $1 - D$  channel has free Euclidean distance satisfying  $d_{free}^2 = 2$ , it is clear that the asymptotic coding gain is 1.8 dB.

A heuristic explanation of why the methods of [66] or [5] generate a more complex trellis code for this rate and ACG is that, in both constructions, the coded-channel output sequences, reduced modulo 2, define a binary convolutional code that is chosen to achieve the largest possible free Hamming distance, for the specified rate

and constraint length. The precoded convolutional code corresponding to the sequences described by Fig. 1 is the block code with codewords 01 and 11. This code has free Hamming distance  $d_{free}^H = 1$ , which is clearly not optimal for rate  $1/2$  binary block codes.

A basic motivation for the research reported in this paper was to understand what underlying properties made the biphas code so efficient, and to determine if the code could be usefully extended. We now examine several key features that will be characteristic of the more general family of MSN trellis codes.

- 1) *Spectral Null Properties:* The (bipolar) biphas code and the dicode channel share a common spectral property. The power spectrum of the bipolar biphas code and the transfer function of the dicode channel both have zero magnitude at zero frequency. To see this, observe that the bipolar code sequences, with random phase, are generated by the finite-state transition diagram (FSTD) in Fig. 3. Using the methods of Gallopoulos, Heegard, and Siegel [16], for example, one can determine that the code power spectrum is given by

$$\Phi_{\text{BIPHASE}}(f) = 2T \sin^2(\pi fT),$$

where it is assumed that the encoder is driven by equally probable binary inputs. The power spectral density (with  $T = 1$ ) is plotted in Fig. 4.

Note also that the frequency response  $H(f)$  of the  $1 - D$  channel [26] is given by

$$H(f) = \iota 2T \sin(\pi fT),$$

where  $\iota$  denotes the square root of  $-1$ . The magnitude of  $H(f)$  (with  $T = 1$ ) is plotted in Fig. 5.

It is readily verified that the code and channel share a spectral null at zero frequency.

- 2) *Distance Properties:* As mentioned above, the biphas-code triples the minimum squared-Euclidean distance at the output of the dicode channel, assuming a binary input restriction. This corresponds to a 4.8-dB gain in distance, or an asymptotic coding gain of 1.8 dB. Note also that the minimum Hamming distance of the binary code is two, a 3-dB gain in Hamming distance relative to the set of all binary sequences.

lossless of finite order can be viewed as “deterministic with bounded delay.”

Fig. 2. Example for bound of Theorem 5.

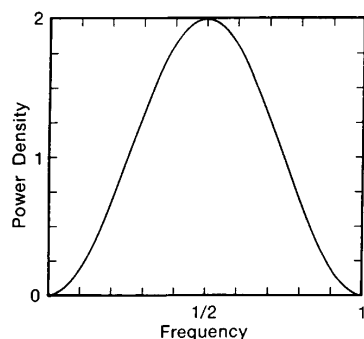


Fig. 4. Power spectral density of bipolar biphasic code.

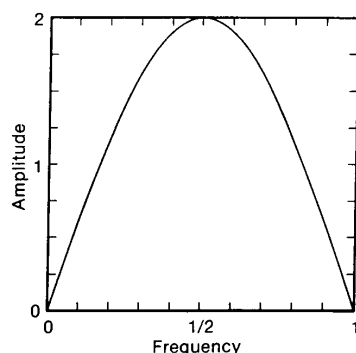


Fig. 5. Frequency response (magnitude) of dicode channel.

- 3) *Runlength-Limitations:* The output sequences of the biphasic-coded dicode channel never have a runlength of more than one zero-sample. The limitation of consecutive zero-samples is critical for decision-directed timing and gain control, as mentioned in the introduction.
- 4) *Efficient Code Implementation:* From Fig. 3, we can see that, starting from any state, the bipolar biphasic code sequences never have an imbalance of symbols 1 and  $-1$  exceeding two; in other words, the running-digital-sum [53] always has magnitude less than or equal to two. This property accounts for the spectral null at zero frequency. It has been shown that any finite-state bipolar code with maximum running-digital-sum bounded in magnitude by two must produce a subset of the sequences generated by Fig. 3, and for this reason, the diagram is considered "canonical" for this running-digital-sum constraint [53]. Therefore, the maximum rate of any such code is bounded above by the Shannon capacity of the canonical diagram, and this capacity is easily proved to be  $C = 1/2$ . It follows that the bipolar biphasic code, which has rate  $1/2$ , achieves the maximum possible rate for this RDS constraint.
- 5) *Viterbi Detector Based on Canonical Diagram:* From Property 4), it can be seen that the Viterbi detector

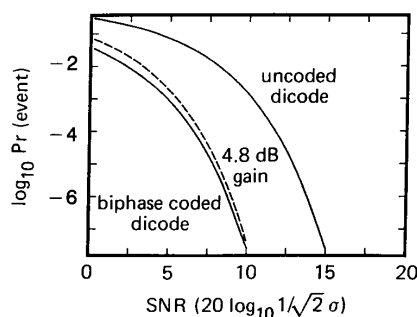


Fig. 6. Performance of biphasic-coded dicode channel.

trellis in Fig. 1 may be thought of as the trellis derived directly from the binary version of Fig. 3. In other words, the Viterbi detector of the bipolar biphasic code may be regarded as a maximum-likelihood detector for sequences with running-digital-sum magnitude bounded by two, transmitted over a dicode channel. Fig. 6 shows the asymptotically tight lower bound on the performance of the biphasic-coded dicode channel with this Viterbi detector. The bound is based upon the well-known expression in [13], where, in this case, the error-coefficient for the coded channel is 1.

#### B. Even-Mark-Modulation for Duobinary Channel

The second MSN-code example is the even-mark-modulation (EMM) code for optical recording [32], [35]. We begin the discussion of this code with a brief review of optical recording channel characteristics, noting similarities and differences relative to magnetic recording channels.

The optical recording channel transfer function resembles that of a lowpass filter. In analogy to the partial-response models for magnetic recording described in [65], one can define a family of models for optical recording with transfer polynomials,  $h(D) = (1 + D)^N$ , for  $N \geq 1$ . The partial-response channel with  $h(D) = 1 + D$  (variously called duobinary, class-1 or PR1) and the channel with  $h(D) = (1 + D)^2$  (PR2) represent the optical recording equivalents of the PR4 and EPR4 channels used in magnetic recording.

Optical recording channels also have certain unique features that have led to the definition of a new class of constrained codes that satisfy asymmetrical runlength-limitations, as described by Davie, *et al.* [8]. Asymmetrical runlength-limited (ARLL) constraints take advantage of the fact that, while the minimum size of a written mark is determined by the laser beam diameter produced by the focusing optics, the minimum space between written marks is governed by the accuracy of positioning of the laser spot, which can be finer than the minimum mark size. The ARLL constraints therefore specify separate minimum and maximum runlength limitations for 1's (written areas) and 0's (unwritten areas). The constraints are de-

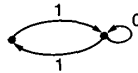


Fig. 7. FSTD for even-mark-modulation sequences.

noted  $(d', k') - (e', m')$ , where  $(d', k')$  represent the minimum and maximum allowable runlengths of 1's, and  $(e', m')$  are the analogous parameters for 0's.

*Remark:* In most magnetic recording applications, binary sequences with a conventional  $(d, k)$  constraint are passed through a precoder of the form  $1/(1 \oplus D)$ , resulting in binary sequences with parameters  $(d', k') - (e', m') = (d + 1, k + 1) - (d + 1, k + 1)$ .

Even-mark-modulation is a coded-modulation technique that was developed for a duobinary channel where the channel inputs are required to satisfy a  $(d', k') - (e', m') = (2, \infty) - (1, \infty)$  constraint. The code sequences used in the EMM method also satisfy the additional requirement that written marks must be *even* in length. The finite-state transition diagram representing these constraints is shown in Fig. 7.

The rate 2/3 code satisfying the EMM constraints (described in [32], [35] and referred to, using a slight abuse of terminology, as the EMM code) provides a bridge from the biphasic code to the more general trellis-coded modulation technique based upon matched-spectral-null codes, particularly with regard to certain code properties related to the use of reduced-complexity Viterbi detectors. As we did previously with the biphasic code, we now highlight the main properties of this code.

- 1) *Spectral Null Properties:* The power spectrum of the maxentropic, bipolar EMM sequences and the transfer function of the duobinary partial-response channel have the common feature of a spectral null at frequency  $f = 1/2T$ . The power spectral density of the bipolar EMM sequences, computed using the technique described in [16], is:

$$\Phi_{EMM}(f) = T \left( \frac{8\lambda}{2 + \lambda} \right) \frac{1 + \cos 2\pi fT}{3 + 2 \cos 2\pi fT},$$

where  $\lambda = (1 + \sqrt{5})/2$ . The power spectral density (with  $T = 1$ ) is plotted in Fig. 8. (The power spectrum also contains discrete lines at integer multiples of  $1/T$ , not shown here). The frequency response of the PR1 channel [26] satisfies:

$$H_{PR1}(f) = 2T \cos \pi fT.$$

The magnitude of this frequency response (with  $T = 1$ ) is plotted in Fig. 9. It is easy to see that both the code spectral density and the channel frequency response vanish at  $f = 1/2T$ .

- 2) *Coding Gain:* The trellis diagram that describes the output of the duobinary channel, with EMM-constrained binary inputs, is easily obtained from Fig. 7 and is shown in Fig. 10. It is not difficult to check that the free Euclidean distance satisfies:

$$d_{free}^2(EMM/PR1) = 4.$$

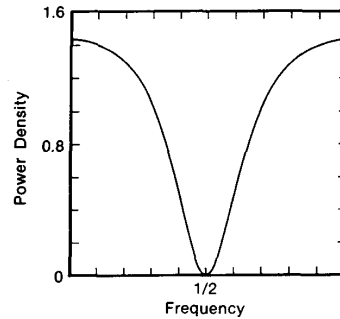


Fig. 8. Power spectral density of EMM sequences.

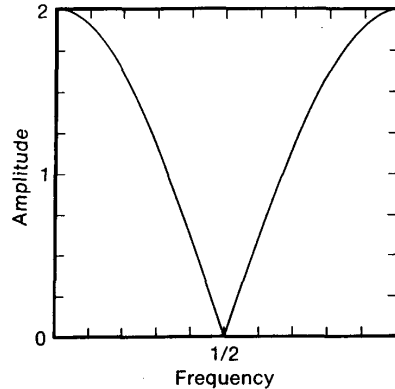


Fig. 9. Frequency response (magnitude) of PR1 channel.

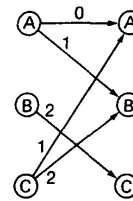


Fig. 10. Trellis for EMM-coded PR1 channel.

A worst-case error event is shown in Fig. 11.

For the  $1 + D$  channel, with binary inputs that are either unrestricted or that satisfy the  $(d', k') - (e', m') = (2, \infty) - (1, \infty)$  constraint, the free distance satisfies:

$$d_{free}^2(PR1) = 2.$$

The EMM constraint therefore doubles the free squared-Euclidean distance of the uncoded channel, representing a distance gain of 3 dB, or, normalizing for the rate 2/3, an asymptotic coding gain of 1.2 dB.

- 3) *Runlength-Limitations:* For the purposes of data-driven timing and gain control, it is desirable to limit the maximum runlength of identical output samples. This requirement translates into a restriction on the

lossless of finite order can be viewed as "deterministic with bounded delay."

Fig. 2. Example for bound of Theorem 5.

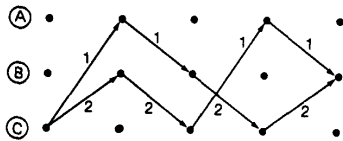


Fig. 11. Worst case error event for EMM-coded PR1 channel.

channel inputs, limiting the number of consecutive symbols 0 and 1, as well as the length of runs of the form 1010... The spectral null constraint naturally forces a limitation on the latter. The other run-length constraints are incorporated into the rate 2/3 EMM code, as described in Property 4).

- 4) *Efficient Code Implementation*: Unlike the finite-state diagram of the biphase code, the diagram underlying the EMM constraint does not correspond to a finite-state encoder. However, code design methods based upon symbolic dynamics (state-splitting) [1], [28] provide techniques for constructing efficient sliding-block codes for the EMM constraint at any rational rate less than its Shannon capacity  $C$ . The capacity of the EMM constraint is given by

$$C = \log_2 \lambda,$$

where  $\lambda$  is the largest real eigenvalue of the adjacency matrix  $A$  of the graph in Fig. 7,

$$A = \begin{bmatrix} 1 & 1 \\ 1 & 0 \end{bmatrix}.$$

It is easy to check that  $\lambda = (1 + \sqrt{5})/2$ , implying that  $C = 0.6923 \dots$ ,

suggesting a practical code rate  $R = 2/3$ .

As previously mentioned, in addition to the EMM constraint, we want to impose additional limitations on the maximum run of 0's and 1's at the channel input in order to facilitate decision-directed timing and gain control. The runlength limits on 1's and 0's were chosen to be  $k' = 12$ ,  $m' = 8$ , as can be seen from the modified EMM FSTD in Fig. 12. With a carefully chosen sequence of state-splittings and state-mergings, the rate 2/3 encoder shown in Table II was designed. The underlying finite-state-machine has eight states. The sliding block decoder requires a decoding window of twelve bits, implying that a single code-bit error can propagate to at most eight bits (one byte) of data, another attractive property from the practical standpoint.

- 5) *Viterbi Detector Based on Canonical Diagram*: The diagram for the bipolar EMM constraint, corresponding to the binary constraint in Fig. 7, is a canonical diagram for bipolar sequences with a spectral null at  $1/2T$ , and with running-digital-sums at  $f = 1/2T$  that assume only values bounded in magnitude by three. The trellis diagram in Fig. 10 therefore provides the basis for maximum-likelihood detection of the (binary) spectral null sequences when used on a  $1 + D$  channel.

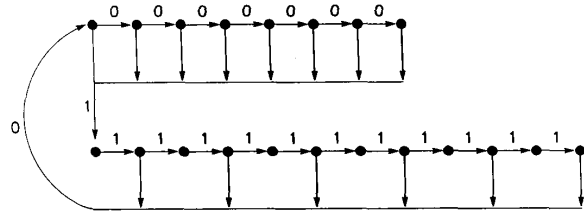


Fig. 12. FSTD for EMM with run-length-limitations.

TABLE II  
ENCODER FOR EVEN-MARK-MODULATION CODE

Data $b_1 b_2$ State $s_1 s_2 s_3$	00	01	10	11
000	011/000	011/001	110/000	110/001
001	001/100	001/101	110/010	011/110
010	000/000	000/011	111/100	111/101
011	001/100	001/101	111/100	111/101
100	100/000	100/001	101/100	101/101
101	111/000	111/001	100/010	111/111
110	000/000	000/001	111/100	111/101
111	000/000	000/001	111/100	000/010

The same trellis can be used to demodulate the rate 2/3 EMM code when it is applied to the  $1 + D$  channel. The trellis structure represents a considerable simplification compared to the structure required for a maximum-likelihood detector based on the 8-state finite-state-machine encoder. Moreover, as we will now explain, the asymptotic performance of the reduced-complexity demodulator approaches that of the maximum-likelihood detector, despite the fact that the trellis generates sequences not contained in the image of the rate 2/3 code.

At moderate-to-high signal-to-noise ratios, the average performance of the maximum-likelihood detector is largely determined by the minimum Euclidean distance between output sequences corresponding to any pair of valid code sequences. For the rate 2/3 EMM code it is easily shown that  $d^2 = 4$  is the minimum. In addition, since the code has finite memory (see Section VI), the maximum length of any error event achieving this distance is bounded by a fixed finite number.

When considering the reduced-complexity trellis in Fig. 10 as the basis for demodulation of the EMM code, we must make note of a characteristic not present in the biphase-coded dicode example: The trellis contains semi-infinite paths beginning at the same state that correspond to sequences with Euclidean distance strictly less than the free distance of the trellis (recall the remark at the beginning of Section II). For example, the paths determined by the state sequences

$$\begin{aligned} C A B C B C \dots \\ C B C B C B \dots \end{aligned}$$

produce outputs

1 1 2 2 2...  
2 2 2 2 2...

having squared-Euclidean distance  $d^2 = 2$ .

The Viterbi detector path memory length required to distinguish these sequences is unbounded, so any truncation of the trellis history would force a decision between survivor sequences at one-half of the free distance, potentially degrading the "worst-case" performance of the system. The reason for this phenomenon—called quasicatastrophic error-propagation [14]—is that the infinite sequence of constrained symbols 1 is generated by two distinct paths in the EMM diagram pictured in Fig. 7.

In the rate 2/3 EMM code, the maximum run-length of 1's is 12, a limit imposed also for the purpose of improved timing recovery. It follows (see Section VI-B) that there is an integer  $\tau$ , which we refer to as the *generalized truncation depth*, such that the squared-Euclidean distance between any channel output sequence of length  $\tau$  produced by a *code* sequence, and any other *trellis* sequence of the same length and generated from the same trellis state, must be at least as large as the free squared-Euclidean distance  $d_{\text{free}}^2 = 4$ . This property of the EMM code, resulting from the elimination of the sequence that causes the quasicatastrophic error-propagation, ensures that the detector based upon the reduced-complexity trellis with a path memory of length at least  $\tau$  will achieve the same asymptotic performance, as the signal-to-noise-ratio increases, as a maximum-likelihood detector for the coded channel. The results of a computer simulation of the EMM-coded PR1 channel are shown in Fig. 13.

C. Additional Applications of Biphase and EMM Codes

The preceding examples—the biphase code and the even-mark-modulation code—illustrate the main properties of MSN trellis codes for partial-response channels. We summarize the key features in the form of the following set of general observations that will be formalized and made precise in the subsequent sections of this paper.

*Observation 1:* Codes with spectral nulls can provide significant increases in the minimum Euclidean distance at the output of partial-response channels when the spectral null frequencies of the code and channel coincide.

*Observation 2:* Efficient spectral null codes with finite-state encoders and sliding block decoders can be constructed from canonical diagrams describing the underlying spectral null constraint.

*Observation 3:* Reduced-complexity trellis structures, derived from the same canonical diagrams, provide the basis for Viterbi detectors which achieve the same asymptotic performance as a maximum-likelihood detector, in the presence of additive, white, Gaussian noise.

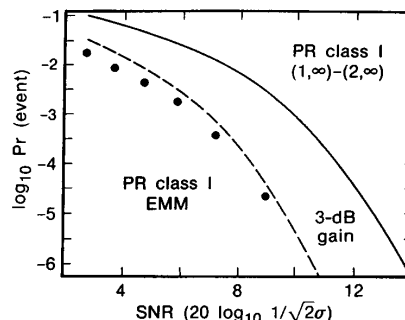


Fig. 13. Simulated performance of EMM-coded PR1 channel.

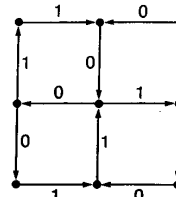


Fig. 14. FSTD for Interleaved Biphase sequences.

With these observations in mind, we now illustrate how the biphase code and the EMM code find new applications in the context of MSN coding.

The interleaved-biphase (IB) code is defined by

$$x_1 x_2 \rightarrow x_1 x_2 \bar{x}_1 \bar{x}_2,$$

where  $x_1, x_2$  are bits and the bar signifies binary complementation. The sequences of the binary IB code are generated by the diagram shown in Fig. 14.

The application of IB to the  $1 - D^2$  (PR4) channel is suggested by the interleaving approach to code design for  $1 - D^N$  channels, as described in [66] and [5]. Since the  $1 - D^2$  channel is simply "interleaved dicode," two copies of the trellis of Fig. 1 can be utilized to describe the even subsequence and the odd subsequence of outputs, respectively. From this it is clear that the distance gain is identical to that of the biphase code on the dicode channel, namely 4.8 dB.

A successful application to the EPR4 channel, with

$$h(D) = 1 + D - D^2 - D^3 = (1 - D)(1 + D)^2$$

is not so obviously anticipated. Fig. 15 shows the trellis diagram representing the sequences at the output of the IB-coded EPR4 channel. (Note that a component of the fourth power of the FSTD is used). From this four-state detector, we find a minimum distance pair of paths giving

$$d_{\text{free}}^2(\text{IB/EPR4}) = 12,$$

as illustrated in Fig. 16. Since the uncoded, binary EPR4 channel has free distance

$$d_{\text{free}}^2(\text{EPR4}) = 4,$$

we see that the interleaved biphase code again achieves 4.8 dB increase in free distance.

lossless of finite order can be viewed as "deterministic with bounded delay."

Fig. 2. Example for bound of Theorem 5.

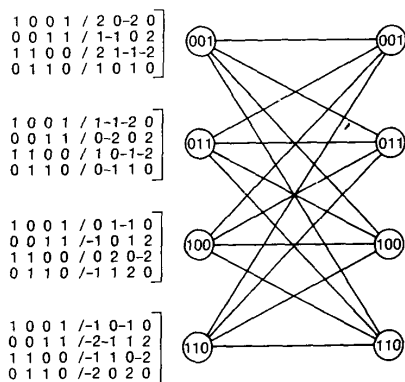


Fig. 15. Trellis for IB-coded EPR4 channel.

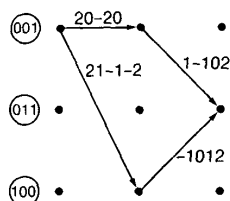


Fig. 16. Worst case error event for IB-coded EPR4 channel.

It is not difficult to verify that the bipolar IB code has first-order spectral nulls at  $f=0$  and  $f=1/2T$ . Referring to [53], we see that the bipolar version of Fig. 14 is a subdiagram of the canonical graph  $G^{0,1/2}$  that generates bipolar sequences with spectral nulls at  $f=0$  and  $f=1/2T$ . The power density spectrum of the bipolar IB code is given by

$$\Phi_{IB}(f) = 2T \sin^2(2\pi fT),$$

and is shown (with  $T=1$ ) in Fig. 17.

The PR4 and EPR4 channels also have spectral nulls in their transfer functions at  $f=0$  and  $f=1/2T$ . Specifically, the PR4 frequency-response is

$$H_{PR4}(f) = i2T \sin(2\pi fT),$$

and the EPR4 frequency-response is

$$H_{EPR4}(f) = i4T \cos(\pi fT) \sin(2\pi fT).$$

The magnitudes of these transfer functions (with  $T=1$ ) are shown in Fig. 18. The correspondence of code spectral null frequencies and the channel null frequencies is clear. The error-coefficient for both the uncoded and IB-coded EPR4 channels is 2. The asymptotically tight lower bound on the performance of the IB-coded EPR4 channel is shown in Fig. 19.

Finally, with regard to runlength-limitations, it is easily checked that at the output of the coded PR4 channel, the maximum runlength of zero-samples is two, and, at the output of the coded EPR4 channel, the maximum runlength of zero-samples is one.

We now discuss the application of the EMM code to the class-2 (PR2) partial-response channel with system

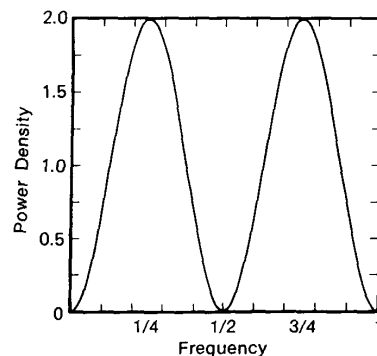


Fig. 17. Power spectral density of bipolar IB sequences.

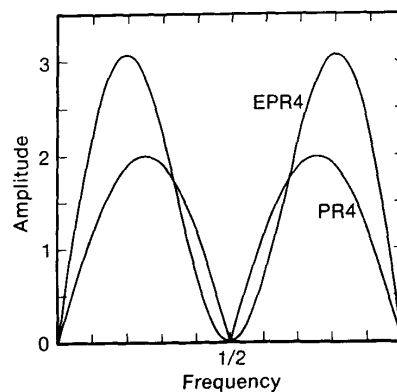


Fig. 18. Frequency response (magnitude) of PR4 and EPR4 channels.

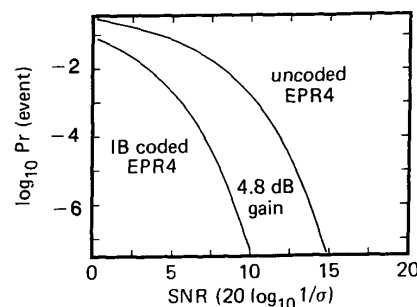


Fig. 19. Performance of IB-coded EPR4 channel.

polynomial  $h(D) = (1 + D)^2$ . Fig. 20 shows the trellis diagram for the sequences at the output of the EMM-coded PR2 channel. The minimum distance error events satisfy

$$d_{free}^2(\text{EMM/PR2}) = 10.$$

An example of such an event is shown in Fig. 21. For the uncoded or ARLL-restricted PR2 channel, the free distance is

$$d_{free}^2(\text{PR2}) = 4.$$

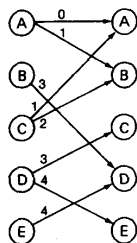


Fig. 20. Trellis for EMM-coded PR2 channel.

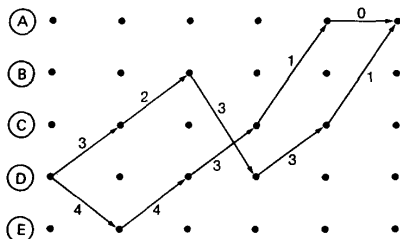


Fig. 21. Worst case error event for EMM-coded PR2 channel.

Therefore, the EMM constraint provides a gain in free distance of 4 dB.

The  $(1 + D)^2$  channel has frequency response

$$H(f) = 4T \cos^2(\pi fT),$$

the magnitude of which (with  $T = 1$ ) is plotted in Fig. 22. Referring to Figure 8, we see that the EMM power spectrum and the PR2 channel have a coincident null at  $f = 1/2T$ . Computer-simulated performance of the EMM-coded PR2 channel is compared to asymptotically-tight performance estimates for the ARLL-coded PR2 channel in Fig. 23. (For the EMM-coded channel, the loss relative to the 4 dB gain suggested by the minimum distance improvement is a result of the large ratio of its error coefficient to that of the ARLL-coded channel).

*Remark:* Some examples, such as the biphasic code and EMM code, provide distance gains which exceed the gains predicted by the matched-spectral-null coding theorem (Theorem 9 in Section V). This behavior appears to be characteristic of codes with relatively low rate and tighter constraints on the running-digital-sum values. As the rate increases, however, the lower bound on gains will reduce to the levels predicted by the theorem. An interesting open problem is to understand and quantify this behavior more precisely.

**D. High-Rate MSN Codes for the Binary Dicode Channel**

In this section, we describe MSN codes for the dicode channel with rates  $R = 2/3$ ,  $R = 3/4$ , and  $R = 4/5$  [36], [37], and we compare their performance in AWGN and the complexity of their detector trellises to those of their counterparts among the Wolf-Ungerboeck codes. They all provide a 3-dB increase in free squared-Euclidean

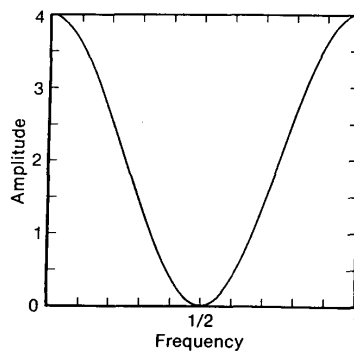


Fig. 22. Frequency response (magnitude) of PR2 channel.

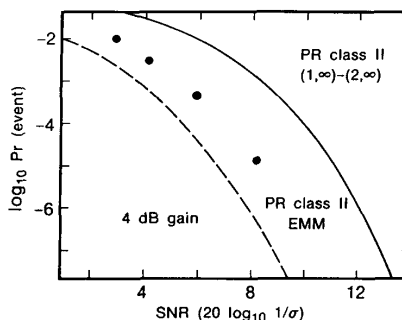


Fig. 23. Performance of EMM-coded PR2 channel.

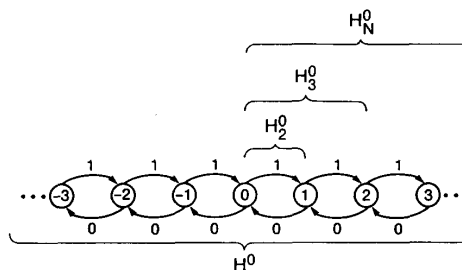


Fig. 24. Subdiagrams of canonical diagram for DC-null.

distance relative to the uncoded, binary dicode channel. The codes were constructed from the subdiagrams with 4, 5, and 7 states, respectively, of the canonical diagram for binary sequences with a spectral null at zero frequency [53], shown in Fig. 24. To simplify the encoder/decoder functions and the detector trellis structures, the MSN codes are implemented as rate 4/6, 6/8, and 8/10 respectively. The encoder for the rate 4/6 code, a finite-state-machine with 3 states, is shown in Table III. The states are denoted by the binary 2-tuple  $s = s_1s_2$ . The input words are the binary 4-tuples  $\mathbf{b} = b_1b_2b_3b_4$ . For a given encoder state  $s$  and input word  $\mathbf{b}$ , the encoder output is a 6-bit codeword  $\mathbf{c} = c_1c_2c_3c_4c_5c_6$  with next state  $\mathbf{t} = t_1t_2$ . The table entry in column  $s$  and row  $\mathbf{b}$

lossless of finite order can be viewed as "deterministic with bounded delay."

Fig. 2. Example for bound of Theorem 5.

TABLE III  
ENCODER FOR RATE 4/6 DC-FREE MSN CODE

Data $s_1s_2$ Data $b_1b_2b_3b_4$	00	10	11
0000	101011/10	001010/00	010110/10
0001	101101/10	001100/00	011001/10
0010	101110/10	010010/00	011010/10
0011	110011/10	010100/00	100011/10
0100	110101/10	011000/00	100101/10
0101	110110/10	100010/00	100110/10
0110	111001/10	100100/00	101001/10
0111	111010/10	101000/00	101010/10
1000	101011/11	001011/10	010110/11
1001	101101/11	001101/10	011001/11
1010	101110/11	001110/10	011010/11
1011	110011/11	010011/10	100011/11
1100	110101/11	001011/11	100101/11
1101	110110/11	001101/11	100110/11
1110	111001/11	001110/11	101001/11
1111	111010/11	010011/11	010101/10

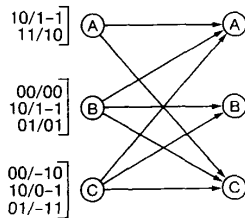


Fig. 25. Trellis for rate 4/6 MSN code on dicode channel.

TABLE IV  
ENCODER FOR RATE 6/8 DC-FREE MSN CODE

$s = 0$	$s = 1$
$A/0$	$\bar{A}/1$
$B/1$	$\bar{B}/0$

List A:

78 71 72 B4 74 B2 B1 B8 5C AC 9C 6C  
C6 C9 CA C5 D8 D1 D2 E4 D4 E2 E1 E8.

List B:

97 9E 9D B9 9B D9 E9 79 A7 AE AD BA  
AB DA EA 7A B3 D3 E3 73 C7 CE CD CB  
57 5E 5D B5 5B D5 E5 75 67 6E 6D B6  
6B D6 E6 76.

represents the output and next state in the form  $c/t$ . The maximum runlength of zero output symbols of the coded system is 2, as is easily seen from the canonical diagram. The reduced-complexity detector trellis for the MSN-coded dicode channel is based upon the second power of the same canonical diagram, and is shown in Fig. 25.

The two-state encoder for the rate 6/8 code is shown schematically in Table IV. For each of the encoder states, represented by the single bit  $s$ , the corresponding column in the table represents the 64 codewords, broken into two subsets of size 24 and 40, and the next state  $t$ . The 24 codewords in set  $A$  and the 40 codewords in set  $B$  are shown in the table. Each 8-bit codeword is described by a pair of hexadecimal symbols. The sets  $\bar{A}$  and  $\bar{B}$  are obtained by bit-wise complementation of the codewords

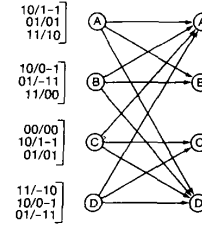


Fig. 26. Trellis for rate 6/8 MSN code on dicode channel.

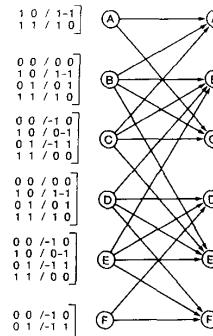


Fig. 27. Trellis for rate 8/10 MSN code on dicode channel.

in sets  $A$  and  $B$ , respectively. Any two maps  $f_1$  and  $f_2$  that assign the 64 data words to the 64 codewords in each column

$$f_1: \{0, 1\}^6 \rightarrow A \cup B,$$

and

$$f_2: \{0, 1\}^6 \rightarrow \bar{A} \cup \bar{B},$$

complete the definition of the encoder. If the maps assign to each codeword and its complement the same data word, the code will be invariant with respect to inversion of the coded dicode channel outputs. The decoder is a block decoder, implementable as a table look-up. The maximum runlength of zero output symbols of the coded system is 3. The reduced-complexity detector trellis for this system is shown in Fig. 26.

An example of a rate 8/10 code with a four-state encoder and block decoder is described in [37]. The maximum zero-runlength at the coded channel output is 5. The reduced-complexity detector trellis for the MSN-coded dicode channel based upon the rate 8/10 code is shown in Fig. 27.

*Remark:* A rate 4/5 MSN code can be derived from the canonical subdiagram with only 6 states, since the diagram has Shannon capacity  $C \approx 0.83$ . However, the complexity of the resulting encoder finite-state-machine would likely be much larger, and the detector trellis would lose some potentially attractive symmetry properties, when compared to a code derived from the 7-state diagram.

We now compare the MSN codes just presented to their counterparts among the Wolf-Ungerboeck codes.

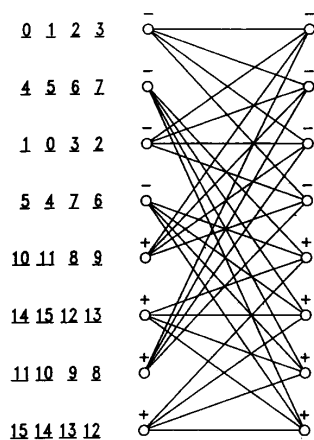


Fig. 28. Trellis for rate 2/3 Wolf-Ungerboeck code on dicode channel.

TABLE V  
EDGE-LABELS FOR WOLF-UNGERBOECK RATE 2/3

- to -		+ to -	
0	0 1 $\bar{1}$	8	0 $\bar{1}$ 0
1	0 0 0	9	0 0 $\bar{1}$
2	1 0 $\bar{1}$	10	$\bar{1}$ 0 0
3	1 $\bar{1}$ 0	11	$\bar{1}$ 1 $\bar{1}$
- to +		+ to +	
4	0 1 0	12	0 $\bar{1}$ 1
5	0 0 1	13	0 0 0
6	1 0 0	14	$\bar{1}$ 0 1
7	1 $\bar{1}$ 1	15	$\bar{1}$ 1 0

From the tables in [66], we selected the codes with the same rates and asymptotic coding gains as the MSN codes just described.

For the rate 2/3 code, the generator matrix is

$$G(D) = \begin{bmatrix} 1 & 1+D & D \\ D & 1 & 1 \end{bmatrix}$$

We inverted the third symbol in each codeword, thereby limiting the maximum zero-runlength at the dicode channel output to 9, as predicted by Lemma 4 of [66]. The trellis structure underlying the encoder/decoder and maximum-likelihood detector is shown in Fig. 28, with edge labels described in Table V.

*Remark:* In Tables V, VI and VII, the symbol  $\bar{1}$  is used to denote -1.

For the rate 3/4 code, the generator matrix is

$$G(D) = \begin{bmatrix} 1 & 1 & 1 & 1 \\ 1 & D & 0 & 1 \\ D & 0 & 1 & 1 \end{bmatrix}$$

Inverting the fourth symbol in each codeword limits the maximum zero-runlength at the dicode channel output to 12 [66]. The trellis structure underlying the encoder/decoder and maximum-likelihood detector is shown in

TABLE VI  
EDGE-LABELS FOR WOLF-UNGERBOECK RATE 3/4

- to -		+ to -	
0	{ 0000 1 $\bar{1}$ 11	8	{ 000 $\bar{1}$ 1 $\bar{1}$ 10
1	{ 010 $\bar{1}$ 10 $\bar{1}$ 0	9	{ 00 $\bar{1}$ 0 1 $\bar{1}$ 0 $\bar{1}$
2	{ 01 $\bar{1}$ 0 100 $\bar{1}$	10	{ 0 $\bar{1}$ 00 10 $\bar{1}$ 1
3	{ 001 $\bar{1}$ 1 $\bar{1}$ 00	11	{ 0 $\bar{1}$ 1 $\bar{1}$ 1000
- to +		+ to +	
4	{ 0001 1 $\bar{1}$ 10	12	{ 0000 1 $\bar{1}$ 11
5	{ 0010 1 $\bar{1}$ 01	13	{ 0 $\bar{1}$ 01 1010
6	{ 0100 10 $\bar{1}$ 1	14	{ 0 $\bar{1}$ 10 1001
7	{ 01 $\bar{1}$ 1 1000	15	{ 00 $\bar{1}$ 1 1 $\bar{1}$ 00

TABLE VII  
EDGE-LABELS FOR WOLF-UNGERBOECK RATE 4/5

- to -		+ to -		- to +		+ to +	
0	{ 10 $\bar{1}$ 00 1 $\bar{1}$ 01 $\bar{1}$	16	{ 00 $\bar{1}$ 00 0 $\bar{1}$ 01 $\bar{1}$	8	{ 00100 0101 $\bar{1}$	24	{ $\bar{1}$ 0100 1 $\bar{1}$ 0 $\bar{1}$ 1
1	{ 1 $\bar{1}$ 1 $\bar{1}$ 0 1000 $\bar{1}$	17	{ 0 $\bar{1}$ 1 $\bar{1}$ 0 0000 $\bar{1}$	9	{ 01110 00001	25	{ 1 $\bar{1}$ 110 10001
2	{ 01 $\bar{1}$ 00 0001 $\bar{1}$	18	{ 1 $\bar{1}$ 100 1001 $\bar{1}$	10	{ 1 $\bar{1}$ 100 10011	26	{ 0 $\bar{1}$ 100 00011
3	{ 001 $\bar{1}$ 0 0100 $\bar{1}$	19	{ 101 $\bar{1}$ 0 1100 $\bar{1}$	11	{ 10 $\bar{1}$ 10 1 $\bar{1}$ 001	27	{ 00 $\bar{1}$ 10 0 $\bar{1}$ 001
4	{ 0010 $\bar{1}$ 01010	20	{ 1010 $\bar{1}$ 11010	12	{ 10 $\bar{1}$ 01 11010	28	{ 00 $\bar{1}$ 01 0 $\bar{1}$ 010
5	{ 01 $\bar{1}$ 1 $\bar{1}$ 00000	21	{ 1 $\bar{1}$ 11 $\bar{1}$ 10000	13	{ 1 $\bar{1}$ 111 10000	29	{ 0 $\bar{1}$ 111 00000
6	{ 1 $\bar{1}$ 10 $\bar{1}$ 10010	22	{ 0 $\bar{1}$ 10 $\bar{1}$ 00010	14	{ 01 $\bar{1}$ 01 00010	30	{ 1 $\bar{1}$ 101 10010
7	{ 10 $\bar{1}$ 1 $\bar{1}$ 1 $\bar{1}$ 000	23	{ 00 $\bar{1}$ 1 $\bar{1}$ 0 $\bar{1}$ 000	15	{ 00111 01000	31	{ 10111 11000

Fig. 29, with edge labels described in Table VI, the binary equivalent of Table II in [66].

Finally, for the rate 4/5 code, the generator matrix is

$$G(D) = \begin{bmatrix} 1+D & 0 & 0 & 0 & 1 \\ 1 & 1+D & 0 & 0 & D \\ 0 & 1 & 1 & 1 & 1 \\ 0 & 1 & 0 & 1+D & D \end{bmatrix}$$

Inverting the third symbol in each codeword limits the maximum zero-runlength at the dicode channel output to 22 [66]. The trellis structure underlying the encoder/decoder and maximum-likelihood detector is shown in Fig. 30, and the edge labels are defined in Table VII.

Computer-simulated performance results (assuming additive, white, gaussian noise) for the rate 3/4 and rate 4/5 MSN-coded dicode channels as well as their Wolf-Ungerboeck counterparts are shown in Figs. 31 and

lossless of finite order can be viewed as "deterministic with bounded delay."

Fig. 2. Example for bound of Theorem 5.

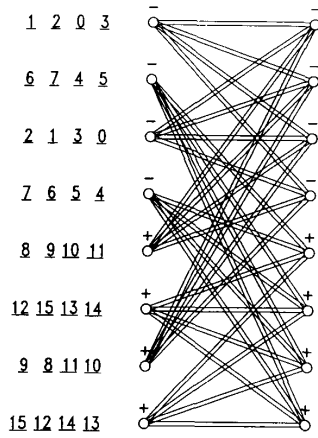


Fig. 29. Trellis for rate 3/4 Wolf-Ungerboeck code on dicode channel.

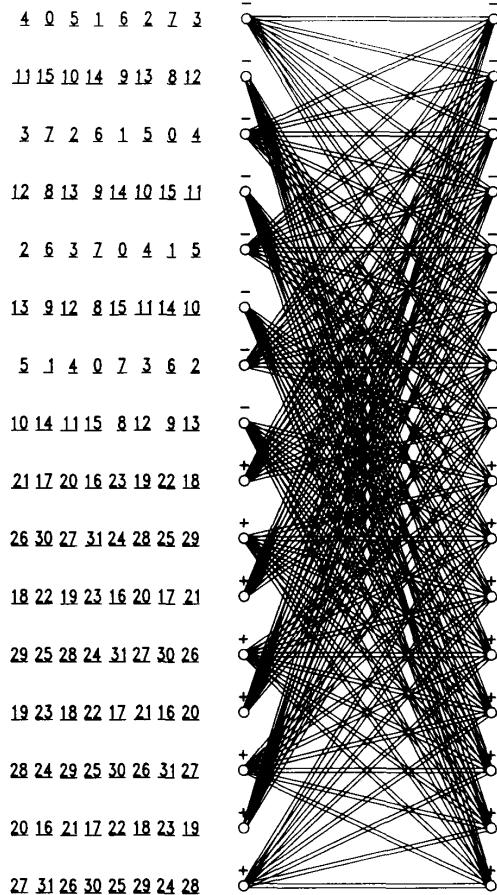


Fig. 30. Trellis for rate 4/5 Wolf-Ungerboeck code on dicode channel.

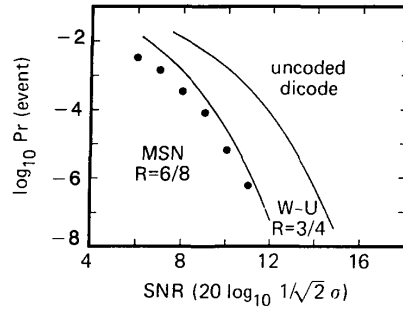


Fig. 31. Performance of rate 3/4 MSN code on dicode channel.

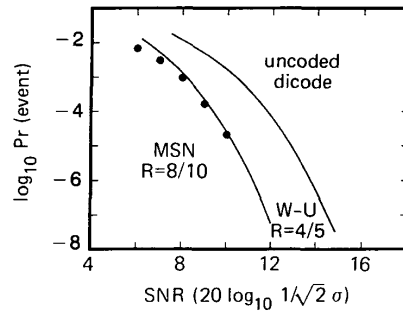


Fig. 32. Performance of rate 4/5 MSN code on dicode channel.

32. In all cases, the path memory was taken long enough to eliminate any performance degradation due to truncation effects (see Section VI). The plots confirm that, at moderate-to-high signal-to-noise-ratios, the reduced-complexity detectors for the MSN codes achieve the same coding gain as would be expected from a maximum-likelihood detector for the MSN-coded dicode channel, and the performance of the MSN codes equals, or better, that of the corresponding precoded convolutional codes.

Although we will make no attempt to rigorously compare the encoder/decoder and detector trellis complexity of MSN codes to that of other codes proposed for partial-response channels, these examples indicate that, at least in some cases, the MSN codes may offer some advantages in terms of implementation. Some issues related to the VLSI implementation of an exploratory MSN code for the dicode channel are addressed by Shung *et al.* in [61]–[63].

*Remarks:* The techniques described in this paper have also been applied to develop new matched-spectral-null trellis codes for data transmission. In that setting, multi-level codes with higher order spectral nulls at zero frequency and at  $f = 1/2T$  have been investigated. Multi-level matched-spectral-null codes for the dicode channel have been developed by Haeb [18], as well as Eleftheriou and Cideciyan [10]–[12]. These codes also incorporate additional constraints to reduce the average power of their codes and improve the coding gain. Some more powerful codes, developed using other *ad hoc* methods,

are treated in [18]. As observed in [10], [18], however, the multilevel codes seem best suited to channels where bandwidth expansion is permitted or the number of signal levels is restricted.

The theory of matched-spectral-null coding also suggests the potential applicability of previously reported binary and multilevel spectral null codes that were developed in a different context, although the issue of quasi-catastrophic error-propagation was not addressed in their design. Notable among these are the codes found by Imminck [23], Imminck and Beenker [25], Monti and Pierobon [55], and Calderbank and Mazo [6].

It should be noted that coset-coding methods have been extended to multilevel partial response channels by Forney and Calderbank [14], Calderbank and Mazo [6], and Kasturia *et al.* [39].

### III. CHARACTERIZATION OF SEQUENCES WITH AN ORDER- $K$ SPECTRAL NULL

In this section, we characterize multilevel sequences, representable as a finite-memory function of a finite-state Markov chain, that have an order- $K$  spectral null at zero frequency or at a nonzero rational submultiple of the symbol frequency. Canonical diagrams for these sequences are also derived.

#### A. Equivalent Conditions for Order- $K$ Spectral Null

We develop several equivalent, necessary and sufficient conditions for an ensemble of sequences over an integer alphabet to have an order- $K$  spectral null at zero frequency or, more generally, at a rational submultiple of the symbol frequency, meaning that the power spectrum and its derivatives through order  $2K - 1$  vanish at the specified frequency. We denote the spectral null frequency by  $f = M/NT$ , where the symbol frequency is  $1/T$ , and  $M, N$  are relatively prime integers. The corresponding complex frequency is  $\omega = e^{-i2\pi M/N}$  with complex conjugate  $\bar{\omega}$ . The case  $f = 0$  corresponds to  $M = 0, N = 1$ .

Throughout this section, we will make use of results, proof techniques, and terminology of [53], [55], [59]. We begin with a few definitions.

Let  $G$  be an irreducible finite-state-transition-diagram (FSTD) with associated Markov chain  $\Gamma$ .

**Definition 1:**  $(G, \Gamma)$  is said to have an *order- $K$  spectral-density null* at  $f$  if the power spectral-density  $\Phi(f)$  satisfies

$$\Phi^{(k)}(f) = 0, \quad k = 0, \dots, 2K - 1,$$

where  $\Phi^{(k)}(f)$  denotes the  $k$ th derivative of  $\Phi(f)$ . If, in addition, there is no discrete spectral line at  $f$ , we say that the system has an *order- $K$  spectral null* at  $f$ .

**Definition 2:** Let  $x = x_0, \dots, x_n$  be a sequence generated by  $G$ . The *order- $k$  running-digital-sum* at  $f = M/NT$ ,

denoted  $\text{RDS}_f^{(k)}(x)$ , is defined by the recursion

$$\text{RDS}_f^{(1)}(x) = \sum_{i=0}^n \omega^i x_i,$$

$$\text{RDS}_f^{(k)}(x) = \sum_{i=0}^n \text{RDS}_f^{(k-1)}(x_0, \dots, x_i), \quad k > 1.$$

**Definition 3:** The finite-state transition diagram  $G$  satisfies an *order- $K$  coboundary condition* at  $f = M/NT$  if there is a family of functions

$$\phi_k: \mathcal{S} \rightarrow \mathbb{C}, \quad k = 1, \dots, K$$

from the state set  $\mathcal{S}$  of  $G$  to the complex numbers  $\mathbb{C}$  such that, for an edge from state  $\sigma$  to  $\tau$  with label  $x$ , the following conditions hold:

$$x = \omega \phi_1(\tau) - \phi_1(\sigma)$$

$$\phi_k(\sigma) = \omega \phi_{k+1}(\tau) - \phi_{k+1}(\sigma), \quad k = 1, \dots, K - 1.$$

Several necessary and sufficient conditions for a first-order ( $K = 1$ ) null at  $f = M/NT$  were first proved by Yoshida [69]. Pierobon [59] rediscovered these conditions for  $f = 0$ . Marcus and Siegel [53], extending the results in [59] to  $f = M/NT$ , rediscovered the conditions in [69], and introduced the concept of a coboundary condition at  $f$  and the related idea of a canonical diagram for spectral null sequences.

Monti and Pierobon [55] then found a necessary and sufficient condition for a spectral null of order  $K$  at  $f = 0$ , and they developed several equivalent characterizations along the lines of those in [53] for the special case  $K = 2$ , motivated by an earlier investigation of so-called  $DC^2$  codes by Imminck [23]. Theorem 1 extends their results, characterizing sequences with order- $K$  spectral null at frequency  $f = M/NT$ . The equivalent, necessary and sufficient conditions are modeled after those in [55] and, as indicated in [31], their derivation involves a fairly straightforward application of the proof techniques employed in [53] and [55]. A similar extension is described in [10], [11].

**Theorem 1:** Let  $(G, \Gamma)$  be as previously stated. The following are equivalent.

- 1)  $(G, \Gamma)$  has an order- $K$  spectral null at  $f = M/NT$ .
- 2)  $G$  satisfies an order- $K$  coboundary condition at  $f$ .
- 3) There exists a family of functions

$$\phi_k: \mathcal{S} \rightarrow \mathbb{C}, \quad k = 1, \dots, K$$

from the state set  $\mathcal{S}$  of  $G$  to the complex numbers  $\mathbb{C}$  such that for every sequence  $x = x_0, \dots, x_n$  generated by a path with state sequence  $\{s_0, s_1, \dots, s_n, s_{n+1}\}$ , the order- $k$  running-digital-sums at  $f$  satisfy

$$\text{RDS}_f^{(k)}(x)$$

$$= \omega^{n+1} \sum_{i=1}^k \left[ \binom{k-1}{k-i} \phi_i(s_{n+1}) - \binom{n+k}{k-i} \phi_i(s_0) \right],$$

for  $k = 1, \dots, K$ . (For  $k = 1$ , the binomial coefficients are taken to be 1).

- 4) There exists a family of functions

$$\phi_k: \mathcal{S} \rightarrow \mathbb{C}, \quad k = 1, \dots, K - 1$$

lossless of finite order can be viewed as "deterministic with bounded delay."

Fig. 2. Example for bound of Theorem 5.

from the state set  $\mathcal{S}$  of  $G$  to the complex numbers  $\mathbb{C}$  such that for every sequence  $\mathbf{x} = x_0, \dots, x_n$  generated by a cycle  $\{s_0, s_1, \dots, s_n, s_{n+1} = s_0\}$  in  $G$  of length a multiple of  $N$ , the order- $k$  running-digital-sums at  $f$  satisfy

$$\text{RDS}_f^{(k)}(\mathbf{x}) = \sum_{i=1}^{k-1} \left[ \binom{k-1}{k-i} - \binom{n+k}{k-i} \right] \phi_i(s_0),$$

for  $k = 1, \dots, K$ . (For  $k = 1$  the sum on the right is interpreted to be 0).

*Proof:* We will prove that 1)  $\Leftrightarrow$  2) and 2)  $\Rightarrow$  3)  $\Rightarrow$  4)  $\Rightarrow$  2).

- 1)  $\Leftrightarrow$  2): For  $f = 0$ , this was proved in [55]. Plugging  $z = e^{-i2\pi M/NT}$  into the power spectral density expressions in [55] gives the general case.
- 2)  $\Rightarrow$  3): This follows from a straightforward calculation.
- 3)  $\Rightarrow$  4): This follows immediately by substituting  $s_{n+1} = s_0$  and  $w^{n+1} = 1$  into 3).
- 4)  $\Rightarrow$  2): For  $f = 0$ , the consistent definition of the functions  $\phi_1, \dots, \phi_K$  is a straightforward extension of the argument in [55]. For  $f = M/NT$ , one must consider two cases, as was done for the  $K = 1$  case [53], corresponding to the possible cycle lengths in  $G$ .

*Case 1:* All cycle lengths are a multiple of  $N$ .

The proof closely follows the lines of the proof for  $f = 0$ .

*Case 2:* Some cycle has length not a multiple of  $N$ .

As in [53], we define, for each state  $\sigma$ , the quantities

$$\phi_1(\sigma) = \frac{\sum_{i=0}^q \omega^i a_i}{\omega^{q+1} - 1},$$

$$\phi_k(\sigma) = \frac{\sum_{i=1}^{q+1} \omega^i \phi_{k-1}(s_i)}{\omega^{q+1} - 1}, \quad k = 2, \dots, K,$$

where  $\{\sigma = s_0, \dots, s_{q+1} = \sigma\}$  is a cycle in  $G$  of length not a multiple of  $N$ , corresponding to the sequence  $a_0, \dots, a_q$ . The proof that the functions are well-defined and the verification of the order- $K$  coboundary condition are routine extensions of the arguments in [53].  $\square$

Before stating a generalization of Theorem 1, we formally define the notion of a *difference sequence*.

*Definition 4:* Let  $\mathbf{x} = x_0, \dots, x_n$  and  $\mathbf{y} = y_0, \dots, y_n$  be sequences which are generated by paths in  $G$  starting at the same state  $\sigma$ . Define the *difference sequence*  $\mathbf{e}$  by

$$e_i = x_i - y_i, \quad i = 0, \dots, n.$$

If the paths also end in the same state  $\tau$ , we call  $\mathbf{e}$  a *difference event*. If, in addition, the end state  $\tau$  coincides with  $\sigma$ , we call  $\mathbf{e}$  a *difference cycle*.

We refer to the polynomial

$$e(D) = \sum_{i=0}^n e_i D^i$$

as the *difference polynomial* corresponding to  $\mathbf{e}$ .

Theorem 2 gives an alternative characterization of sequences with higher order spectral null at  $f = M/NT$ . The equivalent conditions bear a very close resemblance to the characterization of first-order spectral null sequences in [53], the chief distinction being that the generalization to higher order spectral null is most naturally expressed in terms of difference sequences.

*Theorem 2:* Let  $(G, \Gamma)$  be as previously stated. Assume  $G$  generates at least one cycle  $\mathbf{c}$  of length a multiple of  $N$  with vanishing first-order running-digital-sum at  $f$ ; that is,  $\text{RDS}_f^{(1)}(\mathbf{c}) = 0$ . Then, the following are equivalent.

- 1)  $(G, \Gamma)$  has an order- $K$  spectral null at  $f$ .
- 2)  $G$  satisfies an order- $K$  coboundary condition at  $f$ .
- 3) For any difference sequence  $\mathbf{e}$  generated by  $G$ , the order- $k$  running-digital-sums at  $f$ ,  $\text{RDS}_f^{(k)}(\mathbf{e})$ , for  $k = 1, \dots, K$ , lie in a finite range of values, independent of  $\mathbf{e}$  and its length.
- 4) For every difference cycle  $\mathbf{e}$  in  $G$  of length a multiple of  $N$ , the order- $k$  running-digital-sums at  $f$  vanish, for  $k = 1, \dots, K$ . That is,

$$\text{RDS}_f^{(k)}(\mathbf{e}) = 0, \quad k = 1, \dots, K.$$

*Proof:* We will again prove that 1)  $\Leftrightarrow$  2) and 2)  $\Rightarrow$  3)  $\Rightarrow$  4)  $\Rightarrow$  2).

1)  $\Leftrightarrow$  2): The same as in Theorem 1.

2)  $\Rightarrow$  3): This follows from the corresponding proof in Theorem 1. For a difference sequence, the expression in Theorem 1, Part 3) reduces to the form

$$\text{RDS}_f^{(k)}(\mathbf{e}) = \omega^{n+1} \sum_{i=1}^k \binom{k-1}{k-i} [\phi_i(s_{n+1}) - \phi_i(t_{n+1})],$$

which takes values in a finite range, independent of  $\mathbf{e}$  and its length  $n+1$ .

3)  $\Rightarrow$  4): This follows from the corresponding proof in Theorem 1. The expression for the order- $k$  RDS in Theorem 1, Part 4), depends only on the initial state  $s_0$  and therefore vanishes for a difference sequence.

4)  $\Rightarrow$  2): As in Theorem 1, we must consider two cases corresponding to the possible cycle lengths in  $G$ . In each case we will define the boundary functions inductively.

*Case 1:* All cycle lengths are a multiple of  $N$ .

The inductive hypothesis at step  $k+1$  is that the boundary functions  $\phi_l$ ,  $l = 1, \dots, k$  have been defined, and, in particular, the following three conditions apply.

- a) The formula for  $\text{RDS}_f^{(k)}$  in Theorem 1, Part 3), holds.

b) For any cycle  $\{\sigma = s_0, \dots, s_{q+1} = \sigma\}$  in  $G$

$$\sum_{i=0}^q \omega^i \phi_l(s_i) = 0, \quad l = 1, \dots, k-1.$$

c) There is a degree of freedom in the definition of  $\phi_k$ . (That is,  $\phi_k$  is determined up to an additive constant).

Let  $\sigma$  be a state in  $G$ , and let  $s = \{\sigma = s_0, \dots, s_{q+1} = \sigma\}$  and  $t = \{\sigma = t_0, \dots, t_{r+1} = \sigma\}$  be any two cycles at  $\sigma$ . Now, Part 4) states that  $\text{RDS}_f^{(k+1)}(e) = 0$  for any difference cycle in  $G$ . Using the relation

$$\text{RDS}_f^{(k+1)}(x_0, \dots, x_n) = \sum_{i=0}^n \text{RDS}_f^{(k)}(x_0, \dots, x_i),$$

along with the inductively assumed Conditions a) and b), we find after some calculation that there is a constant  $\alpha_k$  such that

$$\frac{\sum_{i=0}^q \omega^i \phi_k(s_i)}{q+1} = \frac{\sum_{i=0}^r \omega^i \phi_k(t_i)}{r+1} = \alpha_k.$$

Applying the condition c), it is not too difficult to see that we can define  $\phi_k(\sigma)$  so as to ensure that the constant satisfies  $\alpha_k = 0$ . We now define the function  $\phi_{k+1}$  by setting  $\phi_{k+1}(\sigma) = 0$ , and pushing the definition along in the obvious manner, as in [53]. One can then verify that the definition is consistent, and therefore the three conditions above are extended to  $\phi_{k+1}$ .

It remains to establish the primary case  $k=1$  of the induction. Let the state  $\sigma$  lie on the cycle  $c$  in the statement of the theorem. By Part 4),  $\text{RDS}_f^{(1)}(e) = 0$  for all difference cycles. Arguing as before, we find that there is a constant  $\alpha_1$  such that

$$\frac{\sum_{i=0}^q \omega^i a_i}{q+1} = \alpha_1,$$

for every cycle at  $\sigma$ . In particular, because of the assumption about  $c$ , we know that  $\alpha_1 = 0$ . The definition of the coboundary function  $\phi_1$  and the completion of the primary case follows from Theorem 1.

Case 2: Some cycle has length not a multiple of  $N$ .

Here, the inductive hypothesis at step  $k+1$  is that the coboundary functions  $\phi_l$ ,  $l = 1, \dots, k$  have been defined, and the following two conditions apply.

a) The formula for  $\text{RDS}_f^{(k)}$  in Theorem 1, Part 3), holds.

b) For any state  $\sigma$  in  $G$  and cycle  $\{\sigma = s_0, \dots, s_{q+1} = \sigma\}$  with length not a multiple of  $N$ ,

$$\phi_l(\sigma) = \frac{\sum_{i=0}^q \omega^i \phi_{l-1}(s_i)}{\omega^{q+1} - 1}, \quad l = 2, \dots, k.$$

(Note that, in this case, there is no degree of freedom in the definition of  $\phi_k$ ). From Part 4), we have

$\text{RDS}_f^{(k+1)}(e) = 0$  for any difference cycle in  $G$ . We use the Conditions a) and b) to conclude that for any two cycles  $s$  and  $t$  at  $\sigma$  of lengths  $q+1$  and  $r+1$  not a multiple of  $N$ ,

$$\frac{\sum_{i=0}^q \omega^i \phi_k(s_i)}{\omega^{q+1} - 1} = \frac{\sum_{i=0}^r \omega^i \phi_k(t_i)}{\omega^{r+1} - 1} = \beta,$$

for some constant  $\beta$ . Defining

$$\phi_{k+1}(\sigma) = \frac{\sum_{i=0}^q \omega^i \phi_k(s_i)}{\omega^{q+1} - 1},$$

we can easily verify that the inductive conditions extend to  $k+1$ .

The primary case is essentially the same argument as in [53]. We also note that the additional assumption in the statement of the theorem, namely the existence of a cycle in  $G$  with vanishing first-order running-digital-sum, is unnecessary in this case.  $\square$

*Remark:* If the assumption about the existence of a cycle with vanishing first-order running-digital-sum is omitted, we can obtain a similar set of equivalent conditions for sequences with a higher order *spectral-density* null at  $f$ . Parts 3) and 4) remain unchanged, but in Part 2), the first-order coboundary condition must be replaced by a *biased coboundary condition*, as developed by Kamabe [27], when  $G$  has period a multiple of  $N$ . Details are left to the reader.

*Remark:* Following an observation in [55], there is an interesting interpretation of the equivalence  $1) \Leftrightarrow 2)$  in Theorems 1 and 2: The sequences generated by  $G$  have an order- $K$  spectral null at  $f$  if and only if the sequences can be obtained by a cascade of  $K$  discrete-time filters, with overall transfer-polynomial  $(1 - \bar{\omega}D)^K$ , applied to an appropriate Moore-machine based upon  $G$ . For  $K \geq 2$ , an alternative proof of the "only if" direction of this equivalence  $1) \Rightarrow 2)$  can be obtained by iteratively applying the corresponding result for  $K=1$ , which follows from the  $D$ -transform representation of the first-order coboundary conditions in [53]. This observation was first pointed out to the authors by C. Heegard [20]. A proof based upon a similar approach also appears in [10].

We now define the order- $k$  power-sums (or, moments) at frequency  $f = M/NT$  of a sequence. These will play an important role in the investigation of distance properties of spectral null codes in Section IV.

*Definition 5:* Let  $x = x_0, \dots, x_n$  be a sequence generated by  $G$ . The *order- $k$  power-sum (or moment)* at  $f = M/NT$ , denoted  $M_f^{(k)}(x)$ , is defined by

$$M_f^{(k)}(x) = \sum_{i=0}^n i^k \omega^i x_i.$$

The following lemma shows that the order- $K$  running-digital-sum at  $f$  can be expressed in terms of the order- $k$  moments at  $f$ , for  $k = 0, \dots, K-1$ .

*Lemma 1:* Let  $x = x_0, \dots, x_{n-1}$  be a sequence of complex numbers. Let  $\omega$  be the primitive, complex  $N$ th root

of unity corresponding to frequency  $f = M/NT$ ,  $\omega = e^{-i2\pi M/N}$ .

Then, for each  $k \geq 1$

$$\text{RDS}_f^{(k)}(\mathbf{x}) = \sum_{j=0}^{k-1} g_j^{(k)}(n) M_f^{(j)}(\mathbf{x}),$$

where

$$g_j^{(k)}(n) = \sum_{l=0}^{k-j-1} g_{j,l}^{(k)} n^l.$$

*Proof:* The proof proceeds by induction. For  $k=1$ , the relation is obvious. Assuming the relation holds for  $k$ , we now extend it to  $k+1$ . The relation follows naturally from the recursive definition of  $\text{RDS}_f^{(k+1)}(x_0, \dots, x_n)$  in Definition 2. Substituting the inductively assumed expression for  $\text{RDS}_f^{(k)}(x_0, \dots, x_i)$  and rearranging the orders of summation, we see that it suffices to show that, for  $0 \leq l \leq k-j-1$ ,

$$\sum_{i=0}^n i^l M_f^{(j)}(x_0, \dots, x_i) = \sum_{m=j}^k f_{l,m}^{(j)}(n) M_f^{(m)}(x_0, \dots, x_n),$$

where  $f_{l,m}^{(j)}(n)$  is a polynomial in  $n$  of degree no larger than  $k+1-m$ . This follows, after some calculation, from the well-known fact that there is a polynomial  $q_l(n)$  of degree  $l+1$  such that

$$q_l(n) = \sum_{r=1}^n r^l,$$

a simple consequence of Euler's summation formula (see, for example Knuth [40, p. 112]).  $\square$

*Example 1:* For  $k=1, 2, 3$  the identities in Lemma 1 are:

$$\begin{aligned} \text{RDS}_f^{(1)}(\mathbf{x}) &= M_f^{(0)}(\mathbf{x}) \\ \text{RDS}_f^{(2)}(\mathbf{x}) &= (n+2)M_f^{(0)}(\mathbf{x}) - M_f^{(1)}(\mathbf{x}) \\ \text{RDS}_f^{(3)}(\mathbf{x}) &= \frac{1}{2}(n^2+5n+6)M_f^{(0)}(\mathbf{x}) \\ &\quad - \frac{1}{2}(2n+5)M_f^{(1)}(\mathbf{x}) + \frac{1}{2}M_f^{(2)}(\mathbf{x}). \end{aligned}$$

*Lemma 2:* The coefficient  $g_{k-1}^{(k)}(n)$  of  $M_f^{(k-1)}(\mathbf{x})$  in the expression for  $\text{RDS}_f^{(k)}(\mathbf{x})$  is given by

$$g_{k-1}^{(k)}(n) = \frac{(-1)^{k-1}}{(k-1)!}.$$

*Proof:* The coefficient in question is independent of  $f$  as well as the sequence  $\mathbf{x}$ , so it suffices to compute its value for  $f=0$  and any sequence  $\mathbf{y}$  whose order- $(k-1)$  moment is nonzero. We will use as the sequence the coefficients of the polynomial  $y(D) = (1-D)^{k-1}$ , and the result will follow from a few general observations (of some independent interest) about running-digital-sums and power-sums. Let  $x(D)$  be the  $D$ -transform of a

sequence  $\mathbf{x} = x_0, \dots, x_n$ . It is easy to check that the series

$$R^{(k)}(D) = \frac{x(D)}{(1-D)^k}$$

is a generating function for the partial order- $k$  running-digital-sums at  $f=0$ , meaning that the coefficient of  $D^i$ ,  $i=0, \dots, n$  is precisely  $\text{RDS}_0^{(k)}(x_0, \dots, x_i)$ . In particular, for  $y(D) = (1-D)^{k-1}$  we see that

$$\text{RDS}_0^{(j)}(\mathbf{y}) = 0, \quad j=1, \dots, k-1,$$

$$\text{RDS}_0^{(k)}(\mathbf{y}) = 1.$$

Turning to the power-sums, we define the polynomial

$$P^{(j)}(\mathbf{x}, D) = \sum_{i=0}^n i^j x_i D^i,$$

having the property that

$$M_0^{(j)}(\mathbf{x}) = P^{(j)}(\mathbf{x}, 1).$$

For  $j \geq 0$ , it is easy to see that

$$P^{(j+1)}(\mathbf{x}, D) = D[P^{(j)}(\mathbf{x}, D)]',$$

where  $[P^{(j)}(\mathbf{x}, D)]'$  is the formal derivative of  $P^{(j)}(\mathbf{x}, D)$  with respect to  $D$ . In particular, for  $y(D) = (1-D)^{k-1}$  we find that

$$M_0^{(j)}(\mathbf{y}) = 0, \quad j=0, \dots, k-2,$$

$$M_0^{(k-1)}(\mathbf{y}) = (-1)^{k-1}(k-1)!,$$

from which the desired result immediately follows.

The following useful fact is a direct consequence of Lemmas 1 and 2.

*Proposition 1:* Let  $\mathbf{x}$  be a sequence. Then, the order- $k$  running-digital-sums at  $f$ ,  $\text{RDS}_f^{(k)}(\mathbf{x})$ , for  $k=1, \dots, K$  are all zero if and only if the order- $j$  moments at  $f$ ,  $M_f^{(j)}(\mathbf{x})$ , for  $j=0, \dots, K-1$ , are all zero.

*Remark:* A similar result, found independently, is developed in [10]. The proof makes use of a nice combinatorial formula for the order- $K$  running-digital-sum:

$$\text{RDS}_f^{(k)}(x_0, \dots, x_n) = \sum_{i=0}^n \binom{n+k-1-i}{k-1} \omega^i x_i.$$

The formula can be verified by an inductive argument based upon certain identities involving binomial coefficients.

Using Theorem 2 and Proposition 1, we obtain the following useful characterization of spectral null sequences.

*Theorem 3:* Let  $(G, \Gamma)$  be as in Theorem 2. Then,  $G$  generates a spectral-density null of order- $K$  at  $f$  if and only if, for every difference event  $e$ , the order- $k$  moments at  $f$  vanish, for  $k=0, \dots, K-1$ .

*Proof:* By irreducibility of  $G$ , we can extend the paths corresponding to any difference event to generate a difference cycle of length a multiple of  $N$ . Part 4) of Theorem 2 and Proposition 1 show that  $G$  generates an order- $K$  spectral null at  $f$  if and only if, for every difference event, the moments at  $f$  through order  $K-1$  are

zero; that is,

$$M_f^{(k)}(\mathbf{e}) = 0, \quad k = 0, \dots, K-1. \quad \square$$

Theorem 4 will make use of Theorem 3 to describe a difference-polynomial interpretation of the second remark after the proof of Theorem 2 that will be very useful in the investigation of distance properties of spectral null sequences in Section IV.

First, we remind the reader of the following standard definition.

*Definition 6:* The  $N$ th cyclotomic polynomial  $\psi_N(D)$  is the unique monic, integer polynomial with minimum degree having  $\omega_N = e^{-i2\pi/N}$  as a zero,

$$\psi_N(\omega_N) = 0.$$

*Example 2:* For  $N = 1, \dots, 6$  we have:

$$\begin{aligned} \psi_1(D) &= 1 - D \\ \psi_2(D) &= 1 + D \\ \psi_3(D) &= 1 + D + D^2 \\ \psi_4(D) &= 1 + D^2 \\ \psi_5(D) &= 1 + D + D^2 + D^3 + D^4 \\ \psi_6(D) &= 1 - D + D^2. \end{aligned}$$

Since  $\text{gcd}(M, N) = 1$ , it follows that  $\psi_N(D)$  is also the minimum degree, integer polynomial with  $\omega = e^{-i2\pi M/N}$  as a zero, and any polynomial with rational coefficients with  $\omega$  as a zero is divisible over the rationals by  $\psi_N(D)$ .

*Theorem 4:* Let  $(G, \Gamma)$  be as in Theorem 2.

- 1) Assume the symbol alphabet is a subset of the complex numbers. Then,  $(G, \Gamma)$  has an order- $K$  spectral null at  $f = M/NT$  if and only if for every difference event  $\mathbf{e}$ , the difference polynomial  $e(D)$  can be written as

$$e(D) = (1 - \bar{\omega}D)^K u(D),$$

where  $u(D) = \sum_{i=0}^m u_i D^i$  is a polynomial with complex-valued coefficients.

- 2) Assume the alphabet is further restricted to be a subset of the rational numbers  $\mathbb{Q}$ . Then,  $(G, \Gamma)$  has an order- $K$  spectral null at  $f = M/NT$  if and only if for every difference event  $\mathbf{e}$ , the difference polynomial  $e(D)$  can be written as

$$e(D) = [\psi_N(D)]^K u(D),$$

where  $u(D) = \sum_{i=0}^m u_i D^i$  is a polynomial with rational-valued coefficients.

*Proof:* Let  $i^{(k)}$  denote the factorial power of  $i$ , for  $0 \leq k \leq i$ , defined by

$$i^{(k)} = \prod_{j=0}^{k-1} (i-j), \quad 1 \leq k \leq i,$$

and, by convention,

$$i^{(0)} = 1 \text{ and } i^{(k)} = 0, \quad k < 0.$$

Using the Sterling number identity (see, for example,

Knuth [41, p. 282]), we can express  $i^k$  as a linear combination of the factorial powers of order  $k$  or less,

$$i^k = \sum_{j=0}^k a_j i^{(j)}.$$

It follows that the order- $k$  moments of  $\mathbf{e}$  can be written in the form

$$M_f^{(k)}(\mathbf{e}) = \sum_{j=0}^k a_j D^j e^{(j)}(D), \quad \text{evaluated at } D = \omega,$$

where  $e^{(j)}(D)$  is the  $j$ th formal derivative with respect to  $D$  of the difference polynomial  $e(D)$ . A straightforward induction shows that the order- $k$  moments, for  $k = 0, \dots, K-1$ , vanish if and only if  $e^{(j)}(D)$  has a zero at  $D = \omega$  for  $j = 0, \dots, K-1$ . Standard factorization arguments then imply that  $e^{(j)}(D)$  is divisible by  $(1 - \bar{\omega}D)^{K-j}$  in the case of complex-valued symbols, or  $\psi_N(D)^{K-j}$  in the rational-valued case. An application of Theorem 3 completes the proof.  $\square$

In analogy to Lemma 3 of [53], we now characterize algebraically the set of frequencies at which order- $K$  spectral nulls can be achieved simultaneously.

*Proposition 2:* If a finite-state code with rational symbol alphabet has an order- $K$  spectral null at  $f = M/NT$ , where  $\text{gcd}(M, N) = 1$ , then it also has an order- $K$  spectral null at frequencies  $f = M'/NT$  for all  $M'$  satisfying  $\text{gcd}(M', N) = 1$ .

*Proof:* By Theorems 1–3, we know that for any difference event  $\mathbf{e}$ , generated by a cycle of length  $rN$  (that is, a multiple of  $N$ ),

$$M_f^{(k)}(\mathbf{e}) = \sum_{i=0}^n i^k \omega^i e_i = 0, \quad \text{for } k = 0, \dots, K-1.$$

Define  $y_i^{(k)} = i^k e_i$ . Then  $y^{(k)}(D) = \sum_{i=0}^n y_i^{(k)} D^i$  is a polynomial with rational coefficients having  $\omega$  as a zero. It follows that  $y^{(k)}(D)$  is divisible by the cyclotomic polynomial  $\psi_N(D)$ , which has zeros at  $\omega^{M'}$  for positive integers  $M'$  less than, and relatively prime to  $N$ . The proposition then follows from another application of Theorem 3.

Having characterized sequences with an order- $K$  spectral null, we note that if a code with spectral density  $\Phi(f)$  is used on a partial-response channel with transfer function  $H(f)$ , the channel output sequence will have a power spectral density  $\Psi(f)$  given by

$$\Psi(f) = \Phi(f)S(f),$$

where we have defined

$$S(f) = |H(f)|^2.$$

In particular, for frequency  $f_0$ , if

$$\Phi^{(k)}(f_0) = 0, \quad k = 0, \dots, 2K-1$$

lossless of finite order can be viewed as “deterministic with bounded delay.”

Fig. 2. Example for bound of Theorem 5.

and

$$S^{(k)}(f_0) = 0, \quad k = 0, \dots, 2L - 1$$

then,

$$\Psi^{(k)}(f_0) = 0, \quad k = 0, \dots, 2(K + L) - 1.$$

This additivity of the orders of the code spectral nulls and channel spectral nulls will play a role in Section V in the determination of bounds on the coding gain for MSN codes when applied to partial-response channels.

### B. Canonical Diagrams

Using methods introduced in [53] and extended in [55], we define canonical diagrams for higher order spectral null constraints with integer-valued code symbols. These diagrams will provide the finite-state representations of spectral null sequences from which sliding block codes can be derived, as well as reduced-complexity detector trellis structures, as described in Section VI.

**Definition 7:** A countable-state transition diagram (CSTD) is a locally-finite, labeled, directed graph with a countable number of states and edge labels drawn from a finite alphabet.

**Definition 8:** A countable-state transition diagram  $G$  is a period- $p$  canonical diagram for a spectral null constraint if:

- every finite-state transition diagram (FSTD)  $H \subset G$  generates a set of sequences with the prescribed spectral null constraint;
- for any period- $p$  FSTD  $G'$  that produces the specified spectral null constraint, there is a label-preserving graph homomorphism of  $G'$  into  $G$ .

The characterization in Section III-A of FSTD's that generate spectral null constraints of order  $K$  at frequency  $f$  may be used as in [53] and [55] to define a canonical diagram  $G$  for these constraints.

The definition of period- $p$  canonical diagrams for order- $K$  spectral null sequences breaks into two cases. The proof that the diagrams defined are indeed period- $p$  canonical is a relatively straightforward extension of the arguments in [53] and [55] and details are, therefore, omitted.

*Case 1:*  $f = M/NT$  and  $p \equiv 0 \pmod{N}$ .

Note that this case includes  $f = 0$ . The state set  $\mathcal{S}$  is the set of  $K$ -tuples

$$\sigma = [\sigma_1, \dots, \sigma_K] \in Z[\omega]^K.$$

For each state  $\sigma$  and element  $b$  in the alphabet there is an edge with label  $b$  from  $\sigma$  to a state  $\tau = [\tau_1, \dots, \tau_K]$ , where

$$\begin{aligned} \tau_1 &= \bar{\omega}(\sigma_1 + pb) \\ \tau_i &= \bar{\omega}(\sigma_i + p\sigma_{i-1}), \quad i = 2, \dots, K-1 \\ \tau_K &= \bar{\omega}(\sigma_K + \sigma_{K-1}). \end{aligned}$$

It is straightforward to verify that  $G$  satisfies an order- $K$  coboundary condition at  $f$ , using the functions  $\phi_k(\sigma) =$

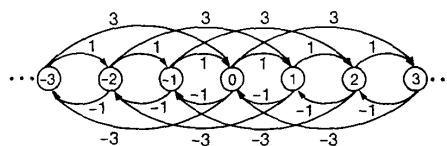


Fig. 33. Canonical diagram for spectral null at 0 (4-AM).

$\sigma_k/p^k$ ,  $k = 1, \dots, K-1$ , and  $\phi_k(\sigma) = \sigma_k/p^{k-1}$ . Moreover, if  $H$  is a period- $p$  FSTD that generates sequences with an order- $K$  spectral null at  $f$ , we can define a label-preserving graph homomorphism from  $H$  to  $G$  in terms of the coboundary functions  $\phi_1, \dots, \phi_K$  on  $H$ . Specifically, the state  $s$  gets mapped to a state in  $G$  according to the rule:

$$s \rightarrow [p\phi_1(s), p^2\phi_2(s), \dots, p^{K-1}\phi_{K-1}(s), p^{K-1}\phi_K(s)].$$

*Remark:* The case corresponding to  $f = 0$ ,  $K = 2$ , and  $p = 1$  was examined in detail in [55]. Another treatment of canonical diagrams can be found in [10].

*Case 2:*  $f = M/NT$  and  $p \not\equiv 0 \pmod{N}$ .

Note that the condition on the period implies that  $f \neq 0$ . The state set of  $G$  is the same as previously stated. For each state  $\sigma$  and element  $b$  in the alphabet there is an edge with label  $b$  from  $\sigma$  to a state  $\tau = [\tau_1, \dots, \tau_K]$ , defined by

$$\begin{aligned} \tau_1 &= \bar{\omega}(\sigma_1 + (\omega^p - 1)b) \\ \tau_i &= \bar{\omega}(\sigma_i + (\omega^p - 1)\sigma_{i-1}), \quad i = 2, \dots, K. \end{aligned}$$

It is not hard to verify that  $G$  satisfies an order- $K$  coboundary condition at  $f$ , using the functions

$$\phi_k(\sigma) = \frac{\sigma_k}{(\omega^p - 1)^k}.$$

Moreover, if  $H$  is a period- $p$  FSTD that generates sequences with an order- $K$  spectral null at  $f$ , we can define a label-preserving graph homomorphism from  $H$  to  $G$  in terms of the coboundary functions  $\phi_1, \dots, \phi_K$  on  $H$ . Specifically, the state  $s$  gets mapped to a state in  $G$  according to the rule:

$$s \rightarrow [(\omega^p - 1)\phi_1(s), (\omega^p - 1)^2\phi_2(s), \dots, (\omega^p - 1)^K\phi_K(s)].$$

*Example 3:* In Figs. 33–36, we illustrate several canonical diagrams for first-order spectral null constraints, based upon the alphabet  $\{\pm 1, \pm 3\}$ . For all but the last of these examples, the corresponding graphs for bipolar signaling may be found in [53], [55]. Specifically, the diagrams correspond to: spectral null at  $f = 0$ , spectral null at  $f = 1/2T$ , simultaneous nulls at  $f = 0$  and  $f = 1/2T$ , and spectral null at  $f = 1/4T$ . Figures depicting canonical diagrams for bipolar, ternary, and quaternary sequences with higher order spectral null at  $f = 0$  or  $f = 1/2T$  can be found in [10], [55].

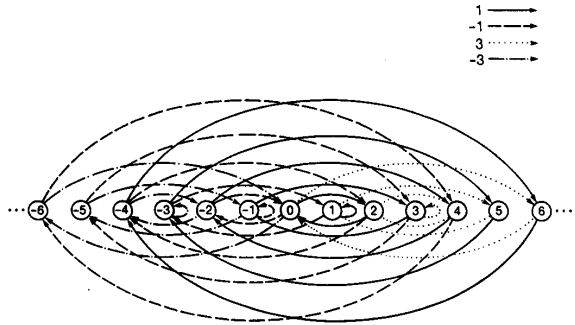


Fig. 34. Canonical diagram for spectral null at 1/2T (4-AM).

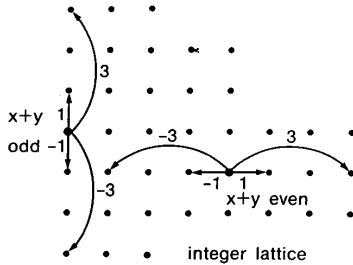


Fig. 35. Canonical diagram for spectral nulls at 0 and 1/2T (4-AM).

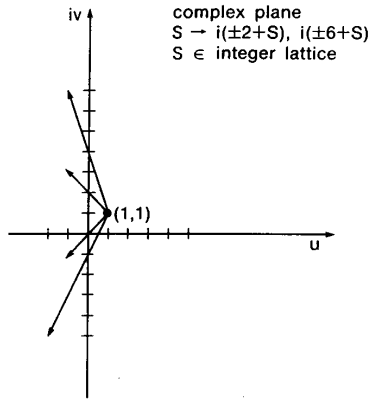


Fig. 36. Canonical diagram for spectral null at 1/4T (4-AM).

IV. DISTANCE PROPERTIES OF SPECTRAL NULL CODES

In this section we develop bounds on the minimum Euclidean distance of multilevel (integer-valued) codes with higher order spectral nulls at frequency  $f = M/NT$ .

A. Distance Properties of Sequences with Spectral Null at Zero Frequency

Immink and Beenker [25] derived a lower bound on the Hamming distance of certain bipolar block codes having a higher-order spectral null at  $f = 0$ . Specifically, they considered codes in which the order- $k$  moment of each

codeword  $x = x_0, \dots, x_n$  vanishes for  $k = 0, \dots, K$ . That is,

$$M_0^{(k)}(x) = \sum_{i=0}^n i^k x_i = 0, \quad k = 0, \dots, K.$$

They call such a code a “ $K$ th-order zero disparity code,” and they demonstrated that the code has an order- $(K + 1)$  spectral null at zero frequency.

We now state the theorem of Immink and Beenker.

*Theorem 5 [25]:* Let  $C$  be a code over the bipolar alphabet  $\{\pm 1\}$  such that for every  $x$  in  $C$ ,

$$M_0^{(k)}(x) = \sum_{i=0}^n i^k x_i = 0, \quad k = 0, \dots, K.$$

Then, for any distinct codewords  $x, y$  in  $C$ ,

$$d^H(x, y) \geq 2(K + 1),$$

where  $d^H(x, y)$  denotes the Hamming distance between the two sequences.

The elegant proof in [25] of this lower bound makes use of Newton’s identities [48, p. 244], which relate power-sums to elementary symmetric polynomials. The following corollary is an immediate consequence of Theorem 5.

*Corollary 1:* Let  $G$  be a FSTD, with edge labels in the bipolar alphabet  $\{\pm 1\}$ , that generates a spectral null of order  $K$  at  $f = 0$ . Let  $x = x_0, \dots, x_n$  and  $y = y_0, \dots, y_n$ , be distinct sequences generated by paths starting at a state  $\sigma$  and ending in a state  $\tau$ . Then, the Euclidean distance between  $x$  and  $y$  satisfies

$$d^2(x, y) \geq 8K.$$

(For the corresponding binary code, the bound is  $2K$ ).

*Proof:* Theorem 3 shows that the difference sequence  $e = e_0, \dots, e_n$ , defined by  $e_i = x_i - y_i$ , satisfies

$$M_0^{(k)}(e) = \sum_{i=0}^n i^k e_i = 0, \quad k = 0, \dots, K - 1.$$

By Theorem 5, the Euclidean distance between  $x$  and  $y$  satisfies  $d^2(x, y) \geq 8K$ . □

In Theorem 6, we develop an extension of the preceding distance bound to integer-valued sequences generated by a FSTD. Two proofs are provided. The first proof is based upon the proof of Theorem 5 due to Immink and Beenker. The second proof makes use of *Descartes’ rule of signs* [21, p. 96] to lower bound the number of sign changes in a sequence produced by a finite-state code with higher-order spectral null at  $f = 0$ .

We first review some background results and terminology.

*Definition 9:* For any set of (complex) numbers,  $A = \{a_1, \dots, a_L\}$ , the *degree- $k$  power-sum* is defined by

$$\tau_k(A) = \sum_{i=1}^L a_i^k.$$

(Compare to Definition 5).

lossless of finite order can be viewed as “deterministic with bounded delay.”

Fig. 2. Example for bound of Theorem 5.

*Definition 10:* The degree- $k$  elementary symmetric polynomial  $\sigma_k(A)$  is defined by:

$$\sigma_0(A) = 1$$

and, for  $k \neq 0$ ,

$$\sigma_k(A) = (-1)^k \sum_{i_1 < \dots < i_k} a_{i_1} \dots a_{i_k}.$$

*Remark:* The elementary symmetric polynomials appear as coefficients of the polynomial

$$\sigma(x) = \sum_{k=0}^L \sigma_k(A) x^k = \prod_{k=0}^L (1 - a_k x).$$

Newton's identities comprise the following relations between the power-sums and the elementary symmetric polynomials:

$$\begin{aligned} \tau_k + \sigma_1 \tau_{k-1} + \dots + \sigma_{k-1} \tau_1 + k \sigma_k &= 0, & k=1, \dots, L \\ \tau_k + \sigma_1 \tau_{k-1} + \dots + \sigma_L \tau_{k-L} &= 0, & k > L. \end{aligned}$$

We now state and prove the generalization of Theorem 5 and Corollary 1.

*Theorem 6:* Let  $G$  be a FSTD with integer alphabet  $\mathcal{A}$  and assume that  $G$  generates sequences with a spectral null of order  $K$  at  $f=0$ . Let  $x$  and  $y$  be as in Corollary 1. Then, the Euclidean distance between  $x$  and  $y$  satisfies

$$d^2(x, y) \geq 2K.$$

*Proof:* Given distinct sequences  $x = x_0, \dots, x_n$  and  $y = y_0, \dots, y_n$  generated by paths starting at state  $\sigma$  and ending at state  $\tau$ , consider the difference event  $e = e_0, \dots, e_n$ , with  $e_i = x_i - y_i$ . Then,  $e_i$  is an integer for all  $i = 0, \dots, n$  and by Theorem 3,

$$M_0^{(k)} = \sum_{i=0}^n i^k e_i = 0, \quad k = 0, \dots, K-1.$$

Let  $I = \{i_1, \dots, i_L\}$  be the set of indices for which  $e_i > 0$ , and let  $J = \{j_1, \dots, j_L\}$  be the set for which  $e_i < 0$ , where each index  $i$  is represented with multiplicity  $|e_i|$  in the appropriate set.

Then, the moment equations imply the following equal-power-sum equations:

$$\sum_{i \in I} i^k = \sum_{j \in J} j^k, \quad k = 0, \dots, K-1.$$

Note that the moment equation for  $k=0$  implies that the sets  $I$  and  $J$  have equal cardinality.

Rewriting this as

$$\tau_k(I) = \tau_k(J), \quad k = 0, \dots, K-1$$

we can apply Newton's identities to conclude that

$$\sigma_k(I) = \sigma_k(J), \quad k = 0, \dots, K-1.$$

If  $L \leq K-1$ , then we could conclude

$$\prod_{i=1}^L (1 - i_i x) = \prod_{j=1}^L (1 - j_j x).$$

But this would imply  $I = J$ , a contradiction because  $I$  and  $J$  as defined are disjoint sets. Therefore,  $L > K-1$ , so

$$|I| = |J| \geq K.$$

This in turn implies

$$\sum_{e_i > 0} |e_i| + \sum_{e_i < 0} |e_i| \geq 2K.$$

Since  $e_i^2 \geq |e_i|$ , we arrive at the desired bound

$$d^2(x, y) = \sum_{i=0}^{n-1} e_i^2 \geq 2K. \quad \square$$

*Remark:* We thank Professor K. Abdel-Ghaffar [17] for suggesting the extension of the Immink-Beenker proof to this more general case. See [10] for another treatment of this result.

*Remark:* As is well-known, Newton's identities apply to finite fields as well, and they play an important conceptual role in the decoding of BCH codes. This link between spectral null codes and algebraic error-control coding can be made more precise by observing that Theorem 6 provides a lower bound on the Lee-metric [3, p. 204] error-correcting capabilities of multilevel spectral null codes [38]. A modified form of Newton's identities provides the basis for an efficient "algebraic" decoding procedure for Lee-error-correcting spectral null codes, as will be described elsewhere.

*Remark:* The proof of this result establishes an interesting connection to the number-theoretic equal-power-sum problem, often associated with Prouhet and Tarry. Immink and Beenker, who first observed this connection, refer to the brief discussion of this problem in Hardy and Wright [19, pp. 328, 338-339]. More details can be found in Hua [22, Chapter 18]. In Section V, we will see how solutions of the equal-power-sum problem relate to the determination of lower bounds on asymptotic coding gains of MSN codes corresponding to null frequency  $f=0$  (and  $f=1/2T$ ). We will also develop a generalization of the equal-power-sum problem and then use the corresponding solutions to extend the lower bounds to codes with spectral null at an arbitrary rational submultiple of the symbol frequency.

For the second proof of Theorem 6, we will keep track of changes in the sign of the symbols in the code difference events. For completeness we make the following definitions.

*Definition 11:* Let  $e = e_0, \dots, e_n$  be a finite, integer-valued sequence. We say that  $e$  has a *sign change* at position  $u$  if  $e_u \neq 0$ , and  $\text{sign}(e_u) = -\text{sign}(e_t)$ , where  $t = \max\{i < u | e_i \neq 0\}$ .

Lemma 3 relates the order  $K$  of the spectral null to the number of sign changes in the difference sequence  $e$ . Lemma 4 then relates the number of sign changes in  $e$  to the Euclidean weight of the corresponding sequence at the output of a  $(1-D)$  channel.

*Lemma 3:* Let  $e(D) = \sum_{i=0}^n e_i D^i$ , where  $e_i$  are integer-valued coefficients, and assume  $e_0 \neq 0$ . If  $e(D)$  is divisible by  $(1-D)^K$ , then the sequence of coefficients  $e = e_0, \dots, e_n$  has at least  $K$  sign changes.

*Proof:* As was pointed out to us by one of the referees, this lemma is a special case of *Descartes' rule of signs*. Let  $e(D)$  be a real polynomial with  $K$  positive real roots, not necessarily distinct. Then the number of sign changes in the sequence  $e$  of coefficients of  $e(D)$ , denoted  $X(e)$ , satisfies

$$X(e) \geq K.$$

(See, for example, Householder [21, p. 96]). An independently discovered proof for the special case of Lemma 3 can be found in the appendix to [36].  $\square$

*Lemma 4:* Let  $g(D) = \sum_{i=0}^n g_i D^i$  be an integer polynomial, with  $g_0 \neq 0$ . Assume the sequence of coefficients  $g = g_0, \dots, g_n$  has  $L$  sign changes. Let  $e(D) = (1 - D)g(D)$ . Then, the Euclidean weight of the sequence  $e = e_0, \dots, e_{n+1}$  satisfies

$$\|e\|^2 = \sum_{i=0}^{m+1} e_i^2 \geq 2(L + 1).$$

*Proof:* We assume, as always, that the polynomial coefficients not explicitly indexed are zero.

One can write the squared Euclidean norm of the output sequence as

$$\|e\|^2 = \sum_{i=0}^{n+1} (g_i - g_{i-1})^2.$$

It is easy to check that if the sequence of coefficients of  $g(D)$  has no sign changes, then

$$\|e\|^2 \geq 2,$$

since the contribution of the term corresponding to the first nonzero coefficient in  $g(D)$  is at least 1, as is the contribution corresponding to the zero coefficient following the last nonzero coefficient.

Suppose that  $g(D)$  has  $L$  changes in sign,  $L \geq 1$ , which occur at coefficients

$$g_{i_1}, g_{i_2}, \dots, g_{i_L}.$$

Let  $W(j)$  equal the partial weight in which the index of summation runs from  $i = 0$  to  $i = j$ ,

$$W(j) = \sum_{i=0}^j (g_i - g_{i-1})^2.$$

It follows that:

$$\begin{aligned} W(0) &\geq 1 \\ W(i_l) - W(i_{l-1}) &\geq 2, \quad l = 1, \dots, L, \text{ and} \\ W(n) - W(i_L) &\geq 1. \end{aligned}$$

The first and third inequalities arise from the contributions corresponding to the first nonzero coefficient and the first zero coefficient after the last nonzero coefficient. To prove the second inequality, one must consider two cases. First, assume that  $g_{i_l-1}$ , the coefficient preceding  $g_{i_l}$ , is nonzero. Then, the sign of  $g_{i_l-1}$  must be the same as the sign of  $g_{i_{l-1}}$ , and opposite to the sign of  $g_{i_l}$ , because  $i_l$  is the first position after  $i_{l-1}$  at which there is a sign change. Therefore, in this case,

$$(g_{i_l} - g_{i_l-1})^2 \geq 4.$$

In the other case, assume  $g_{i_l-1} = 0$ . Let  $g_j$  be the last nonzero coefficient before  $g_{i_l}$ , with  $i_{l-1} \leq j < i_l - 1$ . Then, it is easy to see

$$W(i_l) - W(i_l - 1) \geq 1$$

and

$$W(i_l - 1) - W(j) \geq 1.$$

Since

$$W(j) \geq W(i_{l-1}),$$

the second inequality holds.

Combining the inequalities yields

$$\|e\|^2 = W(n + 1) \geq 2(L + 1).$$

This completes the proof of Lemma 4.  $\square$

*Second Proof of Theorem 6:* Let  $(G, \Gamma)$  have an order- $K$  spectral null at  $f = 0$ . Let  $e$  be a difference event, with corresponding difference polynomial  $e(D)$ . Theorem 4 implies that  $e(D)$  can be factored over the integers as

$$e(D) = (1 - D)^K u(D).$$

By Lemma 3, the polynomial  $f(D) = (1 - D)^{K-1} u(D)$  has at least  $K - 1$  sign changes. Since  $e(D) = (1 - D)f(D)$ , an application of Lemma 4 proves the desired distance bound on the Euclidean weight of the difference event,  $\|e\|^2 \geq 2K$ .  $\square$

*Remark:* This result is easily extended to the channel with  $h(D) = (1 + D)^K$ .

### B. Generalization to Spectral Nulls at $f = M/NT$

In this section, we generalize the lower bound in Theorem 6 to the case of a spectral null of order  $K$  at  $f = M/NT$ , where  $\text{gcd}(M, N) = 1$ . The proof will make use of the number-theoretic quantities known as Legendre symbols, as well as the Gaussian sum formula, to reduce the difference-event moment equations for the order- $K$  spectral null at  $f = M/NT$  to the difference-event moment equations for an order- $K$  spectral null at  $f = 0$ . These, in turn, lead to lower bounds on Euclidean distance by applying the results of the previous section.

We recall the definition of the Euler totient ( $\varphi$ -function).

*Definition 12:* For a positive integer  $N$ , we denote by  $\varphi(N)$  the Euler  $\varphi$ -function, which is defined as the number of positive integers less than and relatively prime to  $N$ .

Theorem 3 and Proposition 2 imply that, for each difference event  $e$  the order- $K$  spectral null at  $f = M/NT$  provides, for  $k = 0, \dots, K - 1$ , a set of  $\varphi(N)$  order- $k$  moment equations at frequency  $f$ . The equations take the form

$$\sum_{i=0}^n i^k \omega_N^m e_i = 0, \quad (E_{m,N}^k),$$

where, as before,  $\omega_N = e^{-i2\pi/N}$ , and  $m$  runs over the set

$\Phi(N)$  of  $\varphi(N)$  integers  $1 \leq m < N$  satisfying

$$\gcd(m, N) = 1.$$

We wish to find a linear combination, with weighting vector  $v = \{v_m | m \in \Phi(N)\}$ , of the moments in equations  $(E_{m,N}^k)$ ,

$$\sum_{(m,N)=1} v_m \sum_{i=0}^n i^k \omega_N^{mi} e_i,$$

yielding a single moment equation, denoted by  $(F_N^k)$ , of the form

$$\sum_{i=0}^n i^k c_i e_i = 0, \quad (F_N^k)$$

for each  $k = 0, \dots, K-1$  where the vector  $c = \{c_0, \dots, c_n\}$  satisfies the property  $c_i \in \{0, \pm c\}$ , for some nonzero constant  $c$ . If we can find, for each index  $i$ , a vector  $v$  such that  $c_i \neq 0$  in  $(F_N^k)$ , then the bound will follow from the proof of Theorem 6.

**Definition 13:** Let  $v$  and  $c$  be as previously stated. We will call such a vector  $v$  a *reduction vector* and the corresponding sequence  $c$  the *mask* associated to  $v$ . The quantity  $c$  will be called the *height* of the mask. (We are grateful to D. Forney for suggesting the *mask* terminology and viewpoint).

**Remark:** Since the ensembles of spectral null sequences under consideration enjoy a stationarity property with regard to the indexing in the moment conditions, it actually suffices to find a single reduction vector and mask. Then, for any index  $i$ , there will be at least one shift of the mask that is nonzero at position  $i$ .

As necessary background, we review some results from number theory that are cited in the course of the proof. (See for example [19], [57].)

In the following lemma, the basic facts needed to calculate the Euler totient  $\varphi(N)$  are summarized.

**Lemma 5 [57, p. 37]:** The Euler  $\varphi$ -function satisfies the following properties:

- $\varphi(2) = 1$ ,
- $\varphi(p) = p - 1$ , for  $p$  an odd prime,
- $\varphi(N_1 N_2) = \varphi(N_1)\varphi(N_2)$  for  $(N_1, N_2) = 1$ ,
- $\varphi(p^l) = p^l - p^{l-1}$ , for  $p$  prime.

**Definition 14:** Let  $p$  be an odd prime. The *Legendre symbol* for a positive integer  $j$ , denoted  $(j/p)$  is defined by:

$$\left(\frac{j}{p}\right) = \begin{cases} 0, & \text{if } j \equiv 0 \pmod{p} \\ 1, & \text{if } j \equiv x^2 \pmod{p} \text{ for some } x \not\equiv 0 \pmod{p} \\ -1, & \text{otherwise.} \end{cases}$$

For integers  $N = p_1 \cdots p_n$  that are a product of distinct odd primes, we have an *extended Legendre symbol* (or *Jacobi symbol*) defined by

$$\left(\frac{j}{n}\right) = \left(\frac{j}{p_1}\right) \cdots \left(\frac{j}{p_n}\right).$$

**Remark:** The sign of  $(j/p)$  indicates whether or not  $j$  is a square-residue  $(\text{mod } p)$ . Some of the basic properties of the Legendre symbols are given in the following lemma.

**Lemma 6 [57, p. 69]:** Let  $p$  be an odd prime, and let  $a$  and  $b$  be integers relatively prime to  $p$ . Then,

- $(a/p) = a^{(p-1)/2} \pmod{p}$
- $(a/p)(b/p) = (ab/p)$  [Multiplicativity]
- $a \equiv b \pmod{p}$  implies  $(a/p) = (b/p)$
- $(a^2/p) = 1, (1/p) = 1, (-1/p) = (-1)^{(p-1)/2}$ .

We will show that a reduction vector  $\{v_m\}$  that reduces  $(E_{m,N}^k)$  to  $(F_N^k)$  can be derived from the Legendre symbols (or Jacobi symbols) associated with  $N$ . The derivation hinges on a key identity for odd prime integers, the Gaussian sum formula.

**Theorem 7 [45, p. 56]:** Let  $p$  be an odd prime integer. Then

$$\begin{aligned} \sum_{m=1}^{p-1} \left(\frac{m}{p}\right) \omega_p^m &= \left[\left(\frac{-1}{p}\right) p\right]^{1/2} \\ &= [(-1)^{(p-1)/2} p]^{1/2} \\ &\stackrel{\text{def}}{=} \gamma_p. \end{aligned}$$

With these number-theoretic tools established, we can now prove the main result of this section.

**Theorem 8:** Let  $G$  be a FSTD, with symbols in an integer alphabet  $\mathcal{A}$ , and assume  $G$  generates sequences with a spectral null of order  $K$  at  $f = M/NT$ . Let  $e$  be a difference event associated to sequences  $x$  and  $y$ . Then, the squared-Euclidean weight of the difference event, or the squared-Euclidean distance between  $x$  and  $y$  satisfies

$$\|e\|^2 \geq 2K.$$

**Proof:** We first prove the theorem in the special case where  $N = p$ , an odd prime. This will illustrate many of the central ideas required in the general case, showing in particular the role that will be played by the Legendre symbols and the Gaussian sum formula.

Since  $\varphi(p) = p - 1$ , the set of order- $k$  moment equations for fixed  $k$  is given by

$$\sum_{i=0}^n i^k \omega_p^{mi} e_i = 0, \quad m = 1, \dots, p-1, \quad (E_{m,p}^k).$$

Let the vector  $v = \{v_1, \dots, v_{p-1}\}$  be defined by

$$v_j = \left(\frac{j}{p}\right).$$

The linear combination of equations  $(E_{m,p}^k)$  prescribed by  $v$  is:

$$\begin{aligned} &v_1 \left(\sum i^k \omega_p^i e_i\right) \\ &+ v_2 \left(\sum i^k \omega_p^{2i} e_i\right) \\ &\vdots \\ &+ v_{p-1} \left(\sum i^k \omega_p^{(p-1)i} e_i\right) = \sum i^k c_i e_i = 0, \end{aligned}$$

where

$$c_i = \sum_{m=1}^{p-1} \left(\frac{m}{p}\right) \omega_p^{mi}. \quad \square$$

The Gaussian sum formula makes it possible to evaluate the coefficients  $\{c_i\}$  explicitly, as we now show.

*Proposition 3:* The coefficients  $\{c_i\}$  satisfy

$$c_i = \begin{cases} \pm \gamma_p, & i \not\equiv 0 \pmod{p} \\ 0, & i \equiv 0 \pmod{p}. \end{cases}$$

*Proof of Proposition 3:* Suppose  $i \not\equiv 0 \pmod{p}$ . By the multiplicativity of the Legendre symbols,

$$\begin{aligned} c_i &= \sum_{m=1}^{p-1} \left(\frac{m}{p}\right) \omega_p^{mi} \\ &= \left(\frac{i}{p}\right)^{-1} \sum_{m=1}^{p-1} \left(\frac{mi}{p}\right) \omega_p^{mi}. \end{aligned}$$

Since  $\{mi|m=1, \dots, p-1\}$  is a complete set of residues modulo  $p$  for  $i \not\equiv 0 \pmod{p}$ , we can rewrite the expression for  $c_i$  as

$$c_i = \left(\frac{i}{p}\right)^{-1} \sum_{j=1}^{p-1} \left(\frac{j}{p}\right) \omega_p^j.$$

Applying the Gaussian sum formula, this expression reduces to

$$c_i = \left(\frac{i}{p}\right)^{-1} \gamma_p = \left(\frac{i}{p}\right) \gamma_p.$$

For  $i \equiv 0 \pmod{p}$ , we get

$$\begin{aligned} c_i &= \sum_{m=1}^{p-1} \left(\frac{m}{p}\right) \omega_p^{mi} \\ &= \sum_{m=1}^{p-1} \left(\frac{m}{p}\right) \end{aligned}$$

since  $\omega_p^p = 1$ . It follows that

$$c_i = 0,$$

since there are exactly  $(p-1)/2$  distinct square residues modulo  $p$ , if  $p$  is an odd prime [57, p. 73].  $\square$

This completes the proof of Theorem 8 for  $N = p$ . We now generalize to the case of  $N = p_1 \cdots p_n$  where the  $p_i$  are distinct odd primes. From this case, the general case  $N = 2^{l_0} p_1^{l_1} \cdots p_n^{l_n}$  will make use of the well-known Chinese remainder theorem, which we state for convenience.

*Lemma 7 (Chinese Remainder Theorem) [57, p. 33]:* Let  $N_1, \dots, N_L$  be distinct positive integers that are pairwise relatively prime. Let  $N'$  be the product of these integers,

$$N' = N_1 \cdots N_L.$$

Let  $r_1, \dots, r_L$  be nonnegative integers. Then, there is a

unique nonnegative integer  $x \leq N'$  that satisfies the following set of congruences:

$$x \equiv r_i \pmod{N_i}, \quad i = 1, \dots, L.$$

If all  $r_i \neq 0$ , then  $x$  belongs to  $\Phi(N')$ .  $\square$

Using the Chinese remainder theorem, we now develop a generalization of the Gaussian sum formula which is applicable to  $N = p_1 \cdots p_n$ .

*Proposition 4 [Generalized Gaussian Sum Formula]:* Let

$$\gamma_N = \sum_{j \in \Phi(N)} \left(\frac{j}{p_1}\right) \cdots \left(\frac{j}{p_n}\right) \omega_N^j.$$

Then

$$\gamma_N = \pm \gamma_{p_1} \cdots \gamma_{p_n}.$$

*Proof:* Let  $\beta = \omega_{p_1} \cdots \omega_{p_n}$ . Then,  $\beta^N = 1$ , and in fact  $N$  is the order of  $\beta$ . Therefore,  $\omega_N = \beta^{m'}$ , for some  $m' \in \Phi(N)$ . Then,

$$\begin{aligned} \gamma_N &= \sum_{j \in \Phi(N)} \left(\frac{j}{p_1}\right) \cdots \left(\frac{j}{p_n}\right) \omega_N^j \\ &= \sum_{j \in \Phi(N)} \left(\frac{j}{p_1}\right) \cdots \left(\frac{j}{p_n}\right) \beta^{m'j} \\ &= \left(\frac{m'}{p_1}\right)^{-1} \cdots \left(\frac{m'}{p_n}\right)^{-1} \sum_{j \in \Phi(N)} \left(\frac{m'j}{p_1}\right) \\ &\quad \cdots \left(\frac{m'j}{p_n}\right) \omega_{p_1}^{m'j} \cdots \omega_{p_n}^{m'j} \\ &= \pm \sum_{j \in \Phi(N)} \left(\frac{j}{p_1}\right) \cdots \left(\frac{j}{p_n}\right) \omega_{p_1}^j \cdots \omega_{p_n}^j. \end{aligned}$$

since  $\{m'j \pmod{N} | j \in \Phi(N)\}$  runs over all of the elements of  $\Phi(N)$ .

From the last remark in Lemma 7, it follows that

$$\begin{aligned} \gamma_N &= \pm \sum_{m \in \Phi(p_1)} \left(\frac{m}{p_1}\right) \omega_{p_1}^m \\ &\quad \cdot \sum_{j \in \Phi(p_2 \cdots p_n)} \left(\frac{j}{p_2}\right) \cdots \left(\frac{j}{p_n}\right) \omega_{p_2}^j \cdots \omega_{p_n}^j \\ &= \pm \gamma_{p_1} \gamma_{p_2 \cdots p_n}. \end{aligned}$$

Repeating this argument  $n-1$  times leads to the desired result.

We now exploit the generalized Gaussian sum formula to define a reduction vector based on the Jacobi symbols. The following proposition generalizes Proposition 3, and provides the reduction vector and mask needed to complete the proof for this case. It shows that we may use the vector

$$v^{(N)} = \left\{ \left(\frac{j}{p_1}\right) \cdots \left(\frac{j}{p_n}\right) \mid j \in \Phi(N) \right\}$$

lossless of finite order can be viewed as "deterministic with bounded delay."

Fig. 2. Example for bound of Theorem 5.

as a reduction vector for  $N$ , with corresponding mask

$$c^{(N)} = \{c_i^{(N)}\}$$

and height  $\gamma_N$  where

$$c_i^{(N)} = \sum_{j \in \Phi(N)} \left(\frac{j}{p_1}\right) \cdots \left(\frac{j}{p_n}\right) \omega_N^j.$$

*Proposition 5:*

$$c_i^{(N)} = \begin{cases} 0, & \text{if } (i, N) \neq 1, \\ \left(\frac{i}{p_1}\right) \cdots \left(\frac{i}{p_n}\right) \gamma_N, & \text{if } (i, N) = 1. \end{cases}$$

*Proof:* The result follows from a more general statement, proved in the Appendix. The stronger statement plays a role in deriving a distance bound for sequences satisfying higher order moment conditions, but failing to satisfy lower order conditions. This “nonstationary” version of Theorem 8 will be addressed elsewhere. This completes the proof of Theorem 8 for the case  $N = p_1 \cdots p_n$ , a product of distinct odd primes.

The generalization to arbitrary  $N = 2^{l_0} p_1^{l_1} \cdots p_n^{l_n}$  now follows from the observation that the cyclotomic polynomial  $\psi_N(D)$  for the primitive  $N$ th roots of unity is given by

$$\begin{aligned} \psi_N(D) &= \psi_{p_1 \cdots p_n}(D^{p_1^{l_1-1} \cdots p_n^{l_n-1}}), & \text{if } l_0 = 0 \\ &= \psi_{p_1 \cdots p_n}(-D^{2^{l_0-1} p_1^{l_1-1} \cdots p_n^{l_n-1}}), & \text{otherwise.} \end{aligned}$$

This relation can be checked by noting that

$$\varphi(N) = 2^{l_0-1} p_1^{l_1-1} \cdots p_n^{l_n-1} \varphi(p_1 \cdots p_n).$$

From [53], it follows that a sequence with nulls at frequencies corresponding to the primitive  $N$ th roots of unity is in fact obtained by interleaving  $2^{l_0-1} p_1^{l_1-1} \cdots p_n^{l_n-1}$  sequences, each with spectral null at frequencies corresponding to the primitive  $2p_1 \cdots p_n$ th roots of unity. Since interleaving preserves minimum distance of difference events, the bounds extend to the general case, completing the proof of Theorem 8.  $\square$

*Remark:* Proposition 5 can be interpreted in signal processing terms: the Legendre/Jacobi symbol sequence for  $N = p_1 \cdots p_n$ ,

$$w_j^{(N)} = \left(\frac{j}{p_1}\right) \cdots \left(\frac{j}{p_n}\right), \quad j = 0, \dots, N-1$$

is invariant (up to a constant factor) under the discrete Fourier transform of length  $N$ . See for example, Schroeder [60].

*Example 4:* Let  $N = 15$ . Then  $N = p_1 p_2$ , where  $p_1 = 3$  and  $p_2 = 5$ . A reduction vector  $v^{(15)}$  of length  $\varphi(15) = 8$  is given by:

$$\begin{aligned} v &= \left\{ \left(\frac{j}{3}\right) \left(\frac{j}{5}\right) \mid j \in \Phi(N) \right\} \\ &= 1 \ 1 \ 1 \ -1 \ 1 \ -1 \ -1 \ -1 \end{aligned}$$

with corresponding period-15 mask defined by

$$\begin{aligned} c &= \left\{ \left(\frac{j}{3}\right) \left(\frac{j}{5}\right) \mid j = 0, \dots, 14 \right\} \\ &= 0 \ c \ c \ 0 \ c \ 0 \ 0 \ -c \ c \ 0 \ 0 \ -c \ 0 \ -c \ -c \end{aligned}$$

and height  $c = \gamma_{15} = i\sqrt{15}$ .

## V. MATCHED SPECTRAL NULL CODE THEOREM FOR PR CHANNELS

In this section we apply the results of Section IV to deduce lower bounds on the asymptotic coding gain of matched-spectral-null codes for partial-response channels. In order to obtain these bounds, we first quantify the free Euclidean distance of partial-response channels with binary (bipolar) or multilevel inputs.

*Definition 15:* The binary (respectively, integer) free distance of the channel  $h(D)$  is given by

$$d_{\text{free}}^2(h(D)) = \min_{e(D)} \|e(D)h(D)\|^2,$$

where  $e(D) = \sum_{i=0}^n e_i D^i$  is an input difference sequence over the ternary (respectively, integer) alphabet, representing the difference between two binary (respectively, integer) signal sequences which differ in only a finite number of places, and the squared-Euclidean weight of a polynomial refers to the sum of the squared coefficients.

We now define the partial-response channels that form the building blocks for the class of channels that we consider in the context of matched-spectral-null codes.

*Definition 16:* A channel with system polynomial  $h(D)$  is called *order- $L$   $N$ -cyclotomic* if

$$h(D) = [\psi_N(D)]^L,$$

where  $N$  is a positive integer and  $\psi_N(D)$  is the  $N$ th cyclotomic polynomial (see Definition 6). In other words, the channel has spectral nulls of order  $L$  at the frequencies, which we denote  $\mathcal{F}_N$ , corresponding to the primitive  $N$ th roots of unity.

*Example 5:* For  $N = 1$ , the system polynomial of the order- $L$  cyclotomic channel is  $(1 - D)^L$ , and for  $N = 2$  it is  $(1 + D)^L$ .

### A. Free Distance for PR Channels: Integer-Valued Inputs

Computing the free distance of general PR channels with integer-valued inputs is an unsolved problem. In the case of channels with order- $L$  spectral null at zero frequency, the problem is closely related to the number-theoretic “equal-power-sums” problem (often associated with Prouhet and Tarry [19]) as discussed in Section IV.

We now exploit this connection to deduce exact values for the free distance of the cyclotomic channel with order- $L$  null at zero frequency—that is, with system polynomial

$$h(D) = [\psi_1(D)]^L = (1 - D)^L$$

—for the cases where

$$1 \leq L \leq 10,$$

under the assumption of integer alphabet,  $\mathcal{A} = \mathbb{Z}$ . We then show how these results can be extended to general order- $L$   $N$ -cyclotomic channels.

*Remark:* Vanucci and Foschini [15] have computed the free distance for channels with system polynomials  $h(D) = (1-D)(1+D)^L$  and  $h(D) = (1+D)^L$  for a range of orders  $L$ , over several equispaced multilevel integer alphabets, up to size 32. It is interesting to compare their results in the range  $1 \leq L \leq 10$  with the exact number-theoretic solutions discussed next.

For  $L \geq 1$ , let  $I(L)$  denote the least integer  $s$  such that there exist disjoint sets of integers  $x_1, \dots, x_s$  and  $y_1, \dots, y_s$ , satisfying the properties:

$$x_1^k + \dots + x_s^k = y_1^k + \dots + y_s^k, \quad k = 0, \dots, L-1,$$

but

$$x_1^L + \dots + x_s^L \neq y_1^L + \dots + y_s^L.$$

These conditions are summarized with the following notation, a slight modification of the notation used in [22]:

$$[x_1, \dots, x_s]_L = [y_1, \dots, y_s]_L.$$

Theorems 5 and 6 in Section IV imply that  $I(L) \geq L$ . The lower bound has been shown to be tight for  $1 \leq L \leq 10$  by using more or less *ad hoc* methods to construct explicit examples of sequences satisfying the conditions [19], [22]. These solutions are shown in Table VIII.

For each value of  $L$  represented in the list previously given, we can define a corresponding ternary sequence  $e^{1,L}$  with Euclidean weight  $2L$ , by setting

$$e_j^{1,L} = \begin{cases} 1, & \text{if } j = x_i, \quad i = 1, \dots, I(L), \\ -1, & \text{if } j = y_i, \quad i = 1, \dots, I(L), \\ 0, & \text{otherwise.} \end{cases}$$

The equal-power-sum conditions imply that the sequence  $e^{1,L}$  satisfies the set of moment equations

$$M_0^{(k)}(e^{1,L}) = 0, \quad k = 0, \dots, L-1$$

and, therefore, by Theorem 4 in Section III-A, the corresponding  $D$ -transform  $e^{1,L}(D)$  satisfies

$$e^{1,L}(D) = (1-D)^L u(D),$$

for some polynomial  $u(D)$  with integer coefficients.

These observation and examples constitute a proof of the following proposition.

*Proposition 6:* Under the assumption of integer alphabet, the free Euclidean distance of the channel with system polynomial  $h(D) = (1-D)^L$ , where  $L \geq 1$ , satisfies

$$d_{\text{free}}^2((1-D)^L) \geq 2L.$$

Moreover, for  $1 \leq L \leq 10$ , the lower bound is achieved.

*Remark:* It follows from Lemma 3 (Descartes' rule of signs) that the ternary sequence  $e^{1,L}$ ,  $1 \leq L \leq 10$  must contain at least  $L$  sign changes. One can easily check that there are, in fact, exactly  $L$  sign changes in each of them.

In Proposition 7, we extend the distance bounds in Proposition 6 to order- $L$   $N$ -cyclotomic channels  $\psi_N(D)^L$ ,

TABLE VIII  
SOLUTIONS TO THE EQUAL-POWER-SUMS PROBLEM FOR  $1 \leq L \leq 10$

$[0]_1 = [1]_1$
$[0, 3]_2 = [1, 2]_2$
$[1, 2, 6]_3 = [0, 4, 5]_3$
$[0, 4, 7, 11]_4 = [1, 2, 9, 10]_4$
$[1, 2, 10, 14, 18]_5 = [0, 4, 8, 16, 17]_5$
$[0, 4, 9, 17, 22, 26]_6 = [1, 2, 12, 14, 24, 25]_6$
$[0, 18, 27, 58, 64, 89, 101]_7 = [1, 13, 38, 44, 75, 84, 102]_7$
$[0, 4, 9, 23, 27, 41, 46, 50]_8 = [1, 2, 11, 20, 30, 39, 48, 49]_8$
$[0, 24, 30, 83, 86, 133, 157, 181, 197]_9 = [1, 17, 41, 65, 112, 115, 168, 174, 198]_9$
$[0, 3083, 3301, 11893, 23314, 24186, 35607, 44199, 44417, 47500]_{10} = [12, 2865, 3519, 11869, 23738, 23762, 35631, 43981, 44635, 47488]_{10}$

for  $N > 1$ . Exact free distance for  $1 \leq L \leq 10$  will be derived by making a simple modification to the sequences  $e^{1,L}$  obtained from Table VIII.

*Proposition 7:* Under the assumption of integer-valued inputs, the free Euclidean distance of the channel with system polynomial  $h(D) = \psi_N(D)^L$ , where  $L \geq 1$ , satisfies

$$d_{\text{free}}^2(\psi_N(D)^L) \geq 2L.$$

Moreover, for  $1 \leq L \leq 10$ , the lower bound is achieved.

*Proof:* The lower bound follows from Theorem 8 of Section IV-B. To prove the last statement, fix the parameter  $N$ , and again let  $\omega$  be a primitive  $N$ th root of unity. To prove the tightness of the bound for a specified value of  $L$ , it suffices to exhibit two disjoint sets of nonnegative integers  $x_1, \dots, x_L$  and  $y_1, \dots, y_L$ , which satisfy the *generalized equal-power-sum conditions* for  $N$  given by

$$\sum_{i=1}^K \omega^{x_i} x_i^k = \sum_{i=1}^K \omega^{y_i} y_i^k, \quad k = 0, \dots, L-1.$$

The corresponding ternary sequence  $e^{N,L}$ , defined by

$$e_j^{N,L} = \begin{cases} 1, & \text{if } j = x_i, \quad i = 1, \dots, L, \\ -1, & \text{if } j = y_i, \quad i = 1, \dots, L, \\ 0, & \text{otherwise,} \end{cases}$$

will then satisfy the moment conditions at  $f = 1/NT$ , namely

$$M_j^{(k)}(e^{N,L}) = 0, \quad k = 0, \dots, L-1.$$

Referring again to Theorem 4 of Section III-A, we will then be able to conclude that the corresponding  $D$ -transform of the sequence can be expressed as

$$e^{N,L}(D) = u(D) \psi_N(D)^L,$$

for some integer polynomial  $u(D)$ . Therefore, the sequence represents a valid output of the channel with system polynomial  $h(D) = \psi_N(D)^L$ , with integer input alphabet. Since, by its definition, the sequence has squared-Euclidean weight  $2L$ , it will achieve the lower bound.

For  $1 \leq L \leq 10$ , we can derive such a sequence by "stretching" the sets of integers  $x_i$  and  $y_i$  in Table VIII, multiplying them by a factor  $N$ . The corresponding sequences  $e^{N,L}$  are defined in terms of the sequences  $e^{1,L}$ ,

lossless of finite order can be viewed as "deterministic with bounded delay."

Fig. 2. Example for bound of Theorem 5.

used to prove Proposition 6:

$$e_j^{N,L} = \begin{cases} e_{j/N}^{1/L}, & \text{if } j \equiv 0 \pmod{N}, \\ 0, & \text{otherwise.} \end{cases}$$

It is easy to verify that this sequence  $e^{N,L}$  satisfies the required moment conditions at  $f = 1/NT$ , and also has Euclidean weight  $2L$ . This completes the proof.  $\square$

### B. Free Distance for PR Channels: Binary Inputs

For the case of channels with a binary input restriction, it appears to be even more difficult to derive general results about free distance. However, we will now prove such a result for the subset of first-order  $N$ -cyclotomic channels

$$h(D) = \psi_N(D),$$

where  $N$  is restricted to have at most 2 distinct odd prime factors, that is  $N = 2^{e_0} p_1^{e_1} p_2^{e_2}$ . The proof is based upon well-known properties of cyclotomic polynomials [54, p. 72].

**Proposition 8:** Let  $N = 2^{e_0} p_1^{e_1} p_2^{e_2}$ . The free distance of the binary cyclotomic channel with  $h(D) = \psi_N(D)$  satisfies:

$$d_{\text{free}}^2(\psi_N(D)) = 2.$$

*Proof:* By Theorem 8 of Section IV-B, we know  $d_{\text{free}}^2 \geq 2$ . For  $N = 1$ , we have  $\psi_1(D) = 1 - D$ , so the result  $d_{\text{free}}^2(\psi_1(D)) = 2$  is trivial. For  $N = p$ , a prime, note that

$$(1 - D)\psi_p(D) = 1 - D^p,$$

so the difference polynomial  $e(D) = 1 - D$  produces output  $1 - D^p$ , which has weight two. Therefore,

$$d_{\text{free}}^2(\psi_p(D)) = 2.$$

For  $N = p^e$ ,  $e \geq 2$ , we have from Section IV that

$$\psi_{p^e}(D) = \psi_p(D^{p^{e-1}}),$$

and, from the previous case,

$$(1 - D^{p^{e-1}})\psi_p(D^{p^{e-1}}) = 1 - D^{p^e},$$

which implies

$$d_{\text{free}}^2(\psi_{p^e}(D)) = 2.$$

If  $N = 2p$ , for  $p$  an odd prime, then

$$\psi_N(D) = \psi_p(-D),$$

so

$$(1 + D)\psi_N(D) = 1 + D^p.$$

The difference polynomial  $e(D) = 1 + D$  therefore yields an output of weight two, so

$$d_{\text{free}}^2(\psi_{2p}(D)) = 2.$$

When  $N = 2^{e_0} p_1^{e_1}$ , the interleaving relation

$$\psi_{2^{e_0} p_1^{e_1}}(D) = \psi_{2p_1}(D^{2^{e_0-1} p_1^{e_1-1}})$$

implies

$$d_{\text{free}}^2(\psi_{2^{e_0} p_1^{e_1}}(D)) = 2.$$

Finally, for  $N = p_1 p_2$  or  $N = 2p_1 p_2$ , with  $p_1$  and  $p_2$  distinct, odd primes, we make use of the relation

$$\psi_{p_1 p_2}(D) = \psi_{p_1}(D^{p_2}) / \psi_{p_1}(D)$$

and

$$\psi_{2p_1 p_2}(D) = \psi_{p_1 p_2}(-D).$$

Then

$$[(1 - D^{p_2})\psi_{p_1}(D)]\psi_{p_1 p_2}(D) = 1 - D^{p_1 p_2}$$

and

$$[(1 + D^{p_2})\psi_{p_1}(-D)]\psi_{2p_1 p_2}(D) = 1 + D^{p_1 p_2}.$$

These relations imply that with difference polynomials

$$e(D) = (1 - D^{p_2})\psi_{p_1}(D),$$

an output sequence with weight 2 is obtained for  $\psi_{p_1 p_2}(D)$ , and with  $e(-D)$ , the minimum weight is obtained on  $\psi_{2p_1 p_2}(D)$ . So,

$$d_{\text{free}}^2(\psi_{p_1 p_2}(D)) = 2$$

and

$$d_{\text{free}}^2(\psi_{2p_1 p_2}(D)) = 2.$$

The interleaving relations for  $N = 2^{e_0} p_1^{e_1} p_2^{e_2}$  and  $N = p_1^{e_1} p_2^{e_2}$  are

$$\psi_{p_1 p_2^{e_2}}(D) = \psi_{p_1 p_2}(D^{p_1^{e_1-1} D^{p_2^{e_2-1}}})$$

and

$$\psi_{2^{e_0} p_1^{e_1} p_2^{e_2}}(D) = \psi_{2p_1 p_2}(D^{2^{e_0-1} p_1^{e_1-1} p_2^{e_2-1}}).$$

The desired results for the final cases follow immediately.

To summarize, then:

$$d_{\text{free}}^2(\psi_{2^{e_0} p_1^{e_1} p_2^{e_2}}(D)) = 2, \quad \text{for } e_0, e_1, e_2 \geq 0. \quad \square$$

The following lemma gives the free Euclidean distance for certain channels, not included in the cases just analyzed, that are of interest in applications.

**Lemma 8:** For each of the following channels

- $h(D) = (1 + D)^2$  [class-2],
- $h(D) = (1 - D)^2$ ,
- $h(D) = (1 - D)(1 + D)^2$  [extended class-4],

the binary free distance is

$$d_{\text{free}}^2(h(D)) = 4.$$

*Proof:* The bounds in Section IV imply that

$$d_{\text{free}}^2(h(D)) \geq 4.$$

It is straightforward to verify that the following difference polynomials, obtained from binary input polynomials, achieve the lower bound for the three channels, respectively:

- $e(D) = 1 - D$ ,
- $e(D) = 1 + D$ ,
- $e(D) = 1$ .

$\square$

### C. Bounds on Asymptotic Coding Gain of MSN Codes

Let  $G$  be a finite-state transition diagram that generates sequences of integers having an order- $K$  spectral null at frequencies  $\mathcal{F}_N$ , corresponding to the primitive, complex  $N$ th roots of unity. If these sequences are applied to the order- $L$   $N$ -cyclotomic channel, the sequences at the channel output will have an order- $(K + L)$  spectral null at frequencies  $\mathcal{F}_N$ , as discussed at the end of Section III-A. We can therefore state the following lower bound on asymptotic coding gain achieved by matched spectral null codes.

*Theorem 9:* Consider a partial-response channel with input alphabet  $\mathcal{A}_{2M} = \{\pm 1, \dots, \pm 2M - 1\}$  and system polynomial

$$h(D) = [\psi_{N_1}(D)]^{L_1} \cdots [\psi_{N_n}(D)]^{L_n},$$

where  $N_1, \dots, N_n$  are distinct nonnegative integers.

Let  $C$  be a rate  $R$ , finite-state code over the alphabet  $\mathcal{A}_{2M}$  with an order- $K_i$  spectral null at frequencies  $\mathcal{F}_i$ , for  $1 \leq i \leq n$ . If the free Euclidean distance of the channel satisfies

$$d_{\text{free}}^2 = 8L,$$

where  $L = \max\{L_i\}$ ,  $1 \leq i \leq n$ , then the asymptotic coding gain of the code  $C$  satisfies the lower bound

$$\text{ACG} \geq 10 \log_{10} \frac{R}{\log 2M} \frac{E_u^{2M}}{E_c} \frac{\max_i (L_i - K_i)}{L},$$

where  $E_u^{2M} = (2M - 1)(2M + 1)/3$  and  $E_c$  represent the average input-symbol power of the uncoded channel and coded channel, respectively.

*Proof:* The proof follows immediately from the results developed earlier in this section.  $\square$

The following two useful corollaries are now easy to verify.

*Corollary 2:* For the order- $L$   $N$ -cyclotomic channel with integer alphabet  $\mathcal{A}_{2M}$ , with  $M$  large enough,

$$\text{ACG} \geq 10 \log_{10} \frac{R}{\log 2M} \frac{E_u^{2M}}{E_c} \frac{(L + K)}{L},$$

for  $N \geq 1$ , provided  $1 \leq L \leq 10$ .

*Corollary 3:* For the first-order  $N$ -cyclotomic channel, where  $N$  has at most two distinct prime factors, as well as for the channels in Lemma 8, with bipolar alphabet  $\mathcal{A}_2$ ,

$$\text{ACG} \geq 10 \log_{10} R(K + 1).$$

*Remark:* Simulation results by Immink [24] can be interpreted as an empirical verification that binary zero-disparity codes of codeword length 4, 6, and 8, applied to a  $1 - D$  channel, achieve the asymptotic coding gain predicted by Theorem 9.

*Remark:* The special case of Corollary 2 corresponding to  $N = 1, 2$  is also discussed in [10].

## VI. MSN CODE DESIGN AND DEMODULATION

In this section, we describe techniques for designing the encoder/decoder mappings for MSN codes, and reduced-complexity Viterbi detectors that provide near-maximum-likelihood performance. The two problems—code construction and code demodulation—are intertwined, the common thread being the canonical diagram representation of spectral null sequences (Section III-B) and, at a more fundamental level, the concepts and methods from symbolic dynamics introduced recently into the context of sliding-block code design for discrete noiseless channels [1], [28], [50].

Following a review of relevant results from symbolic dynamics, we turn to the description and analysis of the trellis-based demodulation of spectral null sequences, the design of MSN codes, and finally, the performance evaluation of the MSN-coded partial-response system.

### A. Symbolic Dynamics Background

This subsection collects some of the basic definitions and results from symbolic dynamics that relate to the representation of constrained sequences by finite-state diagrams and to the construction of efficient sliding block codes. Additional details can be found in [1], [4], [28], [49], [50].

The key properties of spectral null constraints and their canonical diagram representations that will be invoked in the subsequent discussion of reduced-complexity trellis structures (Section VI-B) are summarized at the end of Section VI-A-1.

Similarly, the main coding theorem that will be needed in the construction of efficient sliding-block spectral null codes (Section VI-C) is highlighted at the end of Section VI-A-2.

1) *Background on Sofic Systems:* A *sofic system*  $S$  is the set of all bi-infinite sequences generated by walks on a finite directed graph whose edges are labeled by symbols in a finite alphabet  $\mathcal{A}(S)$ .

A *block* of a sofic system  $S$  is a subsequence that appears in some sequence of  $S$ . A *k-block* is a block of length  $k$ .

The *entropy* (or *capacity*) of the sofic system  $S$  is defined by

$$\text{Cap}(S) = \lim_{k \rightarrow \infty} \frac{\log N(k)}{k},$$

where  $N(k)$  is the number of  $k$ -blocks of  $S$ .

Given two sofic systems  $S_1$  and  $S_2$ , let  $\pi$  be a map from  $S_1$  to  $S_2$

$$\pi: S_1 \rightarrow S_2.$$

The map  $\pi$  is called a *k-block factor map* if there exists a map

$$\pi^*: \{k\text{-blocks of } S_1\} \rightarrow \mathcal{A}(S_2),$$

lossless of finite order can be viewed as “deterministic with bounded delay.”

Fig. 2. Example for bound of Theorem 5.

such that for some integer  $i$ ,

$$(\pi(x))_i = \pi^*(x_{i+i_0}, \dots, x_{i+i_0+k-1}),$$

for every  $x \in S_1$ . The map  $\pi$  is called a factor map if it is a  $k$ -block factor map for some  $k$ .

For a nonnegative, integer square matrix  $A$ , let  $G(A)$  denote the graph defined by the adjacency matrix  $A$ . Also, for such a matrix  $A$ , let  $\{A\}$  denote a sofic system defined by labeling the edges of  $G(A)$  distinctly. Then, for a sofic system  $S$  defined on a labeled graph  $G(A)$ , the natural map

$$\pi: \{A\} \rightarrow S$$

generated by reading off the labels is a one-block factor map.

A matrix  $A$  is *irreducible* if for every  $i, j$  there is a positive integer  $n(i, j)$ , such that

$$[A^{n(i, j)}]_{ij} > 0;$$

that is, there is a path from  $i$  to  $j$  of length  $n(i, j)$ . The irreducible matrix is *aperiodic* if the integer  $n = n(i, j)$  can be chosen to be independent of the states  $i$  and  $j$ , or, in other words, the entries of  $A^n$  are positive. A sofic system is called *irreducible* (respectively, *aperiodic*) if it can be represented by a labeled graph  $G(A)$ , where  $A$  is irreducible (respectively, periodic). A sofic system is said to have *period*  $p$  if it is generated by a labeled graph  $G(A)$ , where the map  $\pi$  is one-to-one almost everywhere and the greatest common divisor of the cycles in  $G$  is equal to  $p$ .

A sofic system  $S$  is called a *subshift of finite type* (SFT) if in some labeled graph representation  $\{A\}$  the natural map  $\pi$  is one-to-one. There is also an intrinsic definition of a SFT that will be important in Section VI-B. Specifically, the system  $S$  is a SFT if there is a positive integer  $k$  and a collection  $C$  of  $k$ -blocks such that

$$S = \{x \in \mathcal{A}(S)^{\mathbb{Z}} \mid x_{i+1}, \dots, x_{i+k} \in C, \text{ for all } i \in \mathbb{Z}\}.$$

The irreducible sofic system  $S$  is called *almost-finite type* (AFT) if, in some labeled graph representation, for every edge  $e$  the natural map  $\pi$  is one-to-one when restricted to the set of bi-infinite paths that are at edge  $e$  at time 0. In other words, the map  $\pi$  is, in a sense, locally one-to-one. An equivalent definition is that the map  $\pi$  is one-to-one on an open set.

A factor map  $\pi$  is *right* (respectively, *left*) *closing* if for every distinct pair  $x$  and  $y$  in  $S_1$ , with  $x_i = y_i$  for all  $i \leq m$  (respectively,  $i \geq m$ ), for some integer  $m$ , we have  $\pi(x) \neq \pi(y)_{S_2}$ . A one-block factor map  $\pi$  is called *right* (respectively, *left*) *resolving* if

$$\pi(a_1 a_2) = \pi(a_1 a'_2) \quad (\text{respectively, } \pi(a_1 a_2) = \pi(a'_1 a_2))$$

implies

$$a_2 = a'_2 \quad (\text{respectively, } a_1 = a'_1).$$

A map is called *biresolving* if it is both right and left resolving.

When  $\pi$  is a 1-block map, a block  $w = w_0, \dots, w_k$  in  $S_2$  is called a *resolving block* if there exists an index  $0 \leq i \leq k$ , and a symbol  $a \in \mathcal{A}(S_1)$  such that whenever we have  $\pi(u_0 \dots u_k) = w$ , then  $u_i = a$ .

There is a useful characterization of AFT systems in terms of these concepts. Namely, the sofic system  $S$  is AFT if it is the image of an irreducible SFT under a map  $\pi$  which is right closing, left closing, and one-to-one almost everywhere (has a resolving block).

Although there are many labeled graphs representing the same irreducible sofic system  $S$ , there is one representation that is in some sense canonical. This representation is called the *minimal Shannon cover* or the *irreducible Shannon cover*. It is the unique irreducible component of maximum entropy in the *future cover*, which is obtained in the following manner.

For every block  $u \in S$ , let

$$F(u) = \{\text{blocks } w \in S \mid uw \in S\}.$$

Consider the labeled graph with state set

$$\mathcal{S} = \{F(u) \mid u \in S\}$$

and edges

$$F(u) \rightarrow F(uj),$$

with label  $j$ , where  $uj$  is a block in  $S$ . It can be shown that this state set  $\mathcal{S}$  is finite. The matrix of this graph, denoted  $A'_S$ , together with the natural factor map

$$\pi'_S: \{A'_S\} \rightarrow S$$

is the future cover of  $S$ . Since  $S$  is irreducible, the graph  $G(A'_S)$  has a unique irreducible component of maximal entropy. The matrix of this component is denoted  $A'_S+$ , the associated SFT is denoted  $\Sigma'_S+$ , and the restriction of the map  $\pi'_S$  to  $\Sigma'_S+$  is denoted  $\pi'_S+$ . We refer to the SFT  $\Sigma'_S+$ , along with the map  $\pi'_S+$  as the *minimal Shannon cover* of  $S$ .

*Remark:* There is an analogous construction based upon a *past cover*, leading to a SFT denoted by  $\Sigma'_S-$ , with factor map  $\pi'_S-$ .

The following proposition summarizes some of the properties of the minimal Shannon cover.

*Proposition 9* [50], [4]: Let  $S$  be an irreducible sofic system with minimal Shannon cover  $\pi'_S+: \Sigma'_S+ \rightarrow S$ . Then,

- 1)  $\pi'_S+$  is onto.
- 2)  $\text{Cap}(S) = \text{Cap}(\Sigma'_S+) = \log(\text{largest eigenvalue of } A'_S+)$ .
- 3)  $\pi'_S+$  is right resolving.
- 4)  $\pi'_S+$  has a resolving block.
- 5)  $\pi'_S+$  is one-to-one if and only if  $S$  is a subshift of finite type (SFT).
- 6)  $\pi'_S+$  is left closing if and only if  $S$  is almost-finite type (AFT).
- 7)  $\Sigma'_S+$  has the minimal number of states among all right resolving presentations of  $S$ , and any right closing factor map from a SFT  $\Sigma_B$  to  $S$  must factor through  $\pi'_S+$ .

As noted in [28], the minimal Shannon cover is uniquely identifiable as the presentation of  $S$  based upon an

irreducible graph, in which, a) for each state, the outgoing edges are labeled distinctly, and b) the sets  $U(s)$  of semi-infinite sequences generated by paths beginning at state  $s$  are distinct.

Let  $H$  be an irreducible subdiagram of a canonical diagram  $G$  for a specified spectral null constraint. Let  $S$  be the sofic system generated by  $H$ , and assume the natural map  $\pi_H: H \rightarrow S$  is one-to-one almost everywhere.

The following remarks establish a connection between the canonical graph representation of  $S$  and its minimal Shannon cover.

*Remarks:*

- 1) The sofic system  $S$  of spectral null constrained sequences is AFT. (*Sketch of proof:* This follows from the fact that the map  $\pi$  is left resolving, right resolving, and one-to-one almost everywhere.)
- 2) The cover defined by  $(H, \pi_H)$  is the same as the minimal Shannon cover  $(\Sigma_S^+, \pi_S^+)$  and its past cover counterpart  $(\Sigma_S^-, \pi_S^-)$ . Viewed as labeled graphs, these covers are isomorphic. (*Sketch of proof:* Since  $\pi_H$  is right resolving, the construction in Proposition 4 of [4] defines a 1-block factor map  $\theta: H \rightarrow \Sigma_S^+$  (with symbols corresponding to edges) from  $H$  to the minimal Shannon cover, such that  $\pi_H = \pi_S^+ \circ \theta$ . Now,  $\pi_H$  is bireolving and one-to-one almost everywhere, so it is one-to-one on an open set. From Corollary 10 of [4], there is an invertible factor map (conjugacy)  $\phi: H \rightarrow \Sigma_S^+$  satisfying  $\pi_H = \pi_S^+ \circ \phi$ . It follows that the maps  $\theta$  and  $\phi$  are the same, and they define a labeled graph isomorphism between  $H$  and  $\Sigma_S^+$ . A similar argument establishes the isomorphism involving  $\Sigma_S^-$ . We also note that the isomorphisms are a special case of a result due to Nasu [5].)
- 3)  $(H, \pi_H)$  has the minimal number of states of any cover  $(\Sigma, \pi)$  of  $S$ , where  $\pi$  is required to be a 1-block map, but need not be right or left resolving. (*Sketch of proof:* Let  $(\Sigma_M, \pi_M)$  be the state-minimal cover of  $S$ . Applying Theorem 9 of [4], with  $(H, \pi_H)$  corresponding to  $(\Sigma_A, \pi)$  and  $(\Sigma_M, \pi_M)$  corresponding to  $(\Sigma_B, \pi_B)$ , we get a 1-block factor map  $\theta: \Sigma_M \rightarrow H$ , such that  $\pi_M = \pi_H \circ \theta$ . An application of Corollary 10, as in the previous remark, establishes a labeled graph isomorphism between  $(H, \pi_H)$  and  $(\Sigma_M, \pi_M)$ .)

We denote the state-minimal cover of the spectral null system  $S$  by  $(\Sigma_S, \pi_S)$ . The fact that the cover determined by the subdiagram  $H$  of the canonical spectral null diagram is state-minimal is very attractive in the context of its use as the basis for the reduced-complexity Viterbi detector defined in Section VI-B.

2) *Sliding-Block Code Background:* The relationship of these concepts to code construction is now addressed, along the lines of the discussion in [28].

Let  $S^+$  denote the set of all semi-infinite subsequences of sequences that belong to  $S$ . That is,  $S^+$  contains the

sequences

$$x_0 x_1 x_2 \cdots$$

for which there is a sequence

$$\cdots x_{-2} x_{-1} x_0 x_1 x_2 \cdots$$

in  $S$ .

A finite-state code from the set of all sequences  $\Sigma_n$  over a finite  $n$ -ary alphabet to  $S$  at rate  $p:q$  is a mapping

$$E: (\Sigma_n)^+ \rightarrow S^+$$

described by a finite-state-machine with inputs drawn from the set of  $p$ -blocks in  $\Sigma_n$  and outputs drawn from the  $q$ -blocks in  $S$ .

The code is called *invertible* if the mapping  $E$  is one-to-one. An invertible finite-state code has a decoder

$$D: \{\mathcal{A}(S)^{z^+}\} \rightarrow (\Sigma_n)^+$$

given by

$$D(E(x)) = x.$$

A finite-state invertible code at rate  $p:q$  is called *noncatastrophic* if whenever  $y \in \mathcal{A}(S)^{z^+}$  and  $z$  is in the image of the encoder  $E$  and the two sequences (or an appropriate shift of each of them) differ in only a finite number of positions, then their images under the decoder mapping,  $D(y)$  and  $D(z)$  also differ in only a finite number of places (after a corresponding shift).

The code is said to have a *sliding-block decoder* if for some integer  $L > 0$ , there is a function from the set of  $q(2L+1)$ -blocks over the alphabet  $\mathcal{A}(S)$  to the  $p$ -blocks in  $\Sigma_n$ ,

$$f: ((\mathcal{A}(S))^q)^{2L+1} \rightarrow (\alpha_1, \cdots, \alpha_n)^p,$$

where  $\{\alpha_1, \cdots, \alpha_n\}$  is the alphabet of  $\Sigma_n$ , such that if  $y$  belongs to the image of  $E$ , and  $y = E(x)$ , then

$$x_i^p = f(y_{i-L}^q, \cdots, y_{i+L}^q), \quad \text{for } i \geq L.$$

It is easy to check that a sliding-block decoder is noncatastrophic.

*Remark:* Techniques for constructing noncatastrophic codes and, more specifically, sliding-block codes, were described in [1], [28]. The existence theorem upon which these methods are based, and the fundamental result of most importance in the consideration of the design of efficient spectral null codes is as follows:

*Theorem 10 [1], [28]:* Let  $S$  be a sofic system, and suppose  $p/q \leq \text{Cap}(S)/\log(n)$ . Then:

- a) There is a finite-state invertible noncatastrophic code from  $n$ -ary data to  $S$  at constant rate  $p:q$ ;
- b) If  $S$  is almost-finite type (AFT), then the code has a sliding-block decoder.

### B. Reduced-Complexity Viterbi Detectors

In this section, we will derive from the canonical diagrams (described in Section III-B) the trellis-structures that will underlie the reduced-complexity demodulators for MSN-coded partial-response channels.

lossless of finite order can be viewed as "deterministic with bounded delay."

Fig. 2. Example for bound of Theorem 5.

Consider a partial-response channel with spectral nulls (of any finite order) in its frequency response at frequencies  $\mathcal{F} = \{f_1, \dots, f_n\}$ . Let  $G$  be a canonical diagram for sequences, based on a finite, integer alphabet, which have spectral nulls (of any order) at  $\mathcal{F}$ , and let  $H$  be an irreducible finite subdiagram of  $G$ . Let  $S$  be the sofic system generated by  $H$ , and assume that the map  $\pi: H \rightarrow S$  is one-to-one almost everywhere. The remarks at the end of Section VI-A-1 imply that  $(H, \pi_H)$  is isomorphic to the state-minimal cover  $(\Sigma_S, \pi_S)$  of  $S$ . Let  $S'$  be the system generated by  $S$  at the output of the channel. It is easy to check that  $S'$  is AFT, that the minimal Shannon cover  $(\Sigma_{S'}, \pi_{S'})$  is derived from  $(\Sigma_S, \pi_S)$  in the obvious manner by incorporating the channel memory, and that it is also a state-minimal presentation of  $S'$ . We then have the following commutative diagram:

$$\begin{array}{ccc} H & \xrightarrow{\mu_H} & H' \\ \downarrow \pi & & \downarrow \pi' \\ S & \xrightarrow{\mu_S} & S' \end{array},$$

where  $H$  and  $H'$  denote the subshifts underlying the minimal covers,  $\pi$  and  $\pi'$  are the natural projections, and the maps  $\mu_H$  and  $\mu_S$  are the surjective maps induced by the channel  $h(D)$ .

Let  $C$  be the image of a sliding-block code from binary data to the constrained system of sequences  $S$  generated by  $H$ , and let  $C'$  be the output sequences of the coded partial-response channel.

We will now develop some ideas related to the use of the trellis structure corresponding to  $H'$  to demodulate the sequences in  $C'$ .

1) *Distance Measures*: First, we define two notions of distance that are important in our later discussion of Viterbi detector performance. These definitions of distance are closely linked to the familiar ideas of free distance and column distance function in the theory of convolutional codes [47, p. 309]. Let  $S$  be a sofic system with multilevel symbol alphabet, and with minimal Shannon cover  $\Sigma_S$ .

*Definition 17*: The *minimum merged distance* of  $S$ , denoted  $d_{<>}(S)$ , is defined as

$$d_{<>}(S) = \min_{(x,y) \in T} d(x,y),$$

where  $T$  is the set of pairs  $(x, y)$  of distinct sequences  $x, y \in S$  having preimages  $\pi_S^{-1}(x)$  and  $\pi_S^{-1}(y)$  in  $\Sigma_S$  that contain representative paths that differ in only a finite number of edges.

Another important notion of distance is the minimum unrestricted distance, denoted  $d_{<}(S)$  as defined as follows.

*Definition 18*: The *minimum unrestricted distance* of  $S$ , denoted  $d_{<}(S)$ , is given by

$$d_{<}(S) = \min_{\substack{(x,y) \in S^2 \\ x \neq y}} d(x,y),$$

where  $S^2$  is the set of all pairs of sequences  $x$  and  $y$  in  $S$ .

*Remark*: For the code sequences of a rate  $1:n$  linear convolutional code  $S$ ,  $\Sigma_S$  corresponds to the state-diagram underlying a minimal noncatastrophic encoder of  $S$  and the minimum merged distance  $d_{<>}(S)$  corresponds to the free distance of  $S$  with respect to the corresponding trellis.

The condition on  $x$  and  $y$  in the definition of  $d_{<>}(S)$  implies that the sequences differ in only a finite number of positions. Moreover, the specified representative paths in  $\Sigma_S$  must agree up to a certain point, at which they diverge; then, after a finite number of steps, they remerge and agree from that point onward. In other words, the representative paths constitute a finite-length error-event. Therefore,  $d_{<>}(S)$  is the minimum-error event in  $\Sigma_S$ .

On the other hand,  $d_{<}(S)$  additionally takes into account the distance between a pair of sequences with representative paths in  $\Sigma_S$  that agree up to a certain point, diverge, and then never remerge. This notion is analogous to the distance measure

$$d_{\infty}(S) = \lim_{i \rightarrow \infty} d_i(S),$$

where  $d_i(S)$  is the column distance of order  $i$  for the linear convolutional code  $S$  [47, p. 309].

*Lemma 9*: The two distance measures satisfy the relation

$$d_{<}(S) \leq d_{<>}(S).$$

*Proof*: This is clear because of the inclusion  $T \subset S^2$ .  $\square$

The following familiar example shows that  $d_{<}(S)$  can be strictly less than  $d_{<>}(S)$ .

*Example 6*: Let  $S$  be the output sequences of the binary 1-D channel. The trellis diagram corresponding to  $\Sigma_S$  is the familiar 2-state structure in Fig. 37. The minimum merged distance is the same as the free distance, as defined in Section II, and

$$d_{\text{free}}(S) = d_{<>}(S) = \sqrt{2},$$

as illustrated by the all 0's sequence and the sequence  $\dots 0 1 -1 0 \dots$  differing by the "diamond" shown in Fig. 37. The minimum unrestricted distance is  $d_{<}(S) = 1$ , however, as can be seen by comparing the all 0's sequence and the sequence  $\dots 0 1 0 \dots$ , represented by paths that diverge but do not remerge, as shown in Fig. 38.

As shown in [13] for uncoded partial-response systems like that of the preceding example, the average probability of error-event for a Viterbi detector is largely determined by signal-to-noise ratios, and the  $d_{<>}(S)$  at moderate-to-high standard underlying trellis is derived from the  $\Sigma_S$ . However, from the practical standpoint of detector implementation, the path memory required to approach the predicted average performance is dependent on the truncation depth, representing the minimum length  $\tau$  with the property that any pair of sequences of length  $\tau$  generated by paths diverging from the same state in the trellis must have distance at least as large as  $d_{<>}(S)$ . Unfortunately, if  $d_{<}(S) < d_{<>}(S)$ , as in the previous

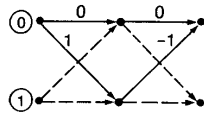


Fig. 37. Dicode sequences with distance  $d_{<}$ .

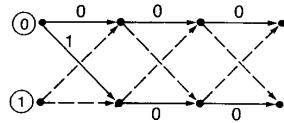


Fig. 38. Dicode sequences with distance  $d_{<}$ .

example, the truncation depth is unbounded. As a result, the system is susceptible to quasicatastrophic error-propagation, where the decoder error-probability may be degraded as a result of path-memory truncation effects [47]. The next subsection identifies the sequences in  $S$  that are responsible for this phenomenon, and shows how the associated performance degradation may be avoided by means of coding.

2) *Quasicatastrophic Sequences*: In this subsection we look at a subset of sequences in  $S$  which we call *quasicatastrophic sequences* that are intimately connected to quasicatastrophic error-propagation and unbounded truncation depth.

*Definition 19*: Let  $S$  be an almost-finite type (AFT) sofic system, with minimal Shannon cover  $\Sigma_S$ , and corresponding factor map  $\pi_S: \Sigma_S \rightarrow S$ . The set  $\mathcal{Q}$  of *quasicatastrophic sequences* in  $S$  is defined by:

$$\mathcal{Q} = \{q \in S \mid |\pi_S^{-1}(q)| > 1\}.$$

In words,  $\mathcal{Q}$  consists of the bi-infinite sequences with multiple distinct preimages in  $\Sigma_S$ , a condition implying that, for each quasicatastrophic sequence  $q$ , there is more than one path in  $\Sigma_S$  that “generates”  $q$ .

*Remark*: From Proposition 9, it follows that the set of quasicatastrophic sequences has measure zero when  $S$  is endowed with its Shannon measure (the measure of maximal entropy).

*Remark*: A similar concept was also introduced in [5] using the terminology “flawed sequences.” In [14], the notion of a quasicatastrophic trellis was defined. We can rephrase that definition in the following manner: The trellis corresponding to  $\Sigma_S$  is quasicatastrophic if and only if the set of quasicatastrophic sequences  $\mathcal{Q}$  in  $S$  is nonempty.

*Example 7*: Let  $S$  be the output sequences of the binary  $1-D$  channel. In this case,

$$\mathcal{Q} = \{q \in S \mid q_i = 0 \text{ for all } i\},$$

that is,  $\mathcal{Q}$  contains simply the all 0’s sequence. If a sequence contains a 1 or  $-1$ , the corresponding edge in the path in  $\Sigma_S$  is uniquely determined, or “resolved.” Since the map  $\pi_S$  is both left- and right resolving, the preimage of  $S$  is then uniquely determined.

The example suggests a useful, alternative characterization of  $\mathcal{Q}$ , given in Lemma 10. First, we recall from Section V-A-1 the definition of a resolving block in  $S$ .

*Definition 20*: A resolving block is a block  $s = s_1 \cdots s_n$  in  $S$  for which there is an index  $i \in [1, \dots, n]$  such that if  $u = u_1 \cdots u_n$  and  $v = v_1 \cdots v_n$  are words in  $\Sigma_S$  with  $\pi_S(u) = s = \pi_S(v)$ , then  $u_i = v_i$ . (In particular, since  $\pi_S$  is right resolving in the case of our canonical diagrams, the  $i$  above can be chosen to be  $n$ .)

*Lemma 10*: Let  $S$  be AFT. Then  $\mathcal{Q}$  is the set of sequences in  $S$  that do not contain a resolving block. Moreover, the set  $\mathcal{Q}$  is a closed subset of  $S$ .

*Proof*: We first show that if  $s \in \mathcal{Q}$ , then  $s$  does not contain a resolving block. For, suppose  $s \in S$  contains a resolving block  $s = s_1 \cdots s_l$ . If  $\pi_S(u) = s$ , then  $u_l$  is uniquely determined. Since  $\pi_S$  is right resolving and left closing, it follows that  $u$  is uniquely determined, so  $s \notin \mathcal{Q}$ .

Conversely, if  $s$  does not contain a resolving block, then, because  $\pi_S$  is both right resolving and left closing, it is easy to see that  $s$  must have at least two preimages.

The fact that  $\mathcal{Q}$  is closed follows from the fact that the sofic system is AFT [50]. This completes the proof.  $\square$

We will now justify our nomenclature by showing how the quasicatastrophic sequences relate to the phenomenon of quasicatastrophic error propagation, as described in [14].

To make the notion of quasicatastrophic error-propagation more precise, we now define a *generalized truncation depth* applicable to this situation.

*Definition 21*: Let  $C$  be a closed shift-invariant subset of  $S - \mathcal{Q}$  (i.e., a subshift of  $S - \mathcal{Q}$ ). Let  $x = \{x_0, x_1, \dots\}$  in  $C$  and  $s = \{s_0, s_1, \dots\}$  in  $S$  be sequences generated by paths that diverge from some state  $\sigma$  in  $\Sigma_S$ . Let  $x^{(n)} = \{x_0, \dots, x_n\}$  and  $s^{(n)} = \{s_0, \dots, s_n\}$ . The *generalized truncation depth* of  $C$  with respect to  $S$ , denoted  $\tau(C, S)$ , is the minimum length  $\tau$  such that

$$d(x^{(\tau)}, s^{(\tau)}) \geq d_{< >}(S),$$

for all such pairs of sequences  $x$  and  $s$ . The following proposition shows that, roughly speaking, one will not experience quasicatastrophic error-propagation if the detector input sequences are restricted to a subset  $C \subset S$  that is disjoint from the set of quasicatastrophic sequences  $\mathcal{Q}$  in  $S$ .

*Proposition 10*: Let  $C$  be a closed shift-invariant subset of  $S - \mathcal{Q}$  (i.e., a subshift of  $S - \mathcal{Q}$ ). Let  $x \in C$ . Then,

- a)  $d(x, s) \geq d_{< >}(S)$ , for any  $s \in S$ , with  $x \neq s$ ;
- b) if  $C$  is a shift of finite type (SFT), the generalized truncation depth  $\tau(C, S)$  is bounded.

*Proof of Part a)*: Since  $x \in S - \mathcal{Q}$ , we have

$$|\pi_S^{-1}(x)| = 1.$$

Let  $\hat{x} \in \pi_S^{-1}(x)$  and  $\hat{s} \in \pi_S^{-1}(s)$ . It suffices to consider the case where  $d(x, s)$  is finite; that is, the sequences differ in only a finite number of positions. We will prove, in this

lossless of finite order can be viewed as “deterministic with bounded delay.”

Fig. 2. Example for bound of Theorem 5.

case, that the set of indexes where  $\hat{x}$  and  $\hat{s}$  differ,  $\{i | \hat{x}_i \neq \hat{s}_i\}$ , is finite, implying that  $x$  and  $s$  are represented by paths in  $\Sigma_S$  that are left and right asymptotic, differing in only a finite number of places. It then will follow that  $d(x, s) \geq d_{< >}(S)$ .

We first show that for any  $x \in C$ , and any integer  $n$ , there must be a resolving block in  $(x_n, x_{n+1}, \dots)$ . If there were not, then the sequence of points in  $S$ ,

$$p = p_0, p_1, \dots, p_k, \dots$$

represented by the sequences  $p_k = \sigma^k(x)$ , where  $\sigma$  is the left-shift operator, would have the property that for any  $k \geq 0$ , the point  $p_k$  would contain no resolving block in components  $(p_k)_i, i \geq n - k$ . Since  $C$  is closed in  $S$ , there is a subsequence  $p_{k_j}, j \geq 0$ , where  $\lim_j k_j \rightarrow \infty$ , which converges to a limit point  $p^* \in C$ . (It helps to think of a zipper in visualizing this convergence.)

Now  $p_{k_j}$  contains no resolving block in components

$$(p_{k_j})_i, \quad i \geq n - k_j,$$

so it follows that  $p^*$  contains no resolving block at all. Therefore,  $p^* \in \mathcal{D}$ . But, by assumption,  $C \subset S - \mathcal{D}$ , which gives a contradiction.

A similar argument shows that for any  $n \in \mathbb{Z}$ , there is resolving block in  $(\dots, x_{n-1}, x_n)$ . So, assume the index set  $I$  on which  $x$  and  $s$  differ satisfies

$$I = \{i | x_i \neq s_i\} \subset [-N, N],$$

for some sufficiently large  $N$ . Since  $\pi_S$  is left closing and right resolving, it follows that  $\hat{x}$  and  $\hat{s}$  must agree asymptotically in the positive and negative directions beyond the first resolving blocks appearing in the components to the right and left of the index set  $I$ . In particular, there is an integer  $M \geq 0$  such that  $\hat{x}_i = \hat{s}_i$ , for  $|i| \geq N + M$ . This completes the proof of part a).  $\square$

*Proof of Part b):* We will prove Part b) by referring to the intrinsic definition of a SFT given in Section VI-A. Suppose, then, that b) does not hold. From the proof of Part a), this would mean that for any integer  $n > 0$ , we can find in  $C$  a block of length greater than  $n$  containing no resolving block of  $S$ . For  $n$  sufficiently large with respect to the parameter  $L$  in the intrinsic definition of the SFT  $C$ , for example  $n > |\mathcal{A}(S)|^L$ , we can extract from the  $n$ -block a subsequence that we can use to define a periodic sequence  $z$  in  $C$  that contains no resolving block of  $S$ , implying that  $z \in \mathcal{D}$ . This conclusion contradicts the fact that  $C$  is disjoint from  $\mathcal{D}$ , proving Part b), and completing the proof of the proposition.

*Corollary 4:* For subshift  $C$  as in Proposition 10,

$$d_{< >}(C) \geq d_{< >}(S).$$

*Proof:* This follows directly from Part a).  $\square$

*Corollary 5:* For a SFT  $C$  as in Proposition 10, the maximum length of minimum distance difference events involving any sequence  $x \in C$  is bounded.

*Proof:* This follows directly from Part b).  $\square$

*Remark:* If  $S$  is a SFT, with minimal Shannon cover  $\Sigma_S$ , it is easy to deduce from Corollary 4 that

$$d_{< >}(S) = d_{< >}(\Sigma_S).$$

In the next section, we show that it is possible to construct a sliding-block code with image in  $S$  that avoids the quasicatastrophic sequences  $\mathcal{D}$ , without incurring additional rate loss.

### C. Sliding-Block Spectral Null Codes

Techniques for constructing sliding-block codes for discrete noiseless channels have been developed in [1], [28], [49], [50]. Such a code has an encoder representable as a synchronous finite-state machine and uses a state-independent decoding rule in the form of a sliding-block decoder. The sliding-block decoder ensures that error propagation is limited when the code is used in applications involving a noisy channel. This section addresses issues related to the construction of sliding-block spectral null codes.

The following lemma shows that one can construct a rate  $p/q$  sliding-block spectral-null code from uncoded  $n$ -ary sequences to the binary spectral-null constraints corresponding to subdiagrams of the canonical diagram  $G$ , for any allowable rate,  $p/q < 1$ .

*Lemma 11:* Let  $p/q < \log n$ . Then there exists a rate  $p/q$  sliding-block code from  $n$ -ary data to binary spectral null constraints. Moreover, the encoder can be defined in such a way that its image is a shift of finite type.

*Proof:* This follows from the work of Petersen [58] and Ashley [2], along with Theorem 10.  $\square$

*Remark:* This result can be extended in a straightforward manner to the canonical diagrams corresponding to spectral null constraints for sequences with finite alphabets contained in the integers. The valid code rates satisfy  $p/q < \log n / \log m$ , where  $m$  is the size of the code symbol alphabet.

*Example 8:* Let  $H_N^0$  denote the FSTD in Fig. 24 that is restricted to  $N$  consecutive states  $0, \dots, N-1$ . The Shannon capacity of the constraint, denoted  $\text{Cap}(H_N^0)$ , is given by the closed form expression:

$$\text{Cap}(H_N^0) = \log_2 2 \cos \frac{\pi}{N+1}, \quad \text{for } N \geq 3,$$

as shown by Chien [7]. It is clear from this formula that the capacities of these systems satisfy

$$\text{Cap}(H_N^0) \rightarrow 1$$

as  $N \rightarrow \infty$ . In particular, to design binary codes with spectral null at  $f = 0$ , with rates  $1/2, 2/3, 3/4$ , and  $4/5$ , one could use the FSTD's  $H_3^0, H_4^0, H_5^0$ , and  $H_6^0$ .

It is clear from Proposition 10 that it is desirable to eliminate quasicatastrophic sequences at the output of the partial-response channel. We now prove, through a series of results, that it is indeed possible to construct

sliding-block spectral null codes that avoids quasicatastrophic sequences at the channel output, without sacrificing any code rate.

Let  $H, S, C$  and  $H', S', C'$  be as in Section VI-B. We first relate the quasicatastrophic sequences in  $S$  to those in  $S'$ . Specifically, we show that if the code sequences  $C$  avoid the quasicatastrophic sequences  $\mathcal{Q} \subset S$ , then the coded-channel output sequences, which we denote by  $C'$ , will avoid the quasicatastrophic sequences  $\mathcal{Q}' \subset S'$ .

*Proposition 11:* The mapping  $\mu_S: S \rightarrow S'$  is one-to-one (injective).

*Proof:* Let  $s, t$  be sequences in  $S$ , with  $\mu_S(s) = \mu_S(t)$ . The difference sequence  $u = s - t$  satisfies

$$\sum_{k=0}^{\deg(h)} u_{n-k} h_k = 0,$$

for each index  $n$ . Given a block of length  $\deg(h)$  in  $u$ ,

$$[u_{n-\deg(h)}, \dots, u_{n-1}],$$

the symbols  $u_n$  and  $u_{n-\deg(h)-1}$  are determined uniquely by the equation. Since the alphabet is finite, there are only a finite number of such blocks, so some block must reappear in  $u$ . Assume, without loss of generality, that  $[u_1, \dots, u_{\deg(h)}]$  reappears. Then  $u$  must be periodic, and it is described by the cycle

$$u_1 \cdots u_{\deg(h)} \cdots u_N,$$

where

$$u_{N+1} u_{N+2} \cdots u_{N+\deg(h)}$$

is the first reappearance of the sequence  $u_1 \cdots u_{\deg(h)}$  in  $u$ .

Now, since  $u$  is periodic, it has a Fourier series, which may be treated mathematically as a discrete spectrum  $U(f)$ . The transform of the defining equation is

$$U(f)H(f) = 0,$$

where  $H(f)$  is the frequency response of the channel  $h(D)$ . Therefore, if  $u \neq 0$ ,  $U(f)$  must consist of nonzero spectral lines at some nonempty subset of the frequencies  $\mathcal{F}$  where  $H(f)$  takes the value zero. But, by assumption,  $S$  consists of sequences whose Fourier spectral component is zero at all of the frequencies in  $\mathcal{F}$ , so  $u = s - t$  would have to have this property as well. Therefore,

$$U(f) = 0$$

and it follows that  $u = 0$ . This implies that  $s = t$ , so  $\mu_S$  is injective as claimed.  $\square$

*Corollary 6:* Let  $\mathcal{Q} \subset S$  and  $\mathcal{Q}' \subset S'$  be the subsets of quasicatastrophic sequences in  $S$  and  $S'$ . Then

$$\mu_S^{-1}(\mathcal{Q}') \subset \mathcal{Q}.$$

In other words,

$$\mu_S(S - \mathcal{Q}) \subset S' - \mathcal{Q}'.$$

*Proof:* Let  $q' \in \mathcal{Q}'$ , with unique preimage  $\mu_S^{-1}(q') = q$ . Since  $q' \in \mathcal{Q}'$ , there are two distinct paths  $p'_1, p'_2 \in H'$  with  $\pi'(p'_1) = \pi'(p'_2) = q'$ . Since  $\mu_H$  is surjective, there

are at least 2 distinct paths  $p_1, p_2 \in H$  with  $\mu_S(p_1) = p'_1$ ,  $\mu_S(p_2) = p'_2$ . By commutativity of the diagram, and injectivity of  $\mu_S$ , we can conclude that  $\pi(p_1) = \pi(p_2) = q$ , implying  $q \in \mathcal{Q}$ .  $\square$

*Remark:* The corollary shows that if the spectral null code is designed to avoid the quasicatastrophic sequences  $\mathcal{Q} \subset S$ , then the channel output sequences will avoid  $\mathcal{Q}' \subset S'$ , as desired. This simplifies the task of constructing the code, since these constraints can be expressed in terms of the code sequences generated by  $H$ , rather than in terms of the channel output sequences described by  $H'$ .

It remains to prove that it is possible to design a code  $C \subset S - \mathcal{Q}$  with rate arbitrarily close to  $\text{Cap}(S)$ . That is, the elimination of quasicatastrophic sequences does not require any reduction in code rate.

*Proposition 12:* Let  $S$  be an AFT sofic system, with quasicatastrophic subshift  $\mathcal{Q}$ . There exists a sequence  $C_1, C_2, \dots$  of subshifts of finite type such that:

$$C_i \subset S - \mathcal{Q}$$

and

$$\sup_i \text{Cap}(C_i) = \text{Cap}(S).$$

*Proof:* The proof is essentially contained in Proposition 3 in [50]. The only remark that needs to be made is that the subshifts of finite type defined in [50] consist of sequences that contain resolving blocks of  $S$  (quasiperiodically, in fact). Therefore, those subshifts must be contained in  $S - \mathcal{Q}$ , by Lemma 10.  $\square$

*Remark:* It is often necessary to incorporate other code constraints in order to ensure compatibility of the channel output sequences with algorithms for timing and gain control [9]. For gain control, more specifically, output sequences with long runs of 0's are to be avoided. More generally, for timing control, output sequences should minimize the length of runs of any identical sample values. In some cases of interest, the spectral null constraint inherently provides very effective runlength constraints. For example, for the  $1-D$  channel with first-order spectral null at zero frequency, the finite-state-transition diagrams  $H_N^0$  in Fig. 24 limit the maximum runlength to  $N-2$ .

For the  $1+D$  channel with binary inputs  $\{0,1\}$ , the canonical subdiagrams limit only the maximum runlength of output 1's, since they incorporate an inherent limitation on the length of runs of the form  $\cdots 1010 \cdots$ . Therefore the input runlengths of 0's and 1's must be further restricted to ensure constraints on the output runlengths of 0's and 2's. For example, as mentioned in Section II-B, the EMM code was designed to restrict the length of the maximum run of 0's (resp. 1's) at the channel input to 8 (resp. 12). See Fig. 12.

The capacity of this modified EMM constraint is approximately 0.6880, as compared to the original EMM capacity  $\log_2((1+\sqrt{5})/2) \approx 0.6942$ . Thus, a sliding-block code with rate  $2/3$  still could be constructed.

lossless of finite order can be viewed as "deterministic with bounded delay."

Fig. 2. Example for bound of Theorem 5.

Runlength limitations such as these will typically reduce the Shannon capacity of the constrained system, but in many applications the parameters can be chosen to minimize the impact on the resulting code rate and code complexity.

#### D. Performance Evaluation of MSN-Coded Channels

The results of the previous section indicate that, when  $d_{<>}(C') = d_{<>}(S')$ , a Viterbi detector using the trellis derived from the minimal cover  $H'$  will provide asymptotically the same error-event probability as a maximum-likelihood detector for  $C'$ , which would use the typically more complex trellis incorporating the structure of the code  $C$  and the channel memory.

The standard bound for the probability of an error event, assuming independent noise samples with Gaussian distribution having mean zero and variance  $\sigma^2$ , is therefore

$$\Pr(\text{event}) \geq N_S Q\left(\frac{d(C', S')}{2\sigma}\right),$$

where  $d(C', S')$  is the minimum distance between any sequence in  $C'$  and any distinct sequence in  $S'$ ,  $Q$  is the complementary error function,

$$Q(x) = \frac{1}{\sqrt{2\pi}} \int_x^\infty e^{-z^2/2} dz,$$

and  $N_S$  is the "error coefficient" that expresses the average number of sequences in  $S'$  at this distance from a sequence in  $C'$ .

We know from Section V that

$$d(C', S') \geq d_{<>}(S') \geq 2(K + L),$$

so the asymptotic performance, in the limit of increasing signal-to-noise ratio, is the same as a maximum-likelihood detector. The error coefficient for the reduced complexity detector may be larger than for the maximum-likelihood detector, but in all of the examples that we have examined in which the rate of the code  $C$  was near the capacity  $\text{Cap}(S)$ , the effect of the difference in error coefficients was insignificant even at low-to-moderate signal-to-noise ratios, as illustrated by the examples of MSN-coded channels in Section II.

We summarize these observations in the form of the following theorem.

*Theorem 11:* Let  $H$ ,  $H'$ ,  $S$ ,  $S'$ ,  $C$ , and  $C'$  be as previously stated. If the Viterbi algorithm based on the trellis derived from  $H'$  is used to detect  $C'$  in additive, independent Gaussian noise with probability density  $\mathcal{N}(0, \sigma^2)$ , the average probability of an error event is tightly bounded by

$$\Pr(\text{event}) \geq N_S Q\left(\frac{d_{<>}(S')}{2\sigma}\right),$$

as  $\sigma^2 \rightarrow 0$ .

Therefore, for moderate-to-high signal-to-noise ratios, the asymptotic performance achieved by the code  $C$ , in

conjunction with the reduced complexity trellis based on  $H'$ , is comparable to the gain promised by the matched-spectral-null code theorem, Theorem 9.

Typically, the complexity of the trellis derived from  $H'$  is considerably simpler than the trellis based upon the code  $C$ , as measured, for example, by number of states, number of edges per trellis stage, or the number of arithmetic/logical operations required per detected data bit. In addition, if  $H$ , and therefore  $H'$ , are periodic with period  $P$ , the code  $C$  and detector trellis can be based upon an irreducible component of the  $P$ th power of  $H$ , denoted  $H^P$ , which is defined as the FSTD with the same states as  $H$ , and with edges and edge labels corresponding to paths of length  $P$  in  $H$ . The trellis will then be appropriate for detecting a code with rate  $p:q$ , where the period  $P$  divides  $q$ .

When the number of states in the trellis is reduced, the path memory hardware is proportionally reduced. If, moreover, the code  $C$  has finite memory and avoids the quasicatastrophic sequences  $\mathcal{Q} \subset S$ , the results of Section VI-B imply that the path memory can be further simplified because of the bounded generalized truncation depth.

*Remark:* A similar approach to "near maximum-likelihood" detection of a spectral null code was reported by Wood [67] in the context of a memoryless channel (that is, without intersymbol interference). He developed a reduced-complexity detector for the binary Miller-squared code, which is a rate 1/2 code with first-order spectral null at zero frequency. The code has free Hamming distance given by

$$d_{\text{free}}^H = 2,$$

representing an increase in minimum distance of 3 dB compared to the uncoded binary channel. The code sequences are generated by the subdiagram  $H_7^0$  of the canonical diagram for a simple spectral null at zero frequency, and the detector represents an approximation to the Viterbi algorithm based on the trellis derived from  $H_7^0$ . The code does contain quasicatastrophic sequences, however.

## VII. CONCLUSION

This paper has presented a new trellis-coded modulation technique applicable to a broad class of partial-response channels. The codes are primarily intended for applications in which the channel input alphabet is fixed. The codes, which we call *matched-spectral-null (MSN) codes*, have zeros in their power spectral density function (and its derivatives) at precisely the same frequencies as the transfer function of the partial-response channel. Systems of integer-valued sequences having higher-order spectral nulls at rational submultiples of the symbol frequency were characterized. Euclidean distance properties of these spectral null constraints were then derived, and a lower bound on the coding gain of MSN codes was proved. Canonical diagrams which characterize higher order spectral null constraints were used to define de-

modulators with reduced-complexity trellises. These were shown to provide performance close to maximum-likelihood detection for efficient sliding-block codes derived from the diagrams. It was shown that elimination of quasicatastrophic sequences from the code could simplify the detector implementation and avoid quasicatastrophic error-propagation.

The theory of MSN codes is appealing from an intuitive standpoint. It is consistent with the well-known adage that “the code spectrum should match the channel transfer characteristics.” In the context of waveform channels with average input-power constraints, this design criterion was made precise by the classical derivations of channel capacity, and the features of a capacity-achieving signal spectrum could be visualized using the “water-filling” interpretation. For input-restricted partial-response channels, the MSN theory identifies a specific, frequency-domain characteristic—the location and order of spectral nulls—and indicates the benefits that can accrue when code and channel match in this respect. An interesting problem for future investigation is the elaboration of this analogy, from both theoretical and practical standpoints.

ACKNOWLEDGMENT

The authors gratefully acknowledge the many colleagues who were kind enough to share their technical thoughts about this work during the course of its development and documentation, in particular: Khaled Abdel-Ghaffar, Jon Ashley, Rob Calderbank, Martin Hassner, Chris Heegard, Tom Howell, Kees Immink, Hiroshi Kamabe, Brian Marcus, Hemant Thapar, Gottfried Ungerboeck, Jack Wolf, Roger Wood, and the referees.

Special thanks go to Dick Blahut and Dave Forney for their careful reading of an earlier draft of this paper, and for many suggestions that improved the paper both stylistically and technically.

The authors additionally thank Hiroshi Kamabe for informing us of several in the Japanese literature papers relevant to spectral null characterization, and Lyle Fredrickson for assistance with computer simulations.

APPENDIX A

In this appendix, we prove a generalization of Proposition 5 that was used to evaluate the mask associated to the reduction vector generated by the sequence of Jacobi symbols in Section IV-B.

*Proposition A1:* Let  $N = p_1 \cdots p_n$ . If  $\{p_{i_1}, \dots, p_{i_L}\}$  is a subset of factors of  $N$ , define

$$c_i^{p_{i_1} \cdots p_{i_L}} = \sum_{j \in \Phi(N)} \left(\frac{j}{p_{i_1}}\right) \cdots \left(\frac{j}{p_{i_L}}\right) \omega_N^{ij}.$$

Then,

$$c_i^{p_{i_1} \cdots p_{i_L}} = \begin{cases} 0, & \text{if } (i, p_{i_1} \cdots p_{i_L}) \neq 1, \\ \pm \varphi\left(\frac{N}{p_{i_1} \cdots p_{i_L}}\right) \gamma_{p_{i_1}} \cdots \gamma_{p_{i_L}}, & \text{if } (i, N) = \frac{N}{p_{i_1} \cdots p_{i_L}}. \end{cases}$$

*Proof:* We assume, without loss of generality, that  $p_{i_1} \cdots p_{i_L} = p_1 \cdots p_L$ . First, assume  $(i, N) = (p_{L+1} \cdots p_n)$ . Then we can write  $i$  in the form

$$i = s(p_{L+1} \cdots p_n),$$

where

$$(s, p_l) = 1, \quad \text{for } l = 1, \dots, L.$$

Since

$$(i, p_l) = 1, \quad \text{for } l = 1, \dots, L,$$

the exponent  $ij$ , where  $j \in \Phi(N)$ , is determined, modulo  $N$ , by the residues

$$r_l = j \pmod{p_l}, \quad l = 1, \dots, L.$$

The number of elements  $j \in \Phi(N)$  with these residues is exactly  $\varphi(p_{L+1} \cdots p_n)$  and we can identify these elements with a specific residue class in  $\Phi(p_1 \cdots p_L)$ . Using the representation of  $i$ , we can therefore rewrite the sum as

$$\varphi(p_{L+1} \cdots p_n) \sum_{j \in \Phi(p_1 \cdots p_L)} \left(\frac{j}{p_1}\right) \cdots \left(\frac{j}{p_L}\right) \omega_{p_1 \cdots p_L}^{sj}.$$

But, the exponent  $sj$  ranges over all residue classes in  $\Phi(p_1 \cdots p_L)$  as  $j$  ranges over these residues, since  $(s, p_1 \cdots p_L) = 1$ . Therefore, we can evaluate  $c_i^{p_1 \cdots p_L}$  as

$$\begin{aligned} c_i^{p_1 \cdots p_L} &= \pm \left(\frac{s}{p_1}\right)^{-1} \cdots \left(\frac{s}{p_L}\right)^{-1} \varphi(p_{L+1} \cdots p_n) \\ &\quad \cdot \sum_{j \in \Phi(p_1 \cdots p_L)} \left(\frac{j}{p_1}\right) \cdots \left(\frac{j}{p_L}\right) \omega_{p_1 \cdots p_L}^j \\ &= \pm \varphi(p_{L+1} \cdots p_n) \gamma_{p_1 \cdots p_L}, \end{aligned}$$

as desired.

We now examine the case where  $(i, p_1 \cdots p_L) \neq 1$ . Suppose that  $N$  can be decomposed into prime factors, as follows:

$$N = (p_1 \cdots p_U)(p_{U+1} \cdots p_L) \cdot (p_{L+1} \cdots p_V)(p_{V+1} \cdots p_n),$$

and that, by the assumption,  $i$  can be written as

$$i = (p_1 \cdots p_U)(p_{L+1} \cdots p_V)s,$$

where

$$(s, p_l) = 1, \quad \text{for } l = U+1, \dots, L, (V+1), \dots, n.$$

We can rewrite the last factor in the expression for  $c_i^{p_1 \cdots p_L}$  as

$$\omega_{N/(i, N)}^{sj}.$$

The value of this quantity is determined by the residues of  $j$  modulo the prime factors of  $N/(i, N)$ ,

$$r_l = j \pmod{p_l}, \quad l = U+1, \dots, L, V+1, \dots, n.$$

lossless of finite order can be viewed as “deterministic with bounded delay.”

Fig. 2. Example for bound of Theorem 5.

Among the elements  $j \in \Phi(N)$ , each such set of residues is realized by

$$\varphi(p_1 \cdots p_U p_{L+1} \cdots p_V)$$

elements. For convenience, we define

$$q = (p_1 \cdots p_U)(p_{L+1} \cdots p_V)$$

and

$$r = (p_{U+1} \cdots p_L)(p_{V+1} \cdots p_N).$$

The coefficient  $c_i^{p_1 \cdots p_L}$  can be evaluated as follows

$$\begin{aligned} c_i^{p_1 \cdots p_L} &= \sum_{u \in \Phi(r)} \sum_{j \in \Phi(q)} \left(\frac{j}{p_1}\right) \cdots \left(\frac{j}{p_U}\right) \left(\frac{u}{p_{U+1}}\right) \\ &\quad \cdots \left(\frac{u}{p_L}\right) \omega_{N/(i,N)}^{su}, \\ &= \sum_{u \in \Phi(r)} \left(\frac{u}{p_{U+1}}\right) \cdots \left(\frac{u}{p_L}\right) \omega_{N/(i,N)}^{su} \\ &\quad \cdot \sum_{j \in \Phi(q)} \left(\frac{j}{p_1}\right) \cdots \left(\frac{j}{p_U}\right), \\ &= \sum_{u \in \Phi(r)} \left(\frac{u}{p_{U+1}}\right) \cdots \left(\frac{u}{p_L}\right) \omega_{N/(i,N)}^{su} \\ &\quad \cdot \left[ \varphi(p_{L+1} \cdots p_V) \sum_{j \in \Phi(p_1 \cdots p_U)} \left(\frac{j}{p_1}\right) \cdots \left(\frac{j}{p_U}\right) \right] \\ &= 0, \end{aligned}$$

since

$$\sum_{j \in \Phi(p_1 \cdots p_U)} \left(\frac{j}{p_1}\right) \cdots \left(\frac{j}{p_U}\right) = 0,$$

as can be seen by combining the Chinese remainder theorem with the fact that

$$\sum_{(j,p)=1} \left(\frac{j}{p}\right) = 0.$$

This completes the proof of the proposition.  $\square$

#### REFERENCES

- [1] R. Adler, D. Coppersmith, and M. Hassner, "Algorithms for sliding block codes," *IEEE Trans. Inform. Theory*, vol. IT-29, no. 1, pp. 5-22, Jan. 1983.
- [2] J. Ashley, "Capacity bounds for channels with spectral nulls," IBM Res. Rep. 5676, May 28, 1987.
- [3] E. Berlekamp, *Algebraic Coding Theory*. New York: McGraw-Hill, 1968.
- [4] M. Boyle, B. Kitchens, and B. Marcus, "A note on minimal covers for sofic systems," *Proc. Amer. Math. Soc.*, vol. 95, no. 3, Nov. 1985, pp. 403-411.
- [5] A. R. Calderbank, C. Heegard, and T. A. Lee, "Binary convolutional codes with application to magnetic recording," *IEEE Trans. Inform. Theory*, vol. IT-32, no. 6, pp. 797-715, Nov. 1986.
- [6] A. R. Calderbank and J. E. Mazo, "Baseband line codes via spectral factorization," *IEEE J. Select. Areas Commun.*, vol. SAC-7, no. 6, pp. 914-928, Aug. 1989.
- [7] T. M. Chien, "Upper bound on the efficiency of DC-constrained codes," *Bell Syst. Tech. J.*, pp. 2267-2287, Dec. 1970.
- [8] N. Davie, M. Hassner, T. Howell, R. Karabed, and P. Siegel, "Method and apparatus for asymmetrical RLL coding," U.S. Patent, 4,949,196, Oct. 10 1990.
- [9] F. Dolivo, "Signal processing for high density digital magnetic recording," in *Proc. COM-PEURO 89*, Hamburg, Germany, May 1989.
- [10] E. Eleftheriou and R. Cideciyan, "On codes satisfying  $M$ th order running digital sum constraints," IBM Res. Rep. RZ 1966, Nov. 1989.
- [11] —, "Multilevel codes with bounded  $M$ th order running digital sum," in *abstracts of papers, IEEE Int. Symp. Inform. Theory*, San Diego, CA, Jan. 14-19, 1990.
- [12] —, "Quaternary codes for partial-response channels," *Proc. 1990 IEEE Global Telecommun. Conf. (Globecom '90)*, vol. 3, San Diego, CA, December 2-5, 1990, pp. 1673-1678.
- [13] G. D. Forney, Jr., "Maximum likelihood sequence detection in the presence of intersymbol interference," *IEEE Trans. Inform. Theory*, vol. IT-18, no. 3, pp. 363-378, May 1972.
- [14] G. D. Forney and A. R. Calderbank, "Coset codes for partial response channels; or coset codes with spectral nulls," *IEEE Trans. Inform. Theory*, vol. 35, no. 6, pp. 925-943, Sept. 1989.
- [15] G. Vannucci and G. Foschini, "The minimum distance for digital magnetic recording partial responses," *IEEE Trans. Inform. Theory*, vol. 37, no. 3, pt. II, pp. 955-960, May 1991.
- [16] A. Gallopoulos, C. Heegard, and P. H. Siegel, "The power spectrum of run-length-limited codes," *IEEE Trans. Commun.*, vol. 37, no. 9, pp. 906-917, Sept. 1989.
- [17] K. Abdel-Ghaffar, private communication, May 1988.
- [18] R. Haeb, "Trellis codes for multilevel partial-response signaling by exploiting the channel memory," IBM Res. Rep. RJ 7025, Sept. 20, 1989.
- [19] G. H. Hardy and E. M. Wright, *An Introduction to the Theory of Numbers*, Fifth ed. Oxford: Oxford Univ. Press, 1979.
- [20] C. Heegard, private communication, Dec. 1987.
- [21] A. S. Householder, *Principles of Numerical Analysis*. New York: McGraw-Hill, 1953.
- [22] L. K. Hua, *Introduction to Number Theory*. Berlin: Springer-Verlag, 1982.
- [23] K. A. S. Immink, "Spectrum shaping with binary DC<sup>2</sup>-constrained codes," *Philips J. Res.*, vol. 40, pp. 40-53, 1985.
- [24] —, "Coding techniques for the noisy magnetic recording channel: A state-of-the-art report," *IEEE Trans. Commun.*, vol. COM-37, no. 5, pp. 413-419, May 1987.
- [25] K. A. S. Immink and G. Beenker, "Binary transmission codes with higher order spectral zeros at zero frequency," *IEEE Trans. Inform. Theory*, vol. IT-33, no. 3, pp. 452-454, May 1987.
- [26] P. Kabal and S. Pasupathy, "Partial-response signaling," *IEEE Trans. Commun.*, vol. 23, no. 9, pp. 921-934, Sept. 1975.
- [27] H. Kamabe, "Spectral lines of codes given as functions of finite Markov chains," *IEEE Trans. Inform. Theory*, vol. 37, no. 3, pt. II, pp. 927-941, May 1991.
- [28] R. Karabed and B. Marcus, "Sliding-block coding for input-restricted channels," *IEEE Trans. Inform. Theory*, vol. 34, no. 1, pp. 2-26, Jan. 1988.
- [29] R. Karabed and P. Siegel, "Matched spectral null trellis codes for partial response channels," presented at *Conf. Commun., Contr. and Signal Processing*, Calif. Inst. of Technol., Pasadena, CA, Apr. 18, 1988.
- [30] —, "Matched-spectral null trellis codes for partial response channels, parts I and II," *Abstracts of Papers, Int. Symp. Inform. Theory*, Kobe, Japan, June 1988, pp. 142-143.
- [31] —, "Matched spectral null trellis codes for partial response channels," in *Proc. Third Workshop on Modulation, Coding, and Signal Processing for Magnetic Recording*, Center for Magnetic Recording Research, UCSD, San Diego, CA, Jan. 8, 1989.
- [32] —, "Even-mark-modulation for optical recording," *Proc. 1989 Int. Conf. Commun. (ICC'89)*, vol. 3, Boston, MA, June 1989, pp. 1628-1632.
- [33] —, "Matched spectral null trellis codes for partial response channels," *IEEE Int. Workshop Inform. Theory*, Cornell University, Ithaca, June 1989.
- [34] —, "Improved trellis codes for partial-response channels," U.S. Patent 4,888,775, Dec. 19, 1989.
- [35] —, "Even-mark-modulation for optical recording," U.S. Patent 4,870,414, Sept. 26, 1989.
- [36] —, "Matched spectral null trellis codes for partial response channels," U.S. Patent 4,888,779, Dec. 19, 1989.

- [37] —, "Phase invariant rate 8/10 matched spectral null code for PRML," U.S. Patent filed Nov. 13, 1989.
- [38] —, "Spectral null codes and number theory," *Proc. 1990 IEEE Int. Workshop on Inform. Theory (IWIT'90)*, Eindhoven, The Netherlands, June 10–15, 1990, p. 34.
- [39] S. Kasturia, J. Aslanis, and J. Cioffi, "Vector-coding for partial-response channels," *IEEE Trans. Inform. Theory*, vol. 36, no. 4, pp. 741–762, July 1990.
- [40] D. Knuth, *The Art of Computer Programming, vol. 1, Fundamental Algorithms*, second ed. Reading, MA: Addison-Wesley, 1973.
- [41] —, *The Art of Computer Programming, vol. 2, Seminumerical Algorithms*, second ed. Reading, MA: Addison-Wesley, 1973.
- [42] H. Kobayashi and D. T. Tang, "Application of partial-response channel coding to magnetic recording systems," *IBM J. Res. Dev.*, vol. 14, pp. 368–375, July 1970.
- [43] H. Kobayashi, "Application of probabilistic decoding to digital magnetic recording systems," *IBM J. Res. Dev.*, vol. 15, no. 1, pp. 64–74, Jan. 1971.
- [44] E. R. Kretzmer, "Generalization of a technique for binary data transmission," *IEEE Trans. Commun. Technol.*, vol. COM-14, p. 67, 1967.
- [45] S. Lang, *Algebraic Numbers*. New York: Addison-Wesley, 1964.
- [46] A. Lender, "Correlative level coding for binary data transmission," *IEEE Spectrum*, vol. 3, no. 2, p. 104, 1966.
- [47] S. Lin and D. J. Costello, Jr., *Error Control Coding: Fundamentals and Applications*. Englewood Cliffs, NJ: Prentice-Hall, 1983.
- [48] F. MacWilliams and N. Sloane, *The Theory of Error-Correcting Codes*. Amsterdam: North-Holland, 1977.
- [49] B. Marcus, "Factors and extensions of full shifts," *Monats. fur Math.*, vol. 88, pp. 239–247, 1979.
- [50] —, "Sofic systems and encoding data," *IEEE Trans. Inform. Theory*, vol. IT-31, no. 5, pp. 367–377, May 1985.
- [51] B. Marcus and P. Siegel, "Constrained codes for partial-response channels," *Proc. Beijing Int. Workshop on Inform. Theory (BIWT'88)*, July 1988, pp. D11.1–D11.4. Also IBM Res. Rep. RJ 6315, June 1988.
- [52] —, "Constrained codes for PRML," IBM Res. Rep. RJ 4371, July 1984 (declassified Sept. 1989).
- [53] —, "On codes with spectral nulls at rational submultiples of the symbol frequency," *IEEE Trans. Inform. Theory*, vol. IT-33, no. 4, pp. 557–568, July 1987.
- [54] J. H. McClellan and C. M. Rader, *Number Theory in Digital Signal Processing, Prentice-Hall Signal Processing Series*. Englewood Cliffs, NJ: Prentice-Hall, pp. 72–78, 1979.
- [55] C. M. Monti and G. L. Pierobon, "Codes with a multiple spectral null at zero frequency," *IEEE Trans. Inform. Theory*, vol. 35, no. 2, pp. 463–471, Mar. 1989.
- [56] M. Nasu, "Topological conjugacy of sofic systems and extensions of automorphisms of finite subsystems of topological markov shifts," *Proc. Special Year in Dynamical Syst. of the Univ. of Maryland, 1986–1987*. New York: Springer-Verlag, 1987.
- [57] I. Niven and H. S. Zuckerman, *An Introduction to the Theory of Numbers*, second ed. New York: John Wiley, 1966.
- [58] K. Petersen, "Chains, entropy, coding," *J. Ergodic Theory Dynamical Syst.*, vol. 6, pp. 415–448, 1987.
- [59] G. Pierobon, "Codes for zero spectral density at zero frequency," *IEEE Trans. Inform. Theory*, vol. IT-30, no. 2, pp. 425–429, Mar. 1984.
- [60] M. Schroeder, *Number Theory in Science and Communication*, second ed. Berlin: Springer-Verlag, 1986.
- [61] C. B. Shung, P. Siegel, G. Ungerboeck, and H. Thapar, "VLSI architectures for metric normalization in the Viterbi algorithm," *Proc. 1990 IEEE Int. Conf. Commun. (ICC'90)*, vol. 3, Atlanta, GA, April 16–19, 1990, pp. 1723–1728.
- [62] C. B. Shung, H.-D. Lin, P. Siegel, and H. Thapar, "Area-efficient architectures for the Viterbi algorithm," *Proc. 1990 IEEE Global Telecommun. Conf. (Globecom'90)*, vol. 3, San Diego, CA, Dec. 2–5, 1990, pp. 1787–1793.
- [63] C. B. Shung, P. Siegel, H. Thapar, and R. Karabed, "A 30 MHz trellis codec chip for partial response channels," *Dig. 1991 IEEE Int. Solid-State Circuits Conf. (ISSCC'91)*, San Francisco, CA, February 13–15, 1991, pp. 132–133.
- [64] P. Siegel, "Recording codes for digital magnetic recording," *IEEE Trans. Magn.*, vol. MAG-21, no. 5, pp. 1344–1349, Sept. 1985.
- [65] H. Thapar and A. Patel, "A class of partial response systems for increasing storage density in magnetic recording," *IEEE Trans. Magn.*, vol. MAG-23, no. 5, pp. 3666–3668, Sept. 1987.
- [66] J. K. Wolf and G. Ungerboeck, "Trellis coding for partial-response channels," *IEEE Trans. Commun.*, vol. COM-34, no. 8, pp. 765–773, Aug. 1986.
- [67] R. Wood, "Viterbi reception of Miller-squared code on a tape channel," *Proc. 4th Int. Conf. Video and Data Recording, IERE Conf. Proc. 54*, Southampton, England, Apr. 1982, pp. 333–343.
- [68] R. W. Wood and D. A. Petersen, "Viterbi detection of class IV partial response on a magnetic recording channel," *IEEE Trans. Commun.*, vol. COM-34, pp. 454–461, May 1986.
- [69] S. Yoshida and S. Yajima, "On the relation between an encoding automaton and the power spectrum of its output sequence," *Trans. IECE Japan*, vol. E59, no. 5, pp. 1–7, May 1976.
- [70] E. Zehavi, "Coding for magnetic recording," Ph.D. dissertation, Univ. California, San Diego, Feb. 1987.

lossless of finite order can be viewed as "deterministic with bounded delay."

Fig. 2. Example for bound of Theorem 5.